POLITECNICO DI TORINO

Corso di Laurea in Ingegneria Biomedica

Tesi di Laurea Magistrale

The mechanical properties of three different bandages and their applicability for fixating patients on positioning aids of operation tables during hip and knee surgery

Relatori

Prof.ssa Cristina BIGNARDI

Prof. Alberto AUDENINO

David PUTZER PhD,MSc

Candidata

Giorgia CARPI

A.A. 2017/2018

Abstract

Arthroplasty is a successful surgical procedure; in 2014, only in Italy, the prosthetic replacement operations achieved the numbers of 175.290[1], of which 67.365 are knee's replacement. A lot of techniques are available for this operation, depending on the positioning of the patient, and lot of used devices too. These are used to immobilize the patient, as the success of the operation depends on the precision of the bone's cut, although the insertion of the prosthesis. In this thesis, the mechanical properties of three bandages are investigated in laboratory and on cadavers. They are evaluated as a medical bandage to immobilize some parts of the patient during the surgical intervention. The three bandages are the iFix, the peha haft and the Coban; the last one is already used in surgical operations. A morphological analysis is done using SEM and the following mechanical tests are performed: the tensile test, the grab test and the tear resistance test. The morphological test showed the structural properties of the bandages: each one seemed anisotropic, and their fibres are different for every orientation. To find if the iFix is isotropic, the mechanical properties of iFix are investigated for all its orientations, and only in the longitudinal direction it is compared with the other two bandages. The mechanical test's results return the maximum force, the breaking force and the two elongations associated. The tensile test's results showed that the iFix had different properties in different orientations, as the longitudinal one should be preferred for its resistance. The three bandages' comparison evidenced that the iFix was less elastic than the other two: they presented the same maximum and breaking force but different elongations, which were higher for the peha haft and the Coban. The grab test is done with wet samples, and it showed that the iFix didn't change its properties while the Coban and the peha haft get the maximum and breaking forces decreased. The last test measured the forces in a sample with a cut of 1 cm on its edge: the iFix showed different forces compared with the tensile test's results, as the tear resistance (maximum force of 60 N) was lower than the tensile resistance (maximum force of 100 N).

To prove if the mechanical properties of the bandages are the same applied on human body, a test on cadavers is done. In this case only the iFix and the Coban were used, as the peha haft wasn't a sterile material, so its usage in such an application is questionable. In this test the sub-bandage pressure is evaluated when a specific traction is applied. The compression is measured with an array of sensors, which are applied on the left leg of the cadaver. The results are shown using colour maps for all the traction's forces. The two bandages presented different points of high compression, on the tibia for the iFix, and near the ankle for the Coban. Results suggest that the iFix is more rigid than the Coban, and it gives a more stable fixation. These results seem to agree with the ones obtained in the laboratory, so the iFix is better for a stable fixation than the Coban, as it could generate unwanted movement of the foot during the surgery.

From our point of view, IFix can be used on lower extremities of the body, as the average pressure was constantly under 10 kPa, and the tests shown its resistance if wet or cut. Our study showed that the iFix gave a stable fixation, which depends on the orientation of the fibres, and it could generate high compressions near the bone. So these two points could limit the usage. Although, further investigation has to be done before clinical usage of IFix

Contents

List of Figures

List of Tables

Chapter 1

1 Introduction

Arthroplasty is a surgical procedure to restore the function of a joint, and it is one of the most commonly performed orthopaedic procedures. The positioning of the patient and the forces applied on the patient are determined by the used instrument in the operation room.

1.1. Arthroplasty

The risk of developing symptomatic osteoarthritis is high; one in four people gets infected; so it is necessary to find a proper treatment for this disorder. Arthroplasty is distinguished by the joint (hip, knee and shoulder): for each disease, there are specific surgical treatments.
In the 20th century Philip Wiles[2] developed the first prosthetic Total Hip Arthroplasty (THA), but his results were lost in the Second World War. The first successful THA is the new generation cemented THA, discovered in 1960.
Only in Italy the number of hip arthroplasties increased: in the last fifteen years, surgical treatment of the knee duplicated, and shoulder treatments rose fourfold. The hip is the most operated joint (56,3%), while the percentage for the knee is 38,6 %, 3,9 % for the shoulder and 0,3 % the ankle. In Italy, 175.290[1] operations were performed in 2014. This value doesn't include the operation of revision.
The total joint replacement is considered a highly successful surgical procedure, in the 2015 the percentage of unsuccessful operation is 1,6 %; so numerous techniques could be developed.

1.1.1. Hip arthroplasty

In the following paragraph the patient positioning is described with the patient in both supine position and lateral position, using an extension table.

For the first one[3] it is necessary an intraoperative manipulation of the operative extremity like abduction, adduction, flexion and extension of the hip; this manipulation allows the access to portions of hip joint. To prevent thrombosis, compression stockings are placed on the contralateral lower extremity, and if extension tables are used, the feet are placed in commercial boots. In this position it is important that the patient and his arm are fixed to the operative table with a safety belt. The contralateral arm is positioned on a board with padding; the abduction of the contralateral shoulder shall not be greater than 60°, and 20° for the flexion. The contralateral arm has to be free, so that the

anesthesia team is able to gain access to the extremity during the operation. For the final position, the bilateral padded feet and ankles are placed into the traction boots and fixed with Velcro straps and tape. A manual traction is also possible: the boots are locked into sliding rail and then placed in traction. The force between the femoral head and acetabulum is between 120 N and 200 N, while the initial traction force is 890 N. An exceeding traction force or duration can cause diseases like pudendal neurapraxia, sciatic nerve injury, lower- extremity skin compromise and genital injury. (*Figure 1.1* [4])

***Figure 1.1**: Supine position for hip arthroplasty*[4]

In the lateral position[5] the patient is put onto his side, while the operative hip is on the top. For a better view of the hip joint it is necessary to do a 'separation' by traction; the force is between 300 N and 500 N. Firstly, the leg is hung by a pulley, so the leg is in traction. In particular, a foot piece and a stretcher are used to hold the leg, and also a padded perineal post for counter traction and a tension meter to gauge the amount of traction applied. The arms are placed in an arm board, between the two arms there is a padding.

***Figure 1.2**: Lateral position for hip arthroplasty*[4]

Describing the two used positions for this kind of operation, it has to be said that the traction, and so the adequate joint distraction, is the most important aspect. More traction could allow the intra-articular manoeuvrability, reduce the risk of intra-articular complications and damage of articular cartilage. High traction forces should be the cause of nerve and soft tissue injury. So Dienst et al.[6] made a study on cadavers about the effects on distraction of the hip joint by traction only, by the combination of traction and distension using air, and the different joint positions on distraction. They

studied eight hip joints in 8 cadavers with the mean age of 79 years; these cadavers are placed in supine position with the pelvis fixed to the table by a belt. This study showed that traction and distension using air is better for joint distraction than only mechanical traction. The risk of neurologic and soft tissue complications may be reduced by breakage of the vacuum phenomenon of the joint by distension. Slight flexion's movements can increase the joint distraction.

1.1.1. Knee arthroplasty

This arthroplasty is the second most performed orthopaedic procedure[7]; a proper positioning of the patient on the table allows an efficient manipulation of the leg and the access to the compartments of the knee. The patient is placed in supine position with the heels at the end of the table. To provide the best positioning of the leg on the holder, the patient's pelvis is moved to the very edge of the operating table (where the holder is placed). When the patient is placed, he is fixed with a safety belt around the waist. The leg is stopped with a holder, otherwise the patient's knee may be placed against the surgeon's chest. A cotton cast padding is used for wrapping the thigh, and around it, a tourniquet with a pressure of 350 mm Hg (for adults) is placed. After that, two possibilities are available: the surgical assistant may put the leg laterally or into valgus to expose the medial compartment or into varus to expose the lateral compartment. In the first case the leg is fixed into the holder, by using straps, and then the end of the bed is lowered. If the surgeon has an assistant, he can push the leg laterally or into valgus to expose the media compartment or into varus to expose the lateral compartment. Otherwise, the surgeon may push the leg on his hip to position the leg laterally into valgus for the medial compartment, and medially into varus on his opposite hip for the lateral compartment. If it is used a lateral post, it is positioned 5 cm over the patient's proximal patella. The post allows to have space for the surgeon to stand between the bed and the ankle with the thigh pressed; also it allows the surgeon to grasp the foot and push it laterally into valgus to expose the medial compartment. When the medial-compartment arthroscopy is completed, the surgeon bends the knee off the end of the table and lowers the post, allowing arthroscopy of the intercondylar notch. Then the knee is pushed to the floor, in this way the hip can be rotated. For this operation it is used surgical draping, which is performed in layers. The first layer is applied by affixing a sticky drape first with the tails going up, placed just distal to the plastic drape applied before preparation of the leg. A second sticky drape may be applied with the tails facing down, angled so the drape covers the ipsilateral arm board. Over the foot another drape is positioned, which has a hole that seals the arthroscopic fluid and prevents it from leaking up under tourniquet. It is also possible to put over the foot a stockinette to seal it off from the arthroscopic field. The stockinette is fixed with a bandage. Then the leg is lowered on the bed, and the surgeon can elevate the post[8].(*Figure 1.3*[9])

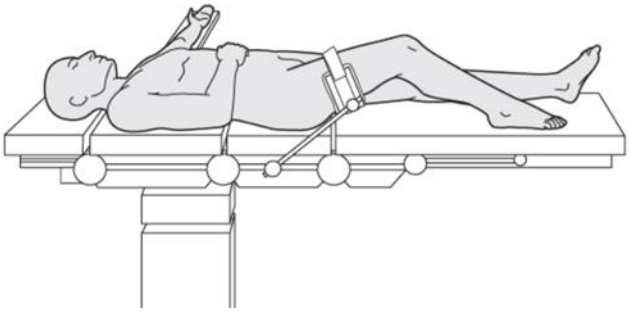

***Figure 1.3**: Position for the knee arthroplasty*[9]

The main factor that leads to negative postoperative outcomes (patient dissatisfaction, loss of thickness of polyethylene tibial bearings, eccentric loading, implant loosening, and eventual early revision), is the incorrect positioning of the total knee arthroplasty components. For a knee's arthroplasty two axis are considered: the gravity axis (GL), which is perpendicular to the ground and passing through the centre of gravity of the body, and the mechanical axis (MA) of the leg, which joins the centre of femoral head with the centre of the tibio-tarsica and passes through the centre of the knee. There are also two lines: the anatomical interline (AJI), which passes through the medial contact between the tibia and femur and the lateral in the coronal plane, and the mechanical interline, which is perpendicular to the MA[10]. The angle β (hip-knee-ankle angle) identifies the anatomical varus, which is usually 3°. The standard technique wants to recreate a neutral MA. Three cuts are done: one distal in the femur, and two perpendiculars to the MA in the tibial part. The obtained mechanical alignment doesn't follow the anatomy but the mechanical needs. [11]

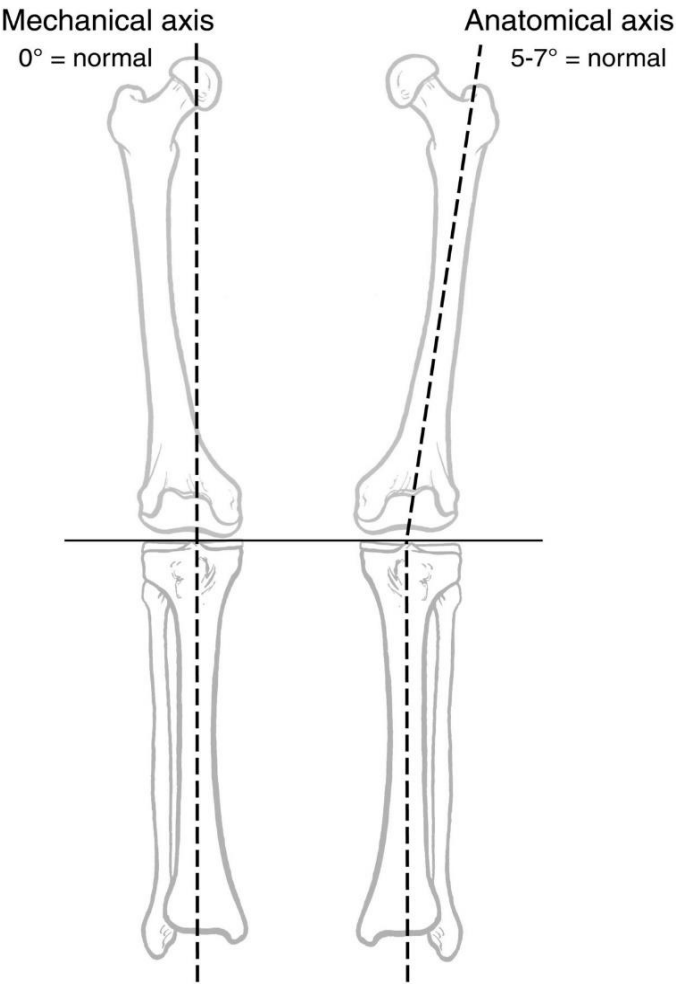

Figure 1.4: *Anatomical references[11]*

To improve mechanical alignment a computer-assisted navigation is used, though it increased the surgical times with no significant improvement in short term clinical outcomes[12]. Daniilidis & Tibesku[12] conducted a study with the purpose of determine whether the patient specific instrumentation (PSI) would lead to a hip-knee-ankle angle (HKA) within ±3° of the ideal alignment of 180°. Four endpoints are measured by radiography: hip-knee-ankle angle (HKA), defined as the angle between the mechanical axis of the femur and the mechanical axis of the tibia, with both lines

crossing at the centre of the knee (*Figure 1.6*); zone of mechanical axis (ZMA), where the tibial base plate is divided into three equal zones (lateral, medial, and central) and the mechanical axis (drawn from the centre of the femoral head to the centre of the ankle), which intersects the tibial base plate, is used to define which zone it passes through (*Figure 1.5*); tibial mechanical axis (TMA), defined as the angle between the line connecting the centre of the ankle and the centre of the knee, and a tangent along the surface of the tibial component; femoral mechanical axis (FMA), defined as the angle between the connecting line between the centre of the femoral head and the centre of the knee, and a tangent along the surface of the femoral component. They are considered ideal for the values: 0° ± 3° varus/valgus for HKA, 90° for TMA and FMA, while for ZMA the TMA passes in the central zone. HKA is calculated as a mean for the entire patient cohort, and additionally patients outside the ± 3° range are noted. The results showed that the use of PSI technology is able to achieve a neutral mechanical axis on average in patients undergoing TKA [12].

***Figure 1.5**: Determination of the ZMA: the tibial plate was divided into three equal zones and the mechanical axis (black line) was defined according to which zone it passes through*[12]

***Figure 1.6**: Knee pre and post operative*[12]

Another system for this kind of operation is Mako Total Knee[13] (*Figure 1.7*). This is a robotic arm assistant. In cadaveric study, this system demonstrated the potential to increase the accuracy of total knee arthroplasty bone cuts and component placement plan. Mako system final bone cuts and final component positions were 5,0 and 3,1 times more precise to plan than the manual total knee arthroscopy control. Sultan et al. [14] wrote a review about the utilization of robotic-arm assisted total knee arthroplasty for soft tissue protection. They found four studies, one cadaver and three clinical. The cadaver study, conducted by Khlopas et al., investigated the presence of soft tissue damage associated with the use of robotic-arm. The results demonstrated no ligament injury in all cadavers prepared using robotic-arm. Furthermore, Park et al. conduced a controlled randomized study:

complications are encountered in the early cases and related to the inappropriate use of small incision and the development of a learning curve. Therefore, the introduction of this new technology may require a learning curve, where the threshold to convert to a manual technique should be low, to avoid complications and longer operative time. In summary, soft tissue complications associated with the use of RTKA have been infrequently reported in the literature and have been mainly related to technical errors and early experience. One cadaver study attempted to directly evaluate the soft tissue integrity with RTKA and demonstrated potential protective advantage with RTKA. Overall, the studied specimens, protection of the PCL, and ability to do the bony resections without the need of patellar eversion or tibial subluxation are demonstrated.

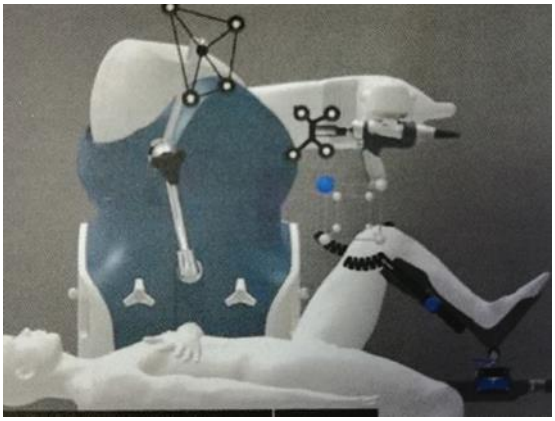

***Figure 1.7**: Mako total knee positioning*[13]

1.1.1. Shoulder arthroplasty

The shoulder arthroplasty is a minimal invasive surgical approach; for this operation the patient can be placed in three positions: lateral decubitus, beach chair and supine.

The lateral decubitus position[15] gives no anatomical orientation and uses traction, so the space in the glenohumeral joint and subacromial space increase, and it is possible a better view. For this approach, firstly the patient is placed in the supine position on the operating table. Then the patient has to be anaesthetized, and the anesthesia performed intravenous access on the inoperative extremity. On the lower extremities it is placed a compression device for the thrombosis. Then the patient is turned onto the inoperative side. There are placed some devices: towels under the head, padded cylinder axillary roll under the axilla, a beanbag under the patient to maintain stability in the lateral position intraoperative. The contralateral arm is placed onto an arm board and it is fixed with a strap. Then safety belts are used over the lateral pelvis to secure the patient to the operative table. Foam padding is positioned between the skin of the patient and the seat belt to avoid irritation of the skin. To prevent a high level of pressure of the bony prominences a pillow is placed between the lower extremities, and also a piece of foam padding over the top of the lower limb ipsilateral on the operative side. The legs are bent with different intensities: the down leg slighter, the upper straighter. Foam padding is positioned between the down leg and the beanbag to reduce pressure; padding can be put over the patient's upper and mid-torso for having stability. The lateral head is covered with padding for more protection. The operative extremity must be put in traction because the joint must be exposed. So an A-frame pulley system is set at the end of the bed, so the arm can be extended. Then a skin traction strip is placed through the end of the pulley system and then attached to the forearm. The operative

extremity is also wrapped in an elastic bandage and traction is generated. For the traction it is used a weight, which is specific for any patient.

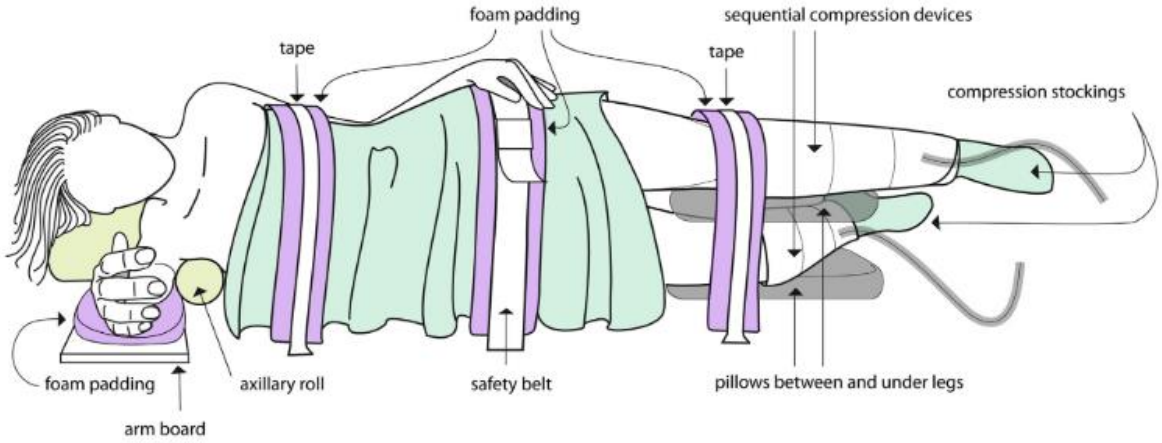

***Figure 1.8**: lateral decubitus for shoulder arthroplasty*[15]

In the beach chair position[16], the patient starts in a supine position on the operating table, and the anesthesia is endotracheal. Compression devices are used to prevent thrombosis. Protective padding is positioned under the heels to prevent compression. Then for the alignment of the greater trochanter with the break, the patient is moved, so the compression of sciatic nerve is prevented. The neutral position is assumed by the head, neck and torso using straps. The head is placed in the head positioner, which must be locked, and the padded head straps are applied across the patient's forehead. Then the operating table is moved by motorized controls to achieve 30° to 40° of the hip flexion and the knee should be flexed 30° for the decrease of the sciatic nerve's tension. A seatbelt is placed around the patient's leg with foam padding, and across the abdomen an additional strap. The posterior aspect of the shoulder is shown removing the ipsilateral back third of the table. The contralateral arm is placed in a padded arm holder, and then the table is tilted for a better access to the shoulder.

***Figure 1.9**: beach chair position for shoulder arthroplasty (ORTHO UND TRAUMA AUF DEM EXTENSIONSTISCH)*

The supine position[17] is not a traditional method for this kind of arthroplasty. It is used when the patient receives a brachial block in the interscalene region. The patient is positioned on the operating table with his head above one of the leg plates. The head is in the neutral position and it is fixed with a tape. The scapular must be free from the table. The operative extremity is connected to a traction device between an adhesive traction tapes. On the traction device it is applied a weight of 3 or 6 kg. The position of the traction should be 45° for forward flexion and 30° for abduction. A sterile waterproof drape is also applied on the suspended arm. This position is good for the view of glenohemoral joint and subacromial space.

***Figure 1.10**: Supine position for shoulder arthroplasty[16]*

All of these positions have different advantages, so they are better for some kind of operations.

1.1.1. Elbow arthroplasty

This procedure was introduced 30 years ago, and it is less popular than the other arthroplasties. Two kind of positions are used: the supine-suspended and the lateral decubitus.

In the supine-suspended position[18], the patient is placed on the operative table with the arm over an arm board. A bracket is applied for the hand, wrist and distal forearm. The mechanical arm holder is brought across the patient's chest from the opposite side. The shoulder is flexed, while the humerus is perpendicular to the floor; then the shoulder is internally rotated and the elbow flexed. This mechanical device allows movements like flexion or extension, and also the access to the anterior and posterior compartments.

The patient is positioned in lateral decubitus position [19] with the operative arm up. A lot of support's devices are positioned: the axillary roll, the bean bag to support the torso, padding under the knees and ankles to prevent the compression. The operative elbow is extended beyond the table, in this way the surgeon can have free access to the medial and lateral aspects of the joint, and also it allows movement like flexion. It is possible to position behind the patient a supporting bean bag. To support

the proximal humerus, a padded arm holder is placed in front of the patient. The arm must be flexed of 90°.

These two methods are different and so they are better for many applications. The lateral decubitus doesn't need a mechanical traction device, it allows free motion during surgery and more anatomic orientation. The supine position is an easier positioning; it allows static positioning without assistant and easy conversation to open surgery for the medial-sided open elbow surgery.

1.1.2. Positioning aids for the operative table

All the examined positions require devices for support the patient, to prevent decubitus, thrombosis and compression's disease. Some of them are analysed and classified in this way: upholstery with viscoelastic foam core, gel pad, operating table accessories, extension table accessories, special units, vacuum mats and patient warming system.[20]

The first two categories change only the materials, although they are used for the same applications. So they have:

- Pillow: which is used for the support of the head in the supine position, it is used in the pre-, mid- and postoperative phase;
- Head rings: for a sure head positioning in supine and lateral position;
- Wedge pillow: which is placed under pelvis of patient in supine position, the leg lies on this side in internal rotation;
- Rolls and half rolls: they relieve the brachial plexus in the patient, placed under the knee or hip for a physiological position;
- Tunnel cushion. Special pad, U-shaped, becomes sideways between the legs of the patient positioned to avoid pressure points. The advantage of this devise is that the weight of the upper leg is not on the lower leg. The pressure on the fibula head of the underlying leg thus becomes reduced to a minimum;
- Special pillow for the knee: this allows a neutral position of the leg in hip area, this is positive also for the lumbar zone.

The operating table accessories are supports that are fixed on the table and that brought the pillows. They are different for their application:

- Attachment for head mounting elements: adjustable with cross handles in 3 joints;
- Arm support device: approaching the arms every storage with the best possible access for the anaesthesiologists;
- Arm protection: it is for a safe storage of the arms on the body, it has an L-padding and two straps, in this way the patient's arm is protected against the side of the operating table, displacement during the operation;
- Radial setting: fastening element for holding and securely attaching accessories to the slide rails of the operating table. A radial adjustment mechanism allows for optimal placement of the accessory;
- Upper arm positioning plate: adaptation to a lateral slide rail of the operating table. For humeral fracture in abdominal and supine position;
- Hand operating table: adaptation to a lateral slide rail of the operating table. It is used for interventions on the arm and hand;
- Fastening three-jointed and body supports: adaptation to the lateral slide rails of the operating table to fix the patient during each storage;

- Side holder: to support the body when folding the operating table;
- Back plate for shoulder operations: back plate with two side removable pads for outdoor storage of the shoulder to be operated on;
- Thorax support: to support the upper body during storage of the patient in a sitting position (beach chair storage);
- Body belt: for body fixation and securing with every storage, but also during patient transport;
- Knee supports: to set up knee-elbow support. Adaptation to the lateral slide rails of the downwardly angled struts of the rectal aggregate;
- Meniscus stab: Angle shape with foam pad roller, adaptable and height adjustable via radial adjusting block on lateral slide rail of the operating table.

***Figure 1.11**: A) Foam pad and B) Gel pad*[19]

***Figure 1.12**: Operating table accessories: A) Bracer, B) Arm support, C) Hand table, D) Goepel leg rest, E) Head rest, F) Helmet*[19]

The extension table accessories are important for arthroplasty; there are devices for extension and rotation:

- Extension sleeve: for variable adjustment of the longitudinal extension during operations on the lower extremities;
- Rotary tilting block: to accommodate footplates (extension shoes) for extensions on the lower extremities;
- Foot plate for extension table: to fix the feet of the patient to the pull spindle unit or foot plate holder. For this application there are also extension shoes that fixes the feet by a system with three belt; they are adaptable. *Figure 1.13*[21].

***Figure 1.13**: Foot plate holder*[20]

About the special units, the motorized knee storage unit is relevant. In this device the electric motor driven knee bearing unit can be controlled by the surgeon by a foot switch, and in knee arthroplasty especially, the intraoperative necessary flexing and stretching movements can be relieved.

The vacuum mats are used for safe patient positioning through good pressure distribution.

The patient warming system is segmented, and custom-tailored blankets can be used individually in any surgical discipline. The idea is that the heat is supplied from above (conductive process).

So for any specific application, there is a specific device. Some of them have similar features, like giving stability or inducing traction or flexion. For example:

- In the shoulder arthroscopy, in beach chair position there are devices of fixation for the head, for the torso, for the leg and for the interested shoulder; these devices are different and they must be adaptable to the patient, so they must be in different sizes.
- In the hip arthroscopy, for each position (supine and lateral) systems of fixation are necessary for the arms, legs and feet. In particular, for the last one there are holders like shoes, so not like tapes.

Some of these devices have the disadvantages to produce ulcers, because they apply a high pressure on the patient's body.

An example for the last point is the 'leg positioner' for the Mako system (produced by Stryker). The *Figure 1.15*[22] shows the components of the system:

- The rail clamp (1);
- The base bar (2);
- The sled (3)
- The simple boot or the boot with bridge (4);
- The extension bar;

- The Coban wrap (*Figure 1.14*).

The rail clamp is positioned on the operating table, and it is used for fixing the base bar, and it allows the horizontal movements of that. The fixing between the bar and the rail clamp is given by the bar's pylon. The bar's movements are not allowed if the pylon is blocked by the rail clamp.

On the bar the sled is installed; it is used for the fixing of the boot, and it can block the movements of the boot. The boot is the place for the patient's leg which is wrapped by the Coban bandage (in three points of the leg).

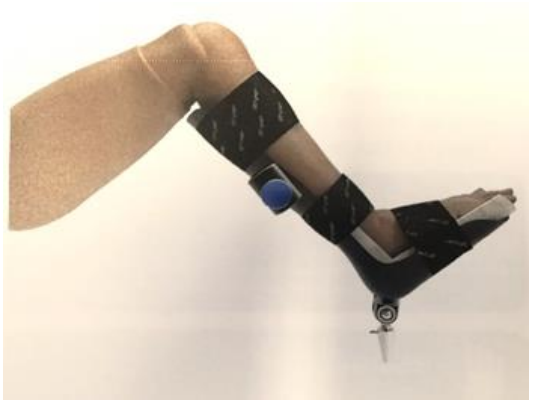

***Figure 1.15**: Leg's fixing in three points*[22]

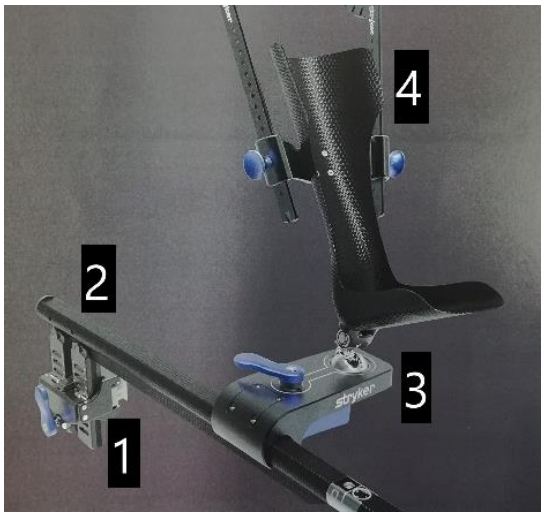

***Figure 1.14**: leg positioner components*[22]

1.1.3. Some Examples for Single Component Compression Bandage

The bandage (the compression bandage in particular) has its principal usage in venous and lymphatic disease. When a bandage is described, the main features are[23]: pressure related to the magnitude of compression applied by the bandage, layers referred to the practice of overlapping layers of bandage material, components related to the construction of the bandage, and elasticity, which denotes the likelihood of the bandage applying a high pressure. Some of the commercial bandages are summarized in the following few paragraphs:

- Ace-bandage (BD, Franklin Lakes, NJ) is an elastic bandage. It is designed to provide support and compression. It is used for body parts such as abdomen, ankle, back, calf, elbow, foot, knee, shoulder and wrist. It doesn't contain natural rubber latex[24].

- Perfekta, Dauerbinde (Lohmann & Rauscher GmbH) are two kind of elastic bandage produced by Lohmann & Rauscher. They are used for the immobilization of limbs, retention of dressing and compression; they can be washed and sterilized. The first one is made with cotton and elastane, and the second with cotton, polyamide and elastane. The Dauerbinde has a characteristic textured woven structure[25].

- Surepress, (ConvaTec, Princeton, NJ) is an elastic wrap that provides sustained graduated compression in an easy to use format. It has extension indicators for easier application and appropriate amount of compression for a variety of leg size[26].

- Profore + (Smith & Nephew UK) is a high compression elastic bandage for use as a part of the PROFORE multi-layer compression bandage system, for large limb sizes. It is made with cotton and elastane. It has a ribbed texture which aids easy application. Its high longitudinal stretch of 170% gives excellent conformability[27].

- Comprilan (BSN Jobst) is an inelastic bandage. It is made with cotton and so it is latex free. It is flexible, sterilizable, reusable and ideal for double banding techniques. Comprilan is used for phlebologic and lymphologic diseases, such as varicosis, thrombophlebitis, phlebothrombosis, chronic venous insufficiency[28].

- Rosidal K, (Lohmann & Rauscher GmbH) is an inelastic bandage made with cotton. It has a lengthwise stretch approximate to 90% and it is sterilizable by steam. It is used to provide powerful compression of the limbs in phlebology. This bandage is also used to treat acute and chronic lymphoedema and to provide support and pressure relief in traumatology and sports medicine[29].

- Pütter bandage, (Paul Hartmann AG): multilayer, single component, inelastic bandage with high stiffness[30]. It is: cohesive, latex free short-stretch bandage with textile elasticity; elasticity of approx. 60 %; cohesive effect on both sides for perfect fit; very high working pressure with light resting pressure; it may also be worn when the patient is in a resting position; breathable; it may be sterilized (by autoclaving at 134 °*C*. It is made with 100 % cotton, with special natural latex free coating.

- Unna boot bandage with inelastic bandage: two components; major component is rigid, bandages with high stiffness. It is a bandage impregnated with calamine lotion and zinc oxide which, when applied over the grafted lower extremity (6 layers), hardens to a semi-rigid dressing resembling a plaster cast. It was invented in 1896 by the German dermatologist Paul Gerson Unna. It adjusts to the leg, calf and foot even during muscle contraction, and can be purchased in stores or made at home with special materials. It needs changing every three to seven days, depending on the exudate and edema. This should be done by a nurse, doctor or a skilled family member. The Unna boot allows patients to carry out their normal daily activities since there is no need to stay in bed to facilitate venous return[31].

The used bandages should resist to high forces, because during an operation the surgeon could apply high forces to move the patient. So in the following chapter the mechanical properties of the bandages will be tested, in particular the tensile resistance.

1.1.4. Tensile test

This test is performed for the material's characterization; it consists in the application of an axial force on a material's sample, which is done using a hydraulic machine. The test sample is clamped in the jaws of the tensile machine, then one end of the machine begins to move in axial direction with a constant speed. So the sample is subjected to a gradual increasing tensile load until failure occurs. The sample starts to change its length, so measurements are recorded throughout the loading operation

by extensometers, and a graph of load against extension (or stress against strain) is produced. The *Figure 1.16*[32] shows a typical result for a test on a mild steel bar, other materials will exhibit different graph.

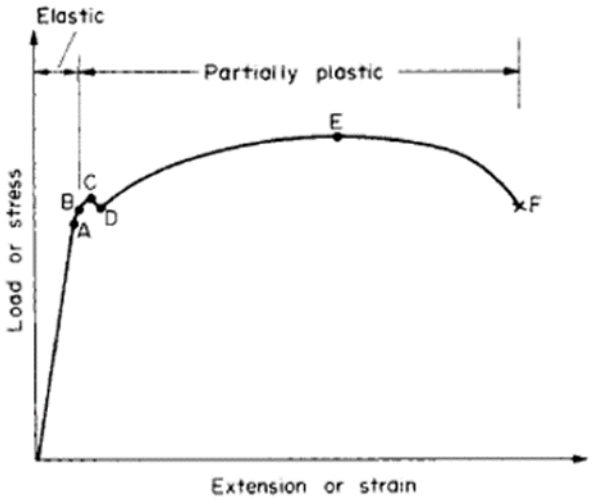

***Figure 1.16**: Typical tensile test curve for mild steel*[31]

For the first part (until A) the material shows an elastic behaviour, so stress is proportional to strain. This is the so-called Hooke's law:

$$E = \frac{stress}{strain} = \frac{\sigma}{\varepsilon}$$

E is the symbol for the modulus of elasticity or Young's modulus.
The point B is called elastic limit and beyond this, plastic deformation occurs and it is permanent, so when the load is removed the material doesn't return in its initial condition.
The point C is called upper yield point, while D is lower yield point.
After point D rapid increases in strain occur without respective high increases in stress. The segment DF shows the ductility of the material, that is the capacity of a material to allow large plastic deformations. A quantitative value of the ductility is obtained by measurements of the percentage elongation:

$$percentage\ elongation = \frac{increase\ in\ gauge\ length\ to\ fracture}{original\ gauge\ length} \times 100$$

For some kind of materials there isn't difference between upper and lower yield points, so in this case a proof stress is used to indicate the start of plastic deformation. The proof stress causes a deformation of 0.1% of the original gauge length (*Figure 1.17*).

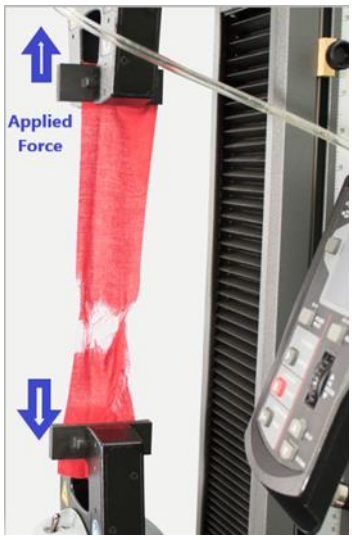

***Figure 1.18**: Tensile machine for texture*[33]

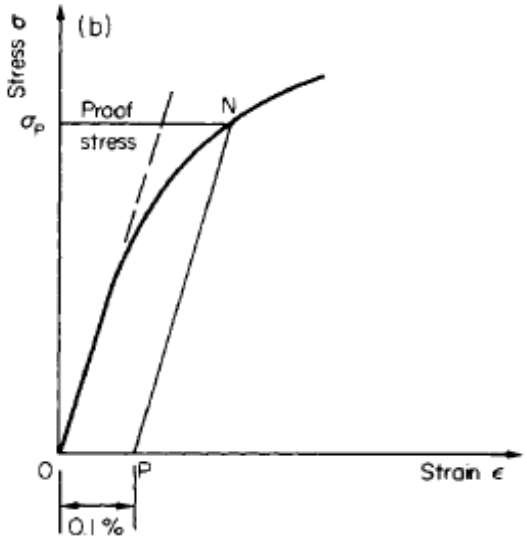

***Figure 1.17**: Determination of 0.1% proof stress*[31]

In *Figure 1.18* it is showed a curve for a mild steel, though for the bandage, that will be tested, the curve has another shape. The sample's section of the bandage is not circular[33] and it could have a section with thickness less than 1 mm (*Figure 1.17*[34]). The bandages, which will be investigated, have a thickness less than 1 mm.
The stress-strain curve for textile has typical regions[33]:

- Toe region, AC, doesn't represent a property of the material, it is caused by an artefact. So it must be correct, in this way it is possible to have the correct value of zero.
- Hooke's region, CD, only for materials with a region of linear behaviour (Hooke's law). The continuation of this region gives the intersection with the zero-stress axis, point B. This point is the real zero-strain point. (*Figure 1.20*)
- BE is the yield offset.
- T' is the point of the stress at braking.

The elastic modulus is calculated by dividing the stress at any point along the line CD by the strain at the same point.
If a material doesn't have a Hooke's region, the correction of the zero point can be made by constructing a tangent to the maximum slope at the inflection point (E') and the intersection with the zero-stress axis gives the point B', which is the real zero-strain point. (*Figure 1.21*) The secant modulus is obtained by dividing the stress at the point G' with the strain in the same point.

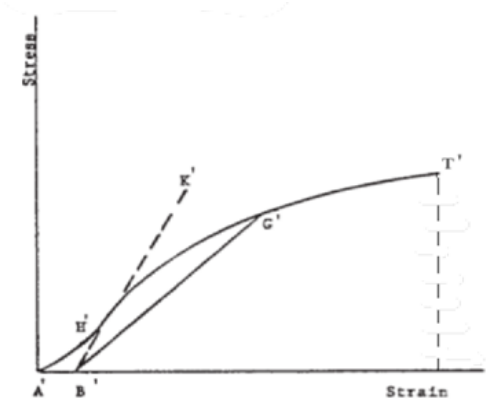

***Figure 1.19**: Material with no Hookean*[32]

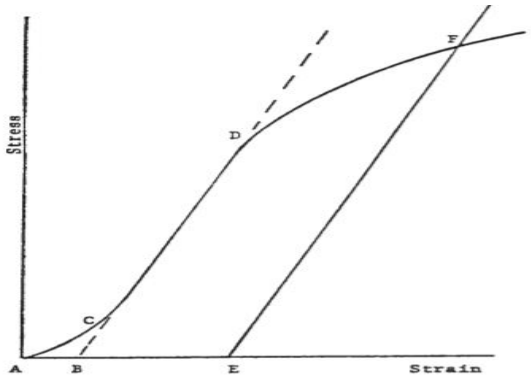

***Figure 1.20**: Material with Hookean*[32]

To obtain the maximum force and the elongation at maximum force for textile fabrics it is used the strip test[35], which is a tensile test where the full width of the sample is gripped in the jaws of the testing machine.

1.1.5. Bandage Stiffness

Stiffness is the resistance of an elastic body to deflection or deformation by an applied force; it is an extensive material property. So for an elastic body it is defined as:

$$k = {}^{F}/_{\delta}$$

Where F is the applied force and δ is the deflection.
The unit of stiffness is Newton per meter. This parameter characterizes the distensibility of a textile. It changes with the position of the sensor, the shape of the body's segment and the consistency of the underlying tissue. The stiffness indices should allow a differentiation between short-stretch (extensibility lower than 100%) and long-stretch material (extensibility more than 100%)[23]. Fabric stiffness under bending deformation is found to influence the interface pressure that a compression garment can apply to a limb.

The stiffness is usually measured in the laboratory (in vitro), but can also be assessed in the individual subject (in vivo).

The measurement in vitro[23] consists in using different extensometer devices to characterize the relationship between the exerted power, required to distend the bandage, and resulting stretch. This relationship can be shown with a "force-elongation" graphic.
The extension of a bandage (in percent elongation) provides a differentiation of compression bandages based on their elasticity; this differentiation is not sufficient for the clinician.

In vivo the stiffness can be defined as the compression rise in the circumference of the leg (in the European prestandard for medical compression hosiery Comité Européen de Normalisation), which is expressed in hectopascals per centimetre (hPacm) or millimetres of mercury per centimetre (mmHgcm). Several studies demonstrated that the difference between the sub bandage pressure

measured in a standing and supine position is indirectly proportional to the stretch length of the bandage[23].
It is defined the static stiffness index (SSI), which is the difference between the interface pressure when standing and lying (mmHg) divided by 1 cm[36]. The SSI may be taken as a useful parameter to characterize in vivo stiffness for all forms of compression bandages including multicomponent multilayer systems in vivo. In the standing position, inelastic bandage systems will produce a higher sub-bandage pressure than elastic bandages resulting in a higher SSI[36].
Liu et al. [37] found that when the bending rigidity of the fabric increases, its ability to apply high pressures increases. This may be related to their findings which state that thick stocking garments with mean thickness of 1.32 mm are able to apply higher amounts of pressure compared to thin stockings with mean thickness of 0.35 mm. Liu et al. [37]considered only the fabric elasticity because the other propriety of the bandage, measured during the test, depended by subjects themselves (such as body posture, muscle tensity..). These testing are only suitable for clinical or laboratory assessments on a small scale, which allows easy realization of unification or standardization.
Suehiro et al. [38] conduced a study to evaluate the interface pressure and stiffness of an elastic multilayer bandage. They found that both the parameters increased linearly for up to five bandages; so the overlapping of bandages raised the stiffness and also the friction.

1.1.6. Others properties

The bandage can be classified on three other factors[39]: the extensibility, the elasticity and the number of components.

- *Extensibility:* it is the ability of the bandage to stretch when a force is applied to it. According to their extensibility the bandage is classified in:

  i) No stretch bandages, that doesn't extend when subjected to a force.
  ii) Short stretch bandages, they are made of cotton and they provide 40 – 90 % extension when subjected to a force.
  iii) Long stretch bandages, they contain elastomers so they have an extension of 140 %.

- *Elasticity:* it is the ability to return to the original length when the tension is removed from the bandage. So there are two kind of bandages according to their elasticity:

  i) Inelastic bandages: they are made of cotton without elastomers.
  ii) Elastic bandages: they contain elastomers such as rubber or lycra.

- *Number of components:* the bandages can be classified according if they are applied alone or with multilayers:

  i) Single component compression bandage consists of one type of compression bandage that is commonly applied over a padding layer.[23]
  ii) Multi-layer single component compression bandage consists of a number of bandages applied usually on top of each other.[23]
  iii) Multi-component short stretch compression banging system consists of three to four different types of bandages and at least one of the components is a short stretch bandage.[40]
  iv) Multi-component elastic compression banging system consists of three to four different types of bandages, and none of the components is classified as a short stretch bandage.[40]

1.1.7. Aim of the study

The purpose of this study is to find a versatile fixation's tool for many of the descripted applications, that holds body's part but also can resist to traction loads. It could be a bandage, used in imaging tests (MRI). This tape fixes the patient to the operative table: it stabilizes the head, the hip and lower spine, upper and extremities.

It has been said that this tape can be resistant to traction and it must not generate pressure that can produce ulcers.

In this study the iFix bandage is tested, and three questions are made:

- The first aim is to determine the maximum force, the breaking force and the two elongations associated of three kinds of bandages (iFix, Coban 3M and peha haft), taken in the longitudinal direction following the testing standard UNI EN 29073-3, testing standard UNI EN 29073-2 (wet) and testing standard UNI EN 29073-4 (tear resistance)

- The second aim is to evaluate the mechanical properties of the iFix bandage in its four directions: longitudinal, transvers, diagonal at 45° and at 135° following the testing standard UNI EN 29073-3. So it is tested the isotropy of the material.

- The last aim is to measure the applied maximum and mean pressure by the iFix and Coban 3M bandages on a cadaver model and to determine its distribution along tibia and forefood.

Chapter 2

2 Morphological and Mechanical Properties of different bandage used in medicine

In *Chapter 1* the properties of the bandage and some examples of commercial bandages were described. The aim of this section is to estimate the mechanical properties of the bandage *iFIX,* produced by *Interventional systems* (iSYS Medizintechnik GmbH). This bandage is used only to immobilize the patient during a test of imaging (for MRI), but it also can be used for different applications in orthopaedic surgery, so the bandage will be tested for maximum traction forces.
There are standards that define elastic or inelastic bandages, though they refer to the compression therapy. One of these is *DIN 61632*[23] (Surgical dressing – Cotton crepe bandages), which is a standard by Deutsches Institut für Normung E.V. (German National Standard). Another is RAL – GZ 387/1[41] (medical compression hosiery); the RAL is an independent organization that recognizes the quality mark for products and services. There isn't a standard for the bandage used during an operation like arthroplasty, so the results of the *iFIX*'s mechanical properties are compared with those of two commercial bandages, *Coban 3M* and *Peha-haft*.

2.1. Background Information

2.1.1. Standard for compression bandage

The main categories of the compression bandage elasticity are defined by the percent elongation of the material, on which is applied a force on bandage width of 10 N/cm; this value is given by the standard DIN 61632[23]. These categories are:

- Rigid or inelastic: it has maximal stretch of 0-10 %.
- Short-Stretch: it has maximal stretch of 10-100 %.
- Long-Stretch or elastic: it has maximal stretch more than 100 %.

This classification is technically acceptable, but the maximal elongations are unlikely to be reached during bandaging, thereby reducing the value of the classification in practical terms.
Partsch et al.[23] classified the bandage doing experiments on 10 legs of volunteers with 26 types of bandages (with different elasticities). They obtained another classification:

- Rigid or inelastic: it has a practical stretch of 0- 10 %.
- Short-Stretch: it has a practical stretch of 20-50%.
- Long-Stretch or elastic: it has a practical stretch of 40-120%.

They also measured the dynamic modulus (given in N/%stretch) for each category, this modulus corresponds to the steepness of the curve at the force – level of 1 N/cm width:

- Rigid: it has a value higher than 30 N/%stretch.
- Short-Stretch: it has a value higher than 0,3 N/%stretch.
- Long-Stretch: it has a value lower than 0,3 N/%stretch.

This classification is used only for single bandage components, and not for multilayer compression bandage system.

The RAL-GZ 387/1[41] gives the quality and test specifications for the medical compression hosiery. One of the tests is about the extensibility in longitudinal and transversal direction. The standard specifies the dimensions of the sample: length of 150 mm and width of 50 mm. The standard specifies that the applied load is 50 N, which is reached within 30 seconds. Its specific doesn't suggest a classification of bandages.

These two standards refer only to bandage with a single component; for the multilayer Al Khaburi et al.[42] presented a study about the effect of multilayer bandage on the interface pressure, applied by compression bandages. They validated the bandage by a test, which estimated the tension-elongation interconnection of the bandage. It is measured the tension developed in the bandage while it is extended at a constant speed of 100 mm/min and loaded with 100 N.

The UNI EN 29073[43]:1993 is about the tensile properties of nonwoven and how to determine them. This standard specifies that the sample has to be 50 mm for width, 200 mm for initial length. The sample is clamped, and it is applied a constant rate of extension of 100 mm/min. The standard shows that it is determined the elongation of the test piece at the maximum breaking strength, and it's expressed as a percentage of nominal initial length. So this standard agrees with the values applied by Al Khaburi in his study.

The last standard will be used to determine the mechanical properties of the bandages, because it is specific for nonwoven. Meanwhile the first standard refers to medical compression hosiery, the second one is referred to multilayer bandages.

2.1.2. Tested Bandages

This chapter has the aim to test the mechanical properties of three bandages, in particular tensile strength. The mechanical properties will set out which one is the proper one for application in arthroplasty. In this operation, as described in *Chapter 1*, the forces applied are high, so the bandage has to fix the body's part and withstand applied forces.
The analysed bandages are iFix, Peha-haft and Coban; the results of the first one are compared with the other two bandages.
The bandages selected are:

- **Peha-haft**[44] (Hartmann Group, Heidenheim an der Brenz, Germany): it is a cohesive conforming bandage, it is composed by 43% viscose, 37% of cotton and 20% polyamide.

Caused by its texture and micro-structured coating it is adhesive to itself. It has an extensibility about 85%.

- **Coban**[45] (3M Health Care, St Paul, Minnesota, United States): it is a self-adherent elastic wrap, and it is obtained from the natural rubber latex. It works as a tape, it compresses, it protects wound sites and it fixes. It is available in sterile and nonsterile versions.
- **iFIX**[46] (iSYS Medizintechnik GmbH, Austria): it is composed by two parts, the iFix Fleece (the bandage), and the iFix Patch (Figure 2.8). The first material is polypropylene fleece, nonwoven, it has a thickness of 0,83 mm, it has a maximum tensile strength of 120 N and an elongation of 70 %; it can be used to wrap the patient. The second one is a patch composed by polyamide extruded, so with an artificial rubber with very good humidity and weather resistance. It has a peel strength 23 N/cm and a shear strength of 100 N/cm. It is used for clamping the iFix Fleece and fixing it to the operative table.

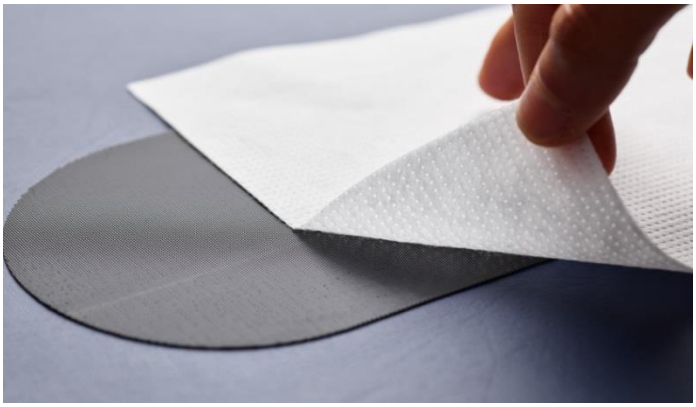

***Figure 2.1**: iFix system: the white bandage is iFix Fleece, the black is iFix Patch*[45]

The polypropylene[47] is a linear hydrocarbon polymer (C_nH_{2n}), it is a versatile polymer because it is available in different forms: mouldings, fibres, tape, film and foam, and it is used for different products. Its great usage is given to its properties, which include: semi-rigid, translucent, chemical resistance, tough, fatigue resistance, heat resistance. The polypropylene fibre is used in applications including tape, strapping, bulk continuous filament, staple fibres, spun bound and continuous filament.
The iFix bandage is made by polypropylene nonwoven. The nonwoven fabric is a method that makes a texture by bonding the fibre together by chemical, mechanical, heat or solvent treatment.
The patch is made by polyamide[48], which is a group of plastics with an amide groups ($CONH$). It has different forms: nylon 6,6; nylon 6,12 etc. The meaning of the two numbers depends on the process of production. The first method consists of a condensation reaction between diamines and dibasic acids, which produces a nylon salt. So in this case the first number is the number of carbon atoms in the diamine, while the second refers to the quantity in the acid. The second method is given by the opening of a monomer with amine and acid groups (lactam ring); in this case the number associated with it is only one, and it refers to the number of atoms in the lactam monomer. The melting point changes for different types of nylon. It is used in the production of films and fibre; this form is semi-crystalline, and it has good thermal and chemical resistance (it can't resist the attack of strong acids like alcohol and alkalis).
The nylon fibre is used in textiles.

2.1 Materials' properties

Two kinds of test are done to investigate the properties of these materials: the first one is morphological and the second one is mechanical. The morphological test is used to analyse the structure of the bandages and it is done with a SEM. The mechanical tests have the aim to evaluate the mechanical properties of the iFix bandage in all of its orientations (longitudinal, transversal, diagonal of 45° and 135°), and to compare the mechanical properties of iFix with Coban and Peha-haft, only in longitudinal directions. The results show the force – elongation curve of each material, and the table with the maximum force and elongation, and with the breaking force and elongation. These values characterize the studied bandages.

A test is also done to evaluate the adhesive force between the iFix fleece and the patch.

2.1.1 Materials and Methods

2.1.1.1 SEM

The SEM images are obtained in the Medichine University's laboratory. They are used samples with square's form and dimensions of 1 cm^2. Four materials are analysed: iFix fleece, iFix patch, Coban and Peha-haft.

Before the examination with the SEM, the samples had to be prepared: it is required a coating of conductive layer of metal (gold). It is done by the machine 'AGAR SPUTTER CATER', set with a time of 45 sec and with a sputter current of 30 $mA/mbar$.The sample is covered with a gold layer (like *Figure 2.9*).

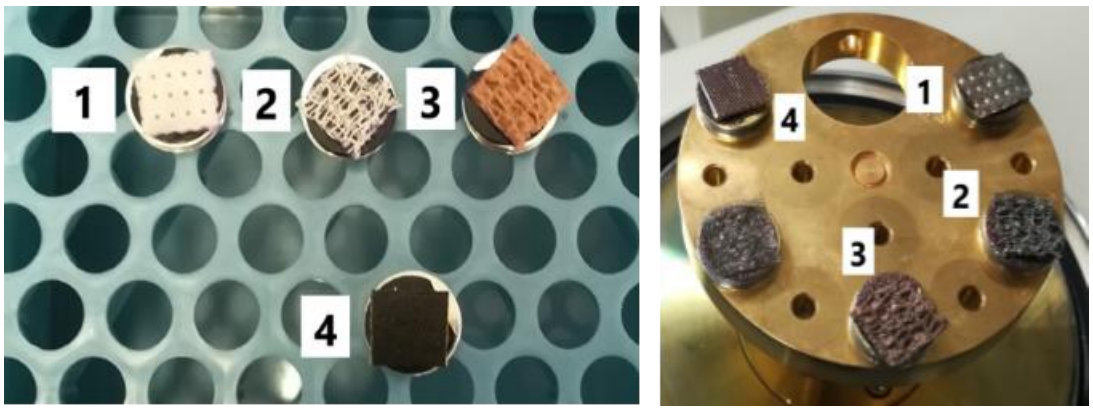

***Figure 2.2**: SEM's samples: 1) iFix fleece, 2) Peha-haft, 3) Coban, 4) iFix patch. The second image shows the samples after coating*

So the samples are positioned in a support, and then into SEM's machine (JEOL JSM 6010LV). The program 'InTouchScope' showed the images; for each sample three images were taken: one with the resolution of 500 μm, one with 200 μm and the last one with 100 μm.

2.1.1.2 Weight of the samples

Before the mechanical tests, the samples are weighed by the high precision balance (SI-603, balance precision: 0,001 g, Denver Instrument, Bohemia, New York).

In the *Appendix A,* the samples' weights are reported. For each bandage, the mean value and the standard deviation are calculated.

2.1.1.3 Mechanical tests

All the described tests are done in the mechanical laboratory of Innsbruck's medicine university. The used tensile machine is a product of Zwick Roell, and the elaboration software is testXpert V11.02 standards.
About the pre load, we had different values for every kind of bandage:

- *IFix:* the pre load was 2 N and the initial speed was 5 mm/min.
- *Coban and Peha -haft:* the pre load was 0,5 N and the initial speed was 20 mm/min.

For all the tests, a statistical test is done to calculate the statistical difference between the groups. The test is ANOVA, and it calculates a P value: if it is under 0,05, the difference among the averages is relevant.

2.1.1.3.1 Tensile test

Different pre load and initial speed are used, because the last two bandages had an elastic behaviour. The used software recorded a force – elongation curve and a table with: the initial length, the maximum force, the breaking force, the strain at the maximum force and at the breaking force. The samples for each bandage were ten with the dimension of 200 mm x 50 mm (*Appendix A*).
The data are elaborated with *Excel 2016* and compared by using the ANOVA test.

Protocol: The test needed the sample to be clamped and then fixed on the tensile machine. To standardize the clamping, a support made in PVC is used. This support is made by a milling machine (Proxxon); the dimensions in mm are indicated in the *Table N°1* in *Appendix B*.
The two lateral rectangles have a thickness of 8 mm, because they are used for positioning the two clamps, the central rectangle for the bandage's sample and the two holes for the bolts.
The clamping force is exercised by using screws with a diameter of 5 mm and a length of 16 mm, and then pressing together 4 aluminium plates (dimensions in *Table N°1* in *Appendix B*).
Because of the adhesive face, the iFix patch is attached on one side.
A standard procedure for mounting the clamps is followed: (*Figure 2.13*):

1. Positioning the four bolts on the two holes.
2. Positioning the two clamps with the adhesive faces on the top.
3. Putting the bandage in the central rectangle.
4. Covering the two extremities of the bandage with other two clamps.
5. Screwing the four screws in the order indicated on the support by a screwdriver with a torque of *2* Nm.

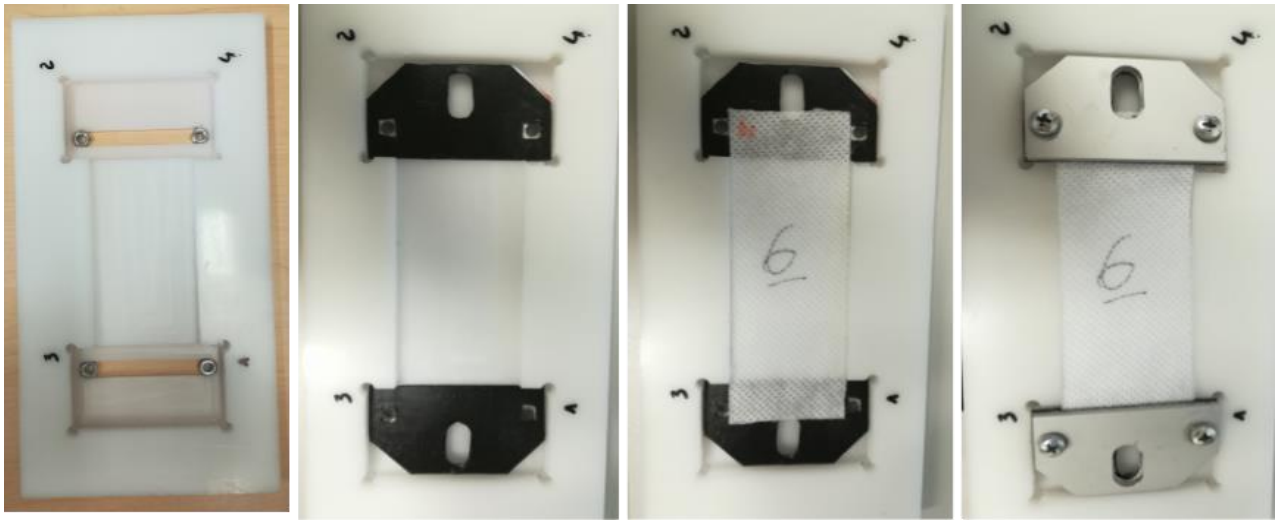

***Figure 2.3**: Used procedure: the last image includes the points 4 and 5*

2.1.1.3.2 Grab test

The grab method is used to determine the tensile strength and it is an alternative method to strip test. This test describes how to obtain the tensile strength in wet samples. The sample is clamped only partially: they are used jaws with dimensions 25 mm x 25 mm. The *Figure 2.6* shows the sample with the areas of the jaws.
It is used a dynamometer with constant speed, one jaw moves and the other not.

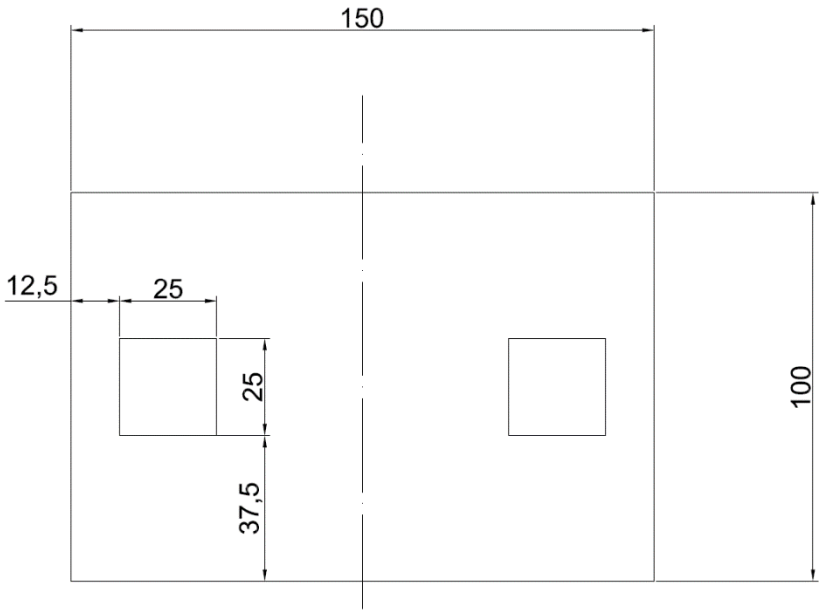

***Figure 2.4**: Grab sample, the white squares are the jaws' areas*

There is a standard for nonwoven textile which describes this test, the UNI EN 29073-2. At the end of the test, we have to calculate the breaking force, the maximum force, the length associated to the maximum force and its percentage.
The length associated to the maximum force and to the breaking force is given by:

$$A_i = 100 \times {}^{\Delta L}/_{L}$$

With A_i as the percentage length of the sample, ΔL the length of the sample given in mm and L the initial length of the sample given in mm.
For this kind of test, the PVC support, the clamps and the samples had different shapes.
The first one is like the sketch in the *Table N° 2* in *Appendix B,* the two small rectangles show the position of the clamps, and the central rectangle the sample's.
The clamp was smaller than the width of the sample, because the fixing area didn't cover all the sample: so the clamp had the dimensions indicated in the *Table N° 2* in *Appendix B*. On the top of the clamp there were thicknesses to prevent sample's deformation; the adhesive part was in a space in the end of the clamp (dimensions 25 mm x 30 mm).

Protocol

The samples had to be wet, so the used procedure is the following:

1. The sample is steeped in distilled water for 5 seconds.
2. It is dried for 5 seconds.
3. It is positioned in the PVC support.
4. It is clamped.
5. It is positioned on the machine for the test.

***Figure 2.5**: Workstation for the Grab test. There are: the box with the distilled water, the PVC support with the sample and the clamps*

2.1.1.3.3 Tear resistance test

The tear resistance test is a tensile test, which measures forces that depend on the fibres of the structure and their composition. The fracture is the sequential break of the wires under tension force.

The standard, which describes this test, is the UNI EN 29073-4. The used sample has a trapezoidal shape, like that in *Figure 2.7*.
It is used dynamometer with constant speed (100 mm/min), and the sample is clamped at its ends.
The software, linked with the traction machine, recorders a series of peaks, and the value of interest is the mean of this peaks for each sample.

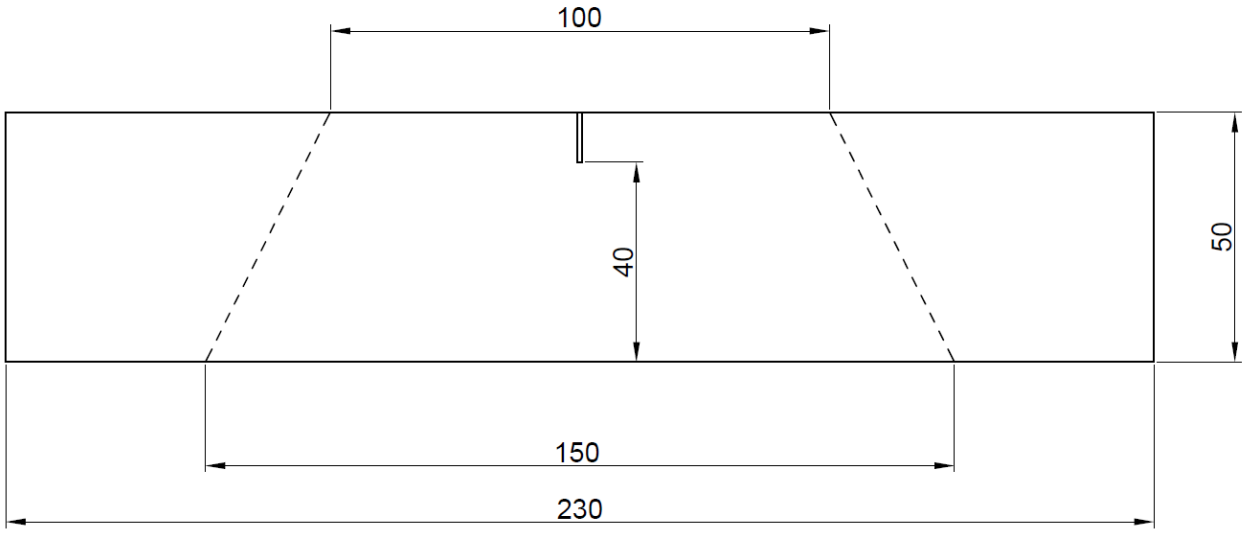

***Figure 2.6**: Trapezoidal sample, the red line is the cut on the sample, it has length of 10 mm*

The test needed the sample to be clamped and then fixed on the tensile machine. For the clamping it is used a support made in PVC. This support is made with a milling machine (Proxxon), the dimensions in mm are indicated in the *Table N° 3* in *Appendix B*.

The two lateral rectangles have a thickness of 8 mm because they are used for positioning the two clamps, the central rectangle for the bandage's sample.
To fix the clamps, they are used screws with a diameter of 5 mm and a length of 16 mm.
The clamps were four, and they were aluminium plates (*Table N° 3* in *Appendix B)*. With the milling machine, they are all pierced. The central hole didn't have an elliptical shape, but a 'T' form, so it was possible to lock it to the tensile machine. Because of the adhesive face, it was attached on one side the iFix patch (black).
To set the sample on the PVC support it is used the same standard procedure of the tensile test, but the torque applied on screwdriver was 2 Nm (in this way the clamps didn't deform).

2.1.1.3.4 Adhesive test

This kind of test is not expected in any standard, so it is made only to measure the range of the adhesive force qualitatively.
Clamps and support were the same of the tensile test. Although, the tested sample was different: it is 150 mm length and it is composed by the fleece and the patch. These two parts were 100 mm long, and for 50 mm they are fixed together. To do that they are pressed by a cylindrical load.
The following figures show: the support and the load used, the sample at the end of the test.

***Figure 2.7**: Sample at the end of the test*

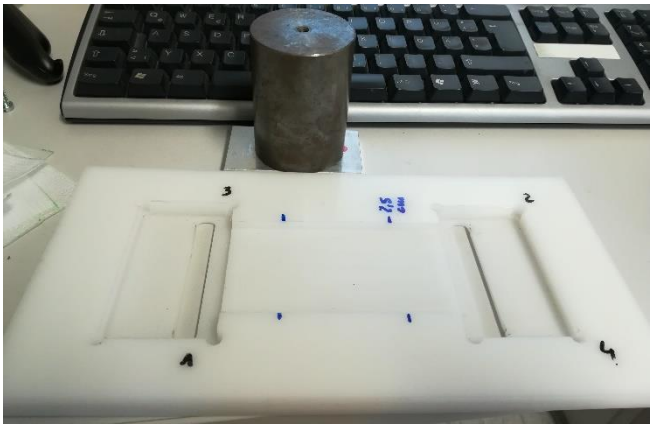

***Figure 2.8**: Support with the indication of the sample's positioning and the load*

The number of evidences were twenty (the first half in the longitudinal orientation and the other half in the transversal); the orientation of the fibres' sample is not considered.

2.1.2 Results

2.1.2.1 SEM

The iFix's structure presents fibres in all directions, but the main orientation is longitudinal. This is shown, easily, in the image with 100 μm resolution, an higher number of fibres is positioned longitudinally. In some points the fibres are melt together, with the resolution of 100 μm it is possible to see also some melting's failures. The melted fibres create structures with two shapes: the biggest is square and it is repeated with regularity, the other is elliptical, not regular and it presents same defects. The iFix patch is made to fix the fibres of the iFix fleece: the structure is regular, and presents cylindrical structure. Thanks to that structure (for the patch) and the square (for the fleece), these two parts can be fixed together.

The Peha-haft bandage has a different structure than the iFix, in fact it shows two kinds of filaments: the first one is entwined as a rope, and these ropes are crossed as a net; the second one is just curly fibre, this kind of fibres crosses the network only in same position and only in one directions. The second type creates a structure with a higher width than the rope made with the first kind of fibres (as shown in *Figure 2.11*). The network provides the adherence at the bandage and also the 'structure', the secondary gives the mechanical resistance in longitudinal direction.

The Coban bandage is an elastic bandage with similar properties of the Peha-haft, while its structure isn't many different. It shows curvy fibres in all directions, which are melted together, as a matrix. In longitudinal direction, the melted fibres make a rope shape, that are separated from each other but they didn't have the same distance. In the image with a resolution of 100 μm, the filaments are more curvy than the others. The longitudinal ropes supply the elasticity and the mechanical resistance in this direction, which is predominant.

The presence of a matrix, which covers all the wires, is better for sterility. In fact, the Peha-haft presents gaps, which can be filled by dirt, bacterias and whatever.

Looking at the structures of the three bandages, it is possible to say something about their mechanical properties, but it's important to prove that with mechanical tests.

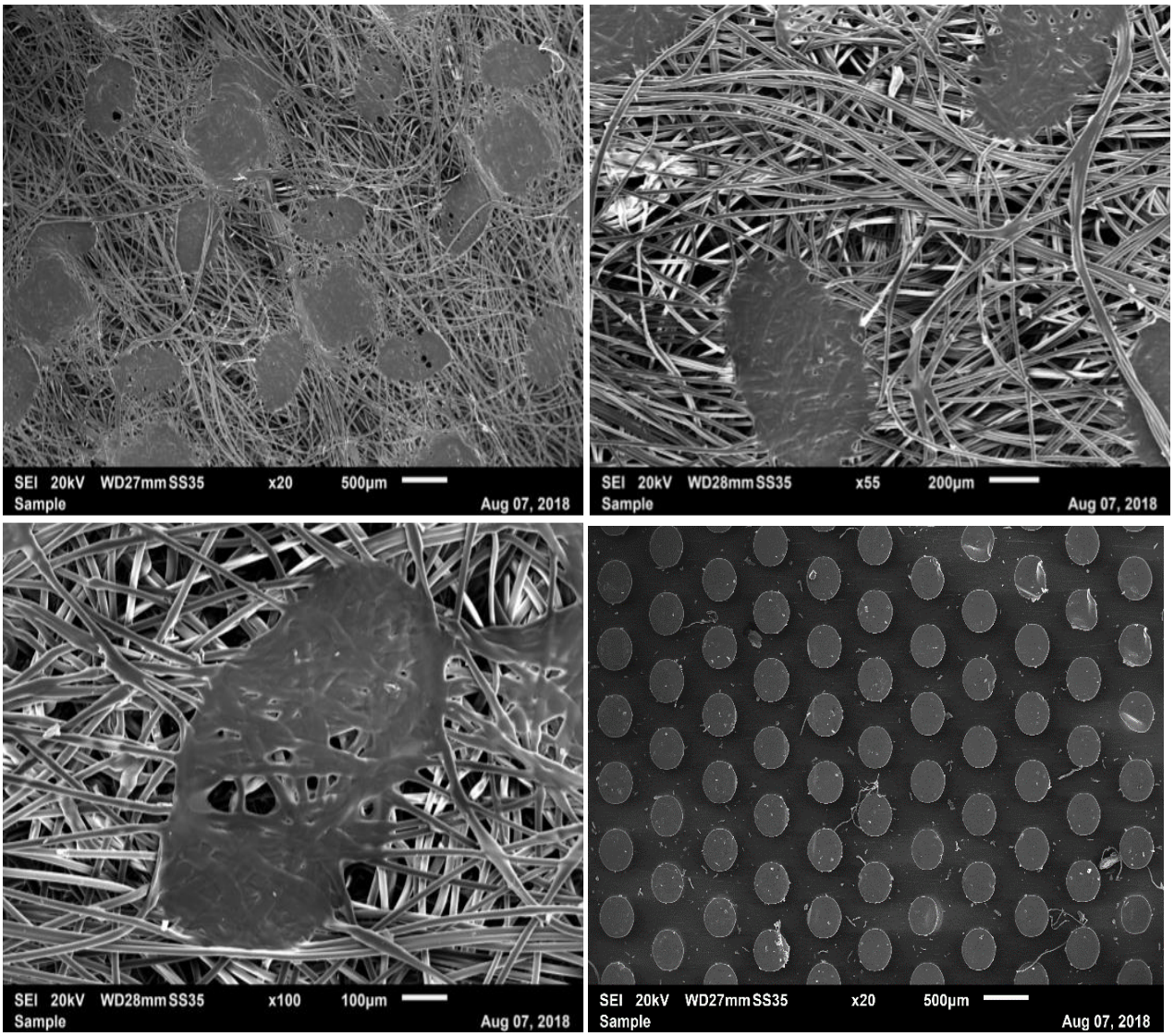

***Figure 2.9**: These four images: the first three show the same iFix sample but with different resolutions: the first one with 500 µm, the second one with 200 µm, the third with 100 µm. The last one (on the right) shows the iFix Patch*

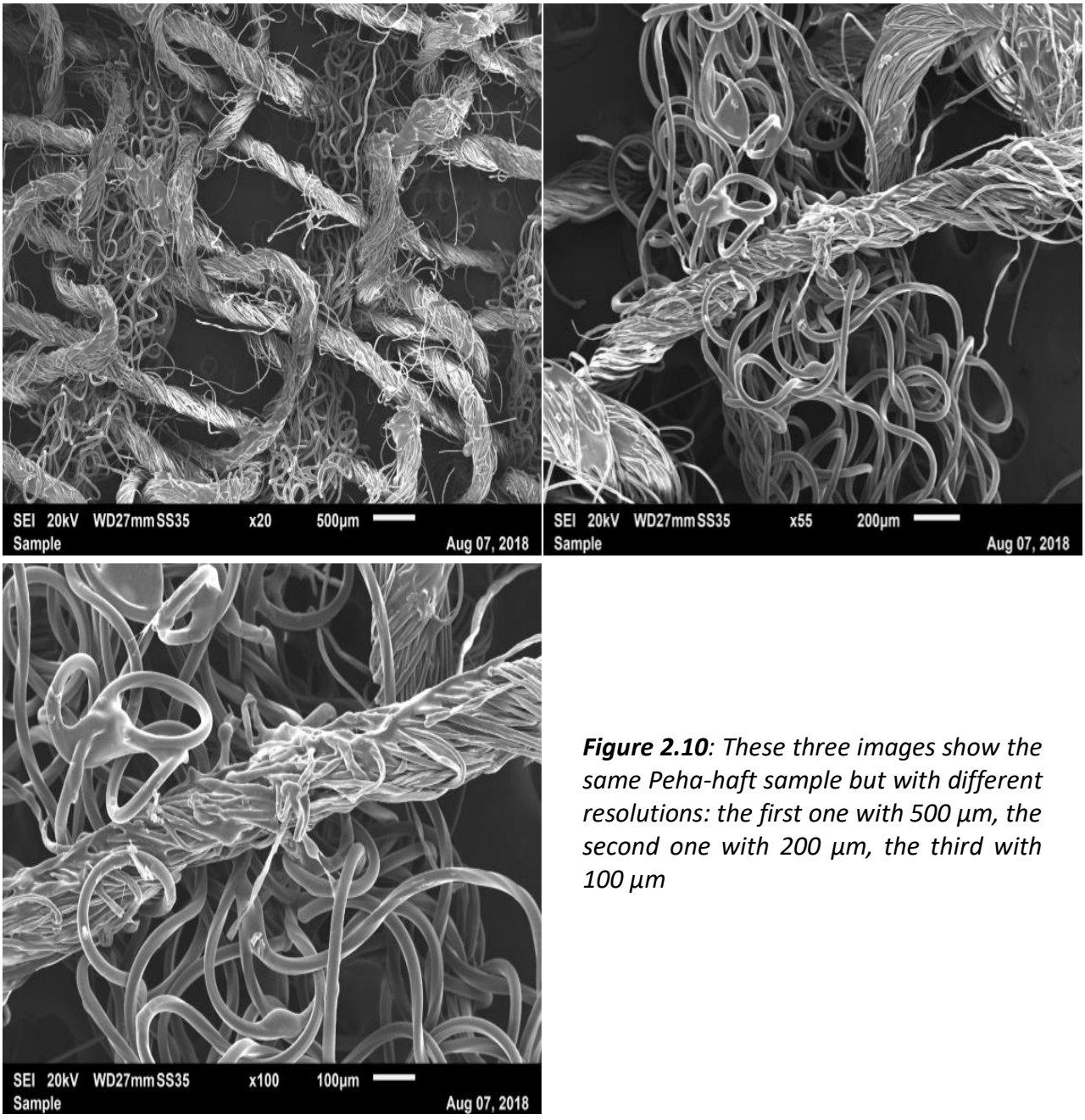

***Figure 2.10**: These three images show the same Peha-haft sample but with different resolutions: the first one with 500 µm, the second one with 200 µm, the third with 100 µm*

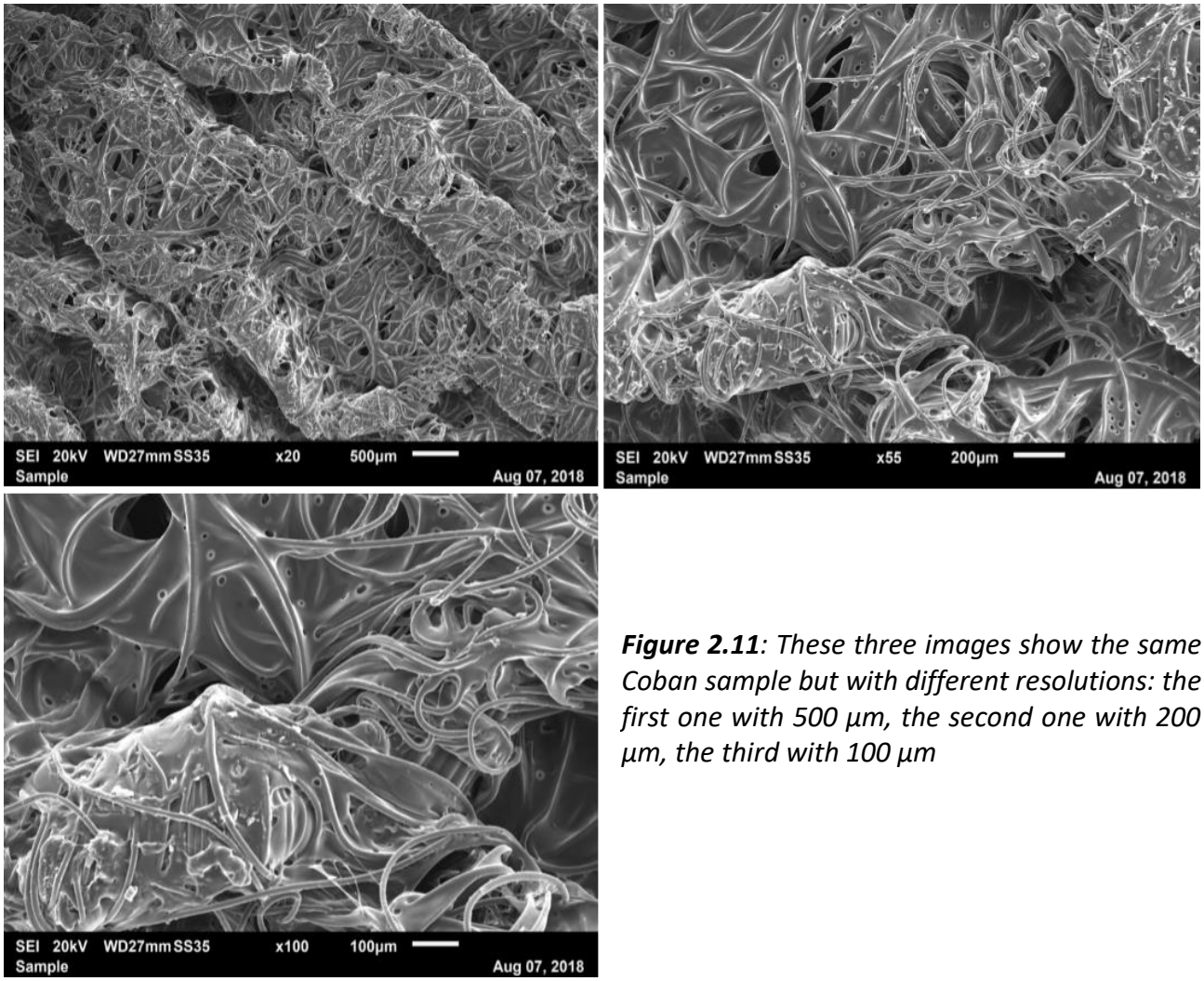

***Figure 2.11**: These three images show the same Coban sample but with different resolutions: the first one with 500 µm, the second one with 200 µm, the third with 100 µm*

2.1.2.2 Weight of the samples

For each bandage the mean value and the standard deviation were calculated. The *Table 2.1* shows the average weight of iFix, Peha-haft and Coban.

***Table 2-1**: Mean weight and standard deviation for the iFix, Coban and Peha-haft for the tensile test*

	Mass (g)
i Fix	
Longitudinal	0,56 ± 0,0577
Transverse	0,64 ± 0,0562
Diag. 45°	0,61 ± 0,0326
Diag. 135°	0,61 ± 0,0205
Coban	
Longitudinal	1,10 ± 0,2731
Peha-haft	
Longitudinal	0,54 ± 0,0396

***Table 2-2**: Mean weight and standard deviation for the tear resistance test*

	Mass (g)
i Fix	
Longitudinal	0,81 ± 0,0563
Transverse	0,77 ± 0,0330
Coban	
Longitudinal	1,84 ± 0,0396
Peha-haft	
Longitudinal	0,80 ± 0,0215

***Table 2-3**: Mean weight and standard deviation for the Grab test*

	Mass (g)
i Fix	
Longitudinal	1,06 ± 0,0327
Transverse	1,08 ± 0,0677
Coban	
Longitudinal	2,39 ± 0,0292
Peha-haft	
Longitudinal	1,04 ± 0,0102

Each table shows that Coban's mass has a higher value than the iFix and the Peha-haft, which have similar weights. The Coban's structure provides a higher weight, in particular for the presence of a matrix, which covers all the fibres.

2.1.2.3 Comparison of mechanical properties of iFix for the different orientations

2.1.2.3.1 Tensile test

The tensile machine shows for each sample the force - displacement curve, which describes the behaviour of the material. The longitudinal orientation shows a different curve from the other three directions (transverse, diagonal at 45°, diagonal at 135°), in particular the bandage's force achieves the maximum, then it decreases for a short time and again it increases until another peak. On the sample this phenomenon can be seen with the formation of a double layer.

In the transverse orientation there isn't the formation of the double layer, so the curve force - displacement shows only one peak at the same value of the maximum longitudinal force, but not at the same maximum longitudinal elongation.

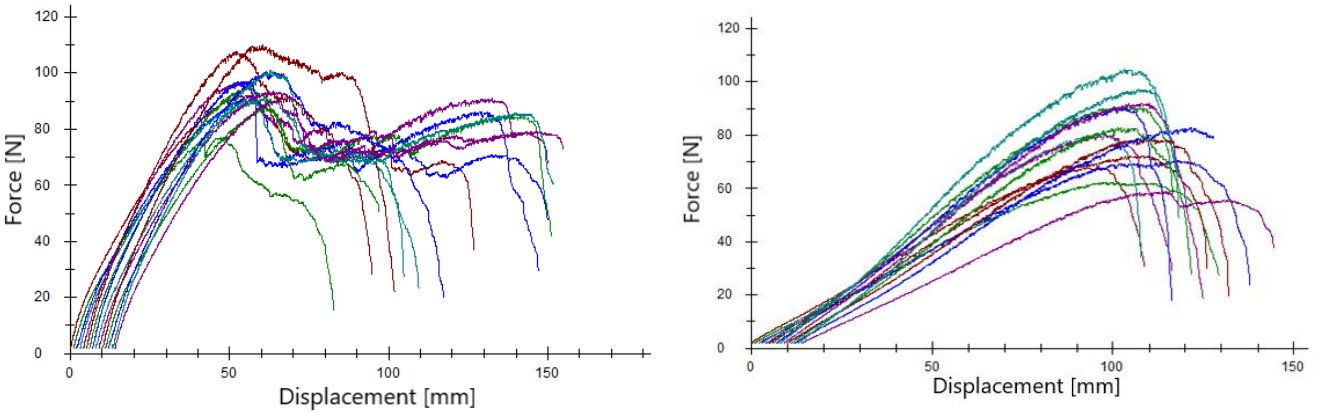

***Figure 2.12**: A) Force displacement curve for longitudinal orientation, B) force displacement curve for transverse orientation. Graphs are shown on different scales*

During the test it is observed that, in the longitudinal orientation, the sample follows these steps:
1. an initial necking of the central area of the sample;
2. the necking increased;
3. the first layer started a delamination;
4. the extremities and the central part of the bandage became thinner;
5. the last resisting layer broke.

For the diagonal orientation at 45° and 135°, the behaviour of the bandage is not always the same, in fact sometime there is a formation of the double layer. The diagonal orientation at 45° has only one peak, while the 135° has two peaks, where the second is near the first one.

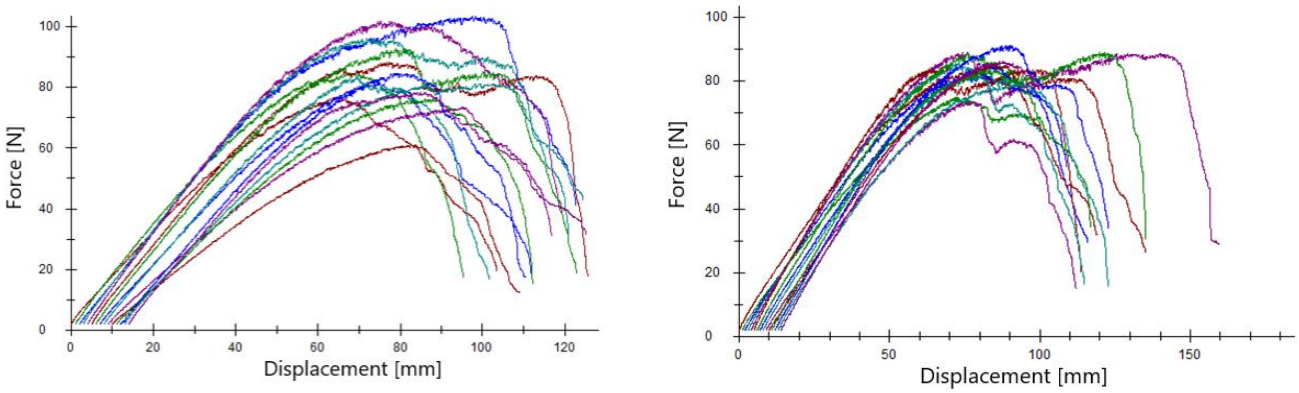

***Figure 2.13**: A) orientation at 45°; B) orientation at 135°. Graphs are shown on different scales.*

The recorded data are analysed by the Excel program.

The first histogram of the *Figure 2.21* shows that the maximum force is higher for the longitudinal direction, lower for the transverse and it is equal for the two diagonal directions. Instead, it is opposite for the elongation at the maximum force, so the material has a higher stiffness in the longitudinal direction than in the transverse.

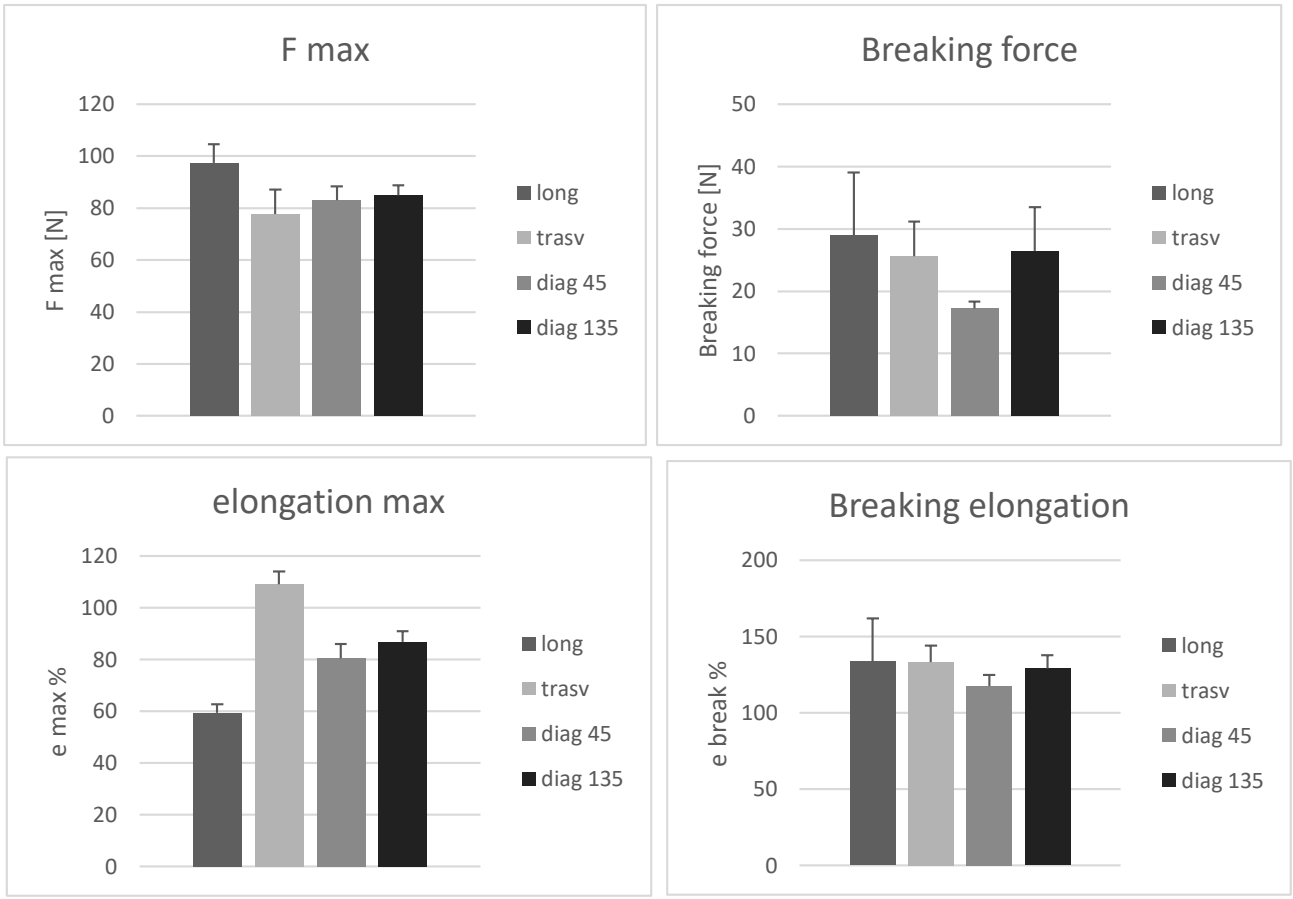

***Figure 2.14**: The four histograms show the comparison between the four orientations*

The dynamic modulus is calculated with the measured values.

***Table 2-4**: The Dinamic modulus for each orientation*

	long	trasv	diag 45	diag 135
Dinamic Modulus	1,64	0,71	1,03	0,98

In longitudinal orientation, the dynamic modulus is 130 % higher than in transverse orientation, 59 % higher than in diagonal at 45°, 67 % higher than in diagonal at 135°. So the dynamic modulus changes with the orientations for the iFix, which is more rigid in the longitudinal than the other orientations.

The shown terms in the *Table 2.2* are:

- SS: sum of differences' square between the four orientations of the iFix.
- DF: degrees of freedom.
- MS: valuation of the variance between the four groups.
- F: the relationship between MS and MSE (variance inside each group).

***Table 2-5**: Results of ANOVA for the tensile test*

ANOVA table	SS	DF	MS	F (DFn, DFd)	P value
F max					
Treatment	2068	3	689,4	F(3,36)=14,69	P<0,0001
Residual	1690	36	46,94		
Total	3758	39			
E% max					
Treatment	10481	3	3494	F(3,36) = 222,1	P<0,0001
Residual	566,4	36	15,73		
Total	11047	39			
Breaking F					
Treatment	781,2	3	260.4	F (3,36) =5,684	P=0,0027
Residual	1649	36	45,81		
Total	2430	39			
E% breaking					
Treatment	1353	3	451	F (3,36) =2,102	P=0,1171
Residual	7725	36	214,6		
Total	9078	39			

This table shows P-values:

- Less than 0,0001 for the maximum force and percentage of elongation, so there is a statistical difference between the four groups.
- Less than 0,05 for the breaking force, so the four groups are statistically different.
- Over 0,05 for the percentage of elongation at break, so for this value the four groups are similar.

To establish which groups are different from the others, the Turkey's test is done. This test compares the different couple of groups, it makes a statistic test, which compares all the combinations of groups' averages. So in the following table are shown: the average of the first group of the couple, the mean of the second, the difference between them, the interval of confidence of the difference and the P value.

***Table 2-6**: Results of Turkey's test for the four groups of iFix's orientations*

Turkey's test	Mean 1	Mean 2	Mean Diff.	95% CI of diff.	Adj. P value
F max					
I-Fix_long vs. I-Fix_tras	97,3	77,7	19,6	11,35 to 27,85	<0,0001
I-Fix_long vs. I-Fix 45°	97,3	82,94	14,36	6,113 to 22,62	0,0002
I-Fix_long vs. I-Fix 135°	97,3	84,89	12,41	4,16 to 20,66	0,0014
I-Fix_tras vs. I-Fix 45°	77,7	82,94	-5,234	-13,49 to 3,018	0,3344
I-Fix_tras vs. I-Fix 135°	77,7	84,89	-7,186	-15,44 to 1,066	0,1066
I-Fix 45° vs. I-Fix 135°	82,94	84,89	-1,952	-10,2 to 6,299	0,9193

E% max					
I-Fix_long vs. I-Fix_tras	50,27	95,72	-45,45	-50,22 to -40,67	<0,0001
I-Fix_long vs. I-Fix 45°	50,27	69,69	-19,42	-24,2 to -14,65	<0,0001
I-Fix_long vs. I-Fix 135°	50,27	75,19	-24,92	-29,7 to -20,14	<0,0001
I-Fix_tras vs. I-Fix 45°	95,72	69,69	26,02	21,25 to 30,8	<0,0001
I-Fix_tras vs. I-Fix 135°	95,72	75,19	20,53	15,75 to 25,31	<0,0001
I-Fix 45° vs. I-Fix 135°	69,69	75,19	-5,495	-10,27 to -0,7173	0,0189
Breaking force					
I-Fix_long vs. I-Fix_tras	28,93	25,6	3,323	-4,829 to 11,48	0,6931
I-Fix_long vs. I-Fix 45°	28,93	17,2	11,73	3,575 to 19,88	0,0024
I-Fix_long vs. I-Fix 135°	28,93	26,5	2,422	-5,73 to 10,57	0,8539
I-Fix_tras vs. I-Fix 45°	25,6	17,2	8,404	0,252 to 16,56	0,0412
I-Fix_tras vs. I-Fix 135°	25,6	26,5	-0,901	-9,053 to 7,251	0,9907
I-Fix 45° vs. I-Fix 135°	17,2	26,5	-9,305	-17,46 to -1,153	0,0200
E% breaking					
I-Fix_long vs. I-Fix_tras	113,2	116,9	-3,697	-21,34 to 13,95	0,9420
I-Fix_long vs. I-Fix 45°	113,2	101,7	11,44	-6,199 to 29,09	0,3152
I-Fix_long vs. I-Fix 135°	113,2	114,4	-1,189	-18,83 to 16,45	0,9978
I-Fix_tras vs. I-Fix 45°	116,9	101,7	15,14	-2,502 to 32,78	0,1143
I-Fix_tras vs. I-Fix 135°	116,9	114,4	2,508	-15,14 to 20,15	0,9806
I-Fix 45° vs. I-Fix 135°	101,7	114,4	-12,63	-30,28 to 5,01	0,2344

The *Table 2.2* as well as *Figure 2.14* shows that:

- About the maximum force, the longitudinal orientation is different than the transverse and the two diagonals. In fact, for the comparison between longitudinal and transverse the P value is less than 0,0001, between the longitudinal and the diagonal at 45° is 0,0002, between longitudinal and 135° is 0,0014. The other comparisons aren't different, so: there isn't difference between the transverse and the diagonal at 45° (P value is 0,3344), between the transverse and the diagonal at 135° (P value is 0,1066), between the two diagonals (P value is 0,9193), which are similar.
- About the breaking force, the diagonal orientation at 45° is different from the other three orientations, so the P values are: between the 45° and the longitudinal 0,0024, between the 45° and the transverse 0,0412, between the 45° and 135° is 0,02. The other comparisons have P values over 0,05: between the longitudinal and the transverse is 0,6931, between the longitudinal and the diagonal at 135° is 0,8539, between the transverse and the diagonal at 135° is 0,9907.
- About the percentage elongation at the maximum force, the P values of all the comparisons are less than 0,05.
- About the percentage elongation at the breaking force, the P values are all over 0,05. Some comparisons have P values near the unity. They are: 0,942 for the transverse vs the longitudinal, 0,9978 for the longitudinal vs 135°, 0,98 for the transverse vs 135°.

2.1.2.3.2 Grab test

For the Grab test two directions are compared only: longitudinal and transverse. The two curves show an initial section, which is linear but has different trend for the two curves. In fact, for the longitudinal this tract finishes at the force of 100 N and at the elongation of 90 mm; for the transversal it finishes

at the force of 120 N and at the elongation of 50 mm; so the last one has a higher trend than the longitudinal. Before the break, the transversal has a section where the trend is zero. In this part the sample starts to break. For the longitudinal, after the maximum force, the sample breaks.

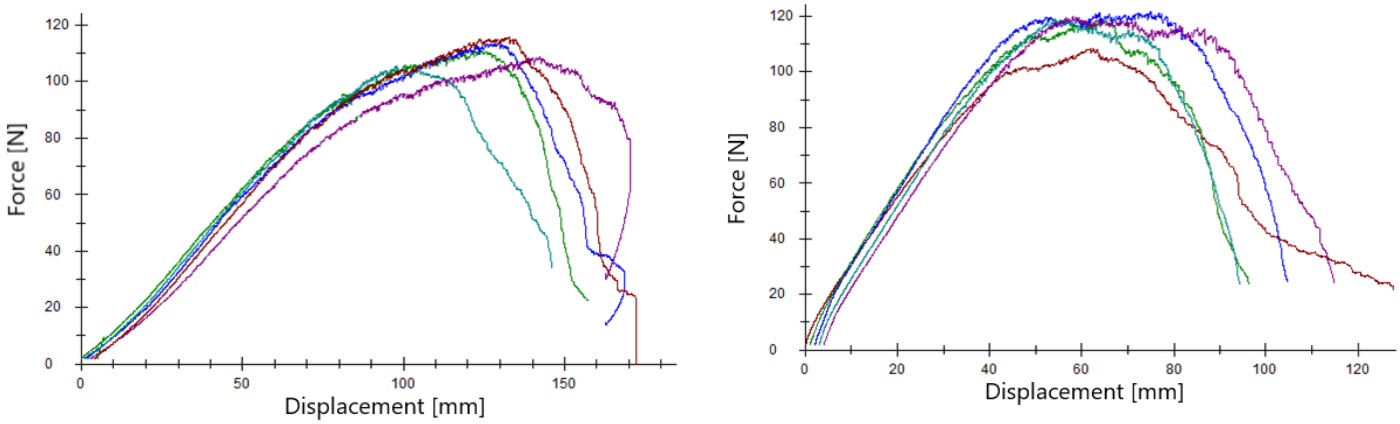

***Figure 2.15**: Force displacement curve for the longitudinal (first figure), for the transverse (second one). Graphs are shown on different scales*

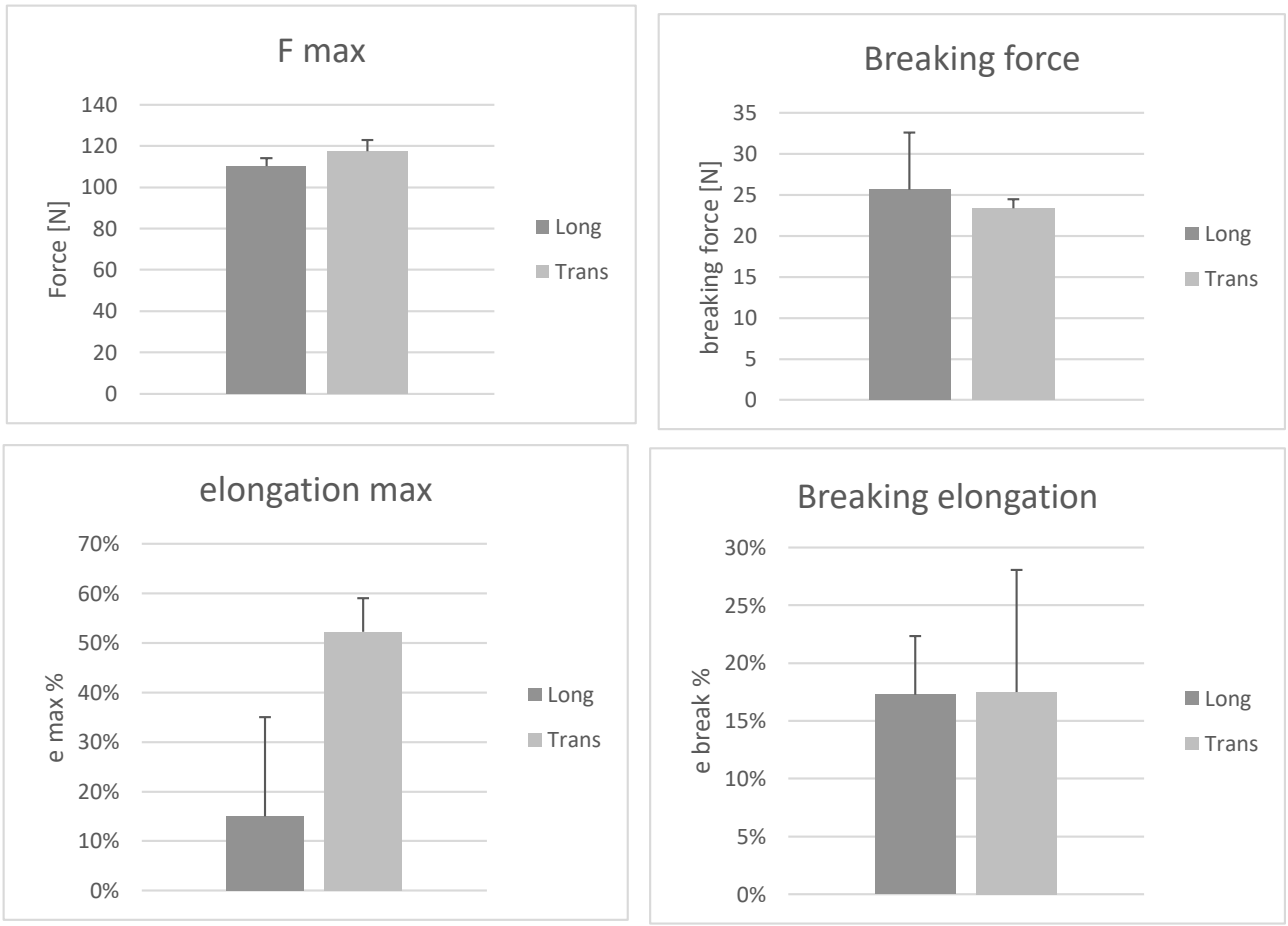

***Figure 2.16**: The four histograms show the comparison between the two orientations*

For the comparison between the two groups, the t test is used. In this case we used the Welch's t test because the variance of these groups are not the same.

The following table shows: P value, the mean of each group, the difference between them and also the confidence's interval of the difference.

***Table 2-7**: Results for the t test*

t test table	P value	Mean 1	Mean 2	Mean Diff.	95% CI of diff.
F max	0,0364	110,1 ± 1,633	117,4 ± 2,365	7,334 ± 2,874	0,6084 to 14,06
E % max	0,0045	15 ± 8,153	52,4 ± 3,043	37,4 ± 8,702	16,38 to 58,42
F break	0,0045	25,64 ± 4,008	23,39 ± 0,4897	-2,247 ± 4,038	-19,15 to 14,65
E % break	0,6325	25,64 ± 4,008	23,39 ± 0,4897	-2,247 ± 4,038	-13,6 to 14,4

This table shows that:

- The P value is less than 0,05 for the maximum force and elongation, and also for the force of break. So the two directions are different for these values, there isn't a similarity between them.
- For the percentage of elongation at break, the directions are similar, in fact the P value is 0,6325.

In *Table 2.7* and *Figure 2.15* the Grab test shows that there isn't statistical difference between longitudinal and transverse direction, when the samples are impregnated in distilled water.

A significant difference (p = 0,0045) is found for the maximum elongation, where the longitudinal had a 71% lower value than the transverse. For the breaking force, a statistical significant difference could be found and *Graph 2.15* shows that longitudinal resists to higher breaking forces than transverse (8,7 % higher).

2.1.2.3.3 Tear resistance test

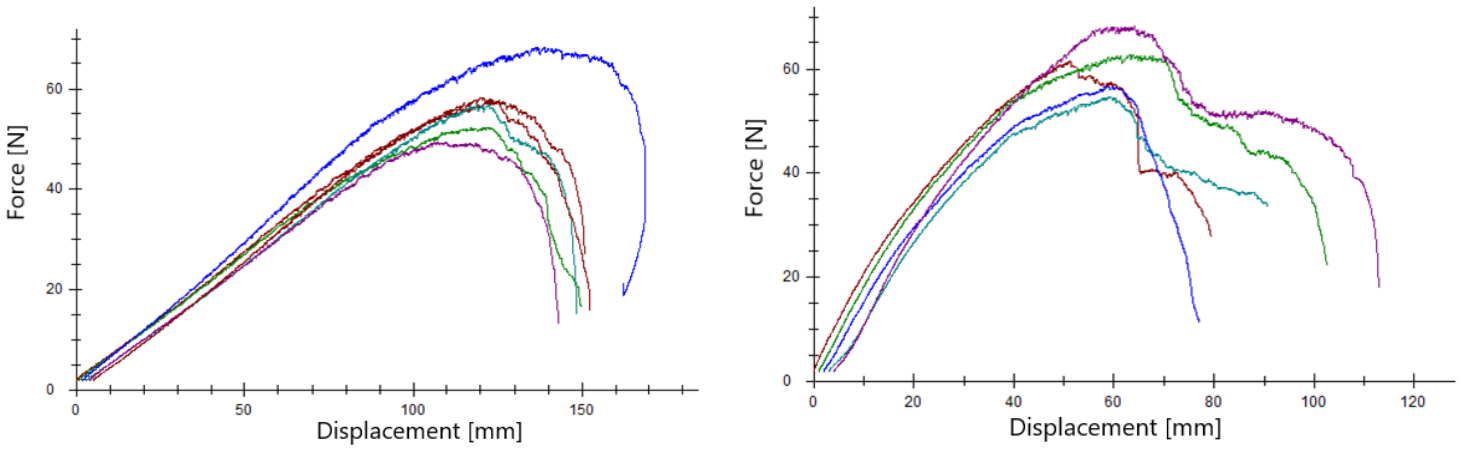

***Figure 2.17**: A) Longitudinal's force displacement curve; B) transverse's force displacement curve. Graphs are shown on different scales*

During the test, it is observed that for the longitudinal orientation the sample broke at one of the two extremities, so the cut seems to be not important for breaking, while for the transverse it broke in the middle, near the cut of 1 cm. The two curves show that behaviour: the longitudinal has only one peak and its first stroke has a lower trend than the transverse, so it is more elastic in this direction. After the peak, the longitudinal breaks. The transverse has another peak because there is the formation of a second layer and so, in a second moment it breaks.

In *Figure 2.18* the histograms show that: the maximum force has similar values, which doesn't reach statistical significance (*Table 2.8* p = 0.1044). Maximum elongation is statistical significant higher for the longitudinal orientation than the transverse (p<0.0001 *Table 2.8*). The two samples break at different forces, the longitudinal has a statistical significant lower value (p = 0,3027 *Table 2.8*) but with a higher elongation than the transverse.

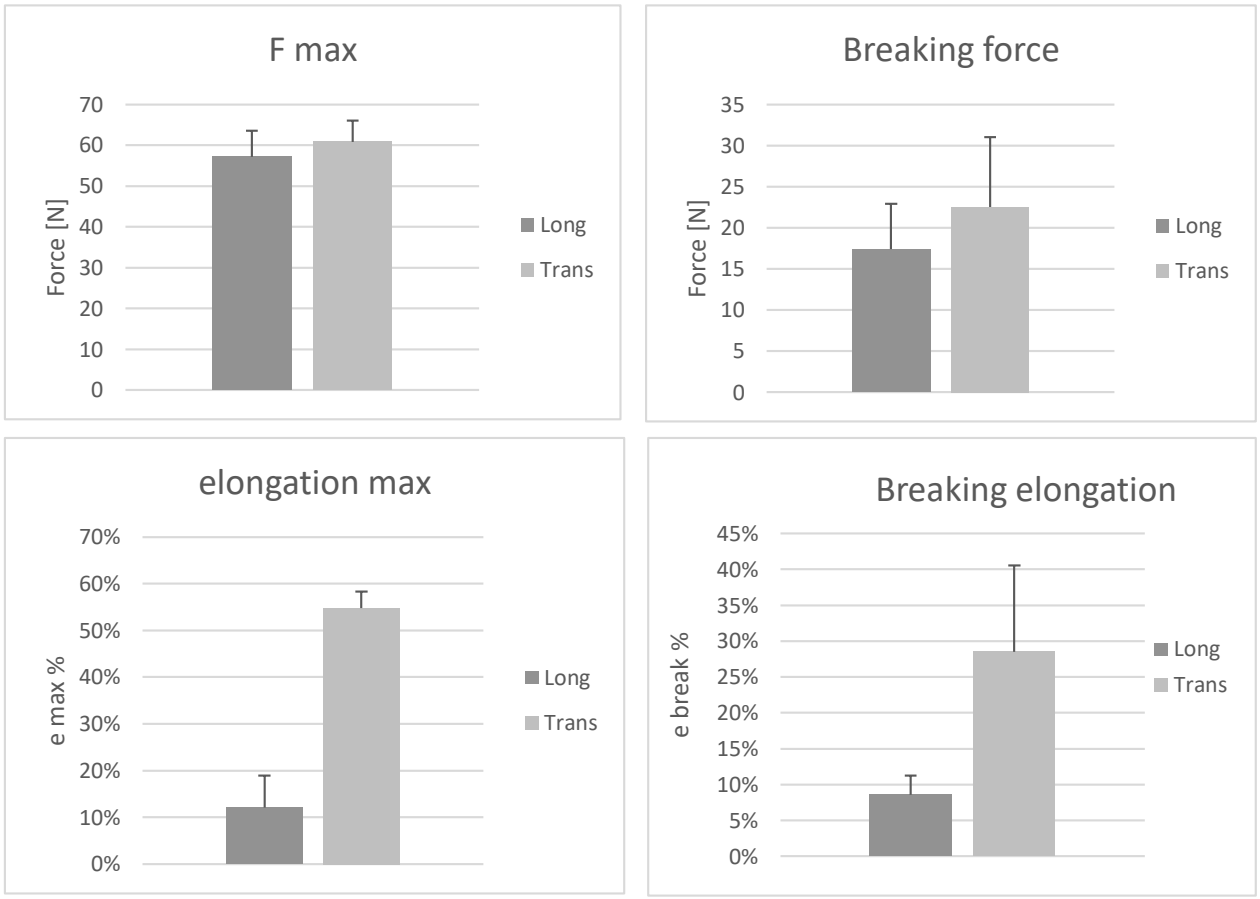

***Figure 2.18**: The four histograms show the comparison between the two orientations*

The following table confirms the consideration made by the observation of the histograms: the two forces are similar for the two directions, in fact the P values are over 0,05; about the percentages of elongation the two directions are different, so the P values are under 0,05.

***Table 2-8**: Results of the t test for the tear resistance*

t test table	P value	Mean 1	Mean 2	Mean Diff.	95% CI of diff.
F max	0,1044	57,11 ± 2,637	60,74 ± 2,37	3,632 ± 3,546	-4,389 to 11,65
e max	<0,0001	12 ± 2,708	57,38 ± 1,858	45,38 ± 3,284	37,88 to 52,88
Breaking force	0,3027	17,42 ± 2,458	22,49 ± 3,825	5,068 ± 4,547	-5,741 to 15,88
e break	0,0181	8,6 ± 1,166	28,6 ± 5,316	20 ± 5,442	5,397 to 34,6

2.1.2.4 Comparison of the mechanical properties of the iFix, Coban and Peha-haft in the longitudinal orientation

2.1.2.4.1 Tensile test

The comparison between the three bandages is done in the same way of that of four directions. First, the force - displacement curves are observed: Coban and Peha-haft show an elastic behaviour; in fact, for low forces they have a high elongation (i.e. Coban with a force of 10 N there is an elongation of 100 mm). After this first tract, the two materials have different trends: for the Coban, until the peak, the slope of the curve increases, and then there is the breakup; for Peha-haft before the breakup the downhill is rich of peaks, which are caused by the breaking of single fibres.

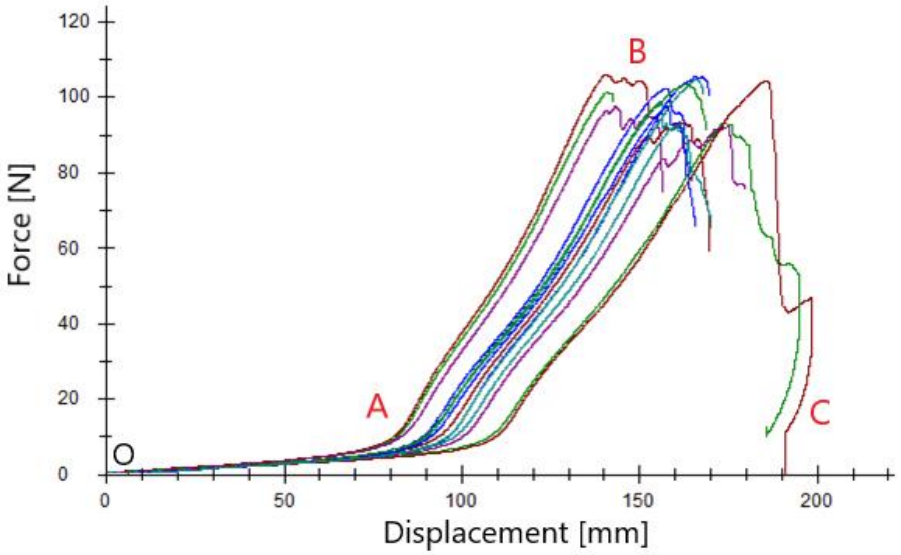

***Figure 2.19**: Force - displacement curve of Coban*

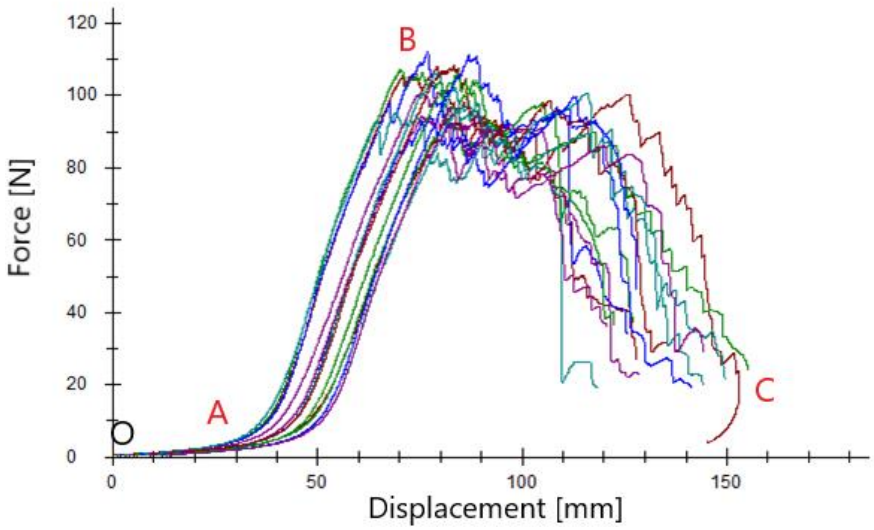

***Figure 2.20**: Force - displacement curve of Peha-haft*

During the test, samples of Coban and Peha-haft don't follow the same steps. For the first one, they are:

1. The sample's length increases with small increments of force (OA);
2. The sample starts to reduce its section (necking) (AB);
3. The sample starts to break, usually near one end (point B);
4. The sample broke (point C).

For the second one:

1. The sample's length increases with small increments of force (OA);
2. The sample starts to reduce its section (necking) (AB);
3. The single wires start to break (point B).
4. The sample broke (point C).

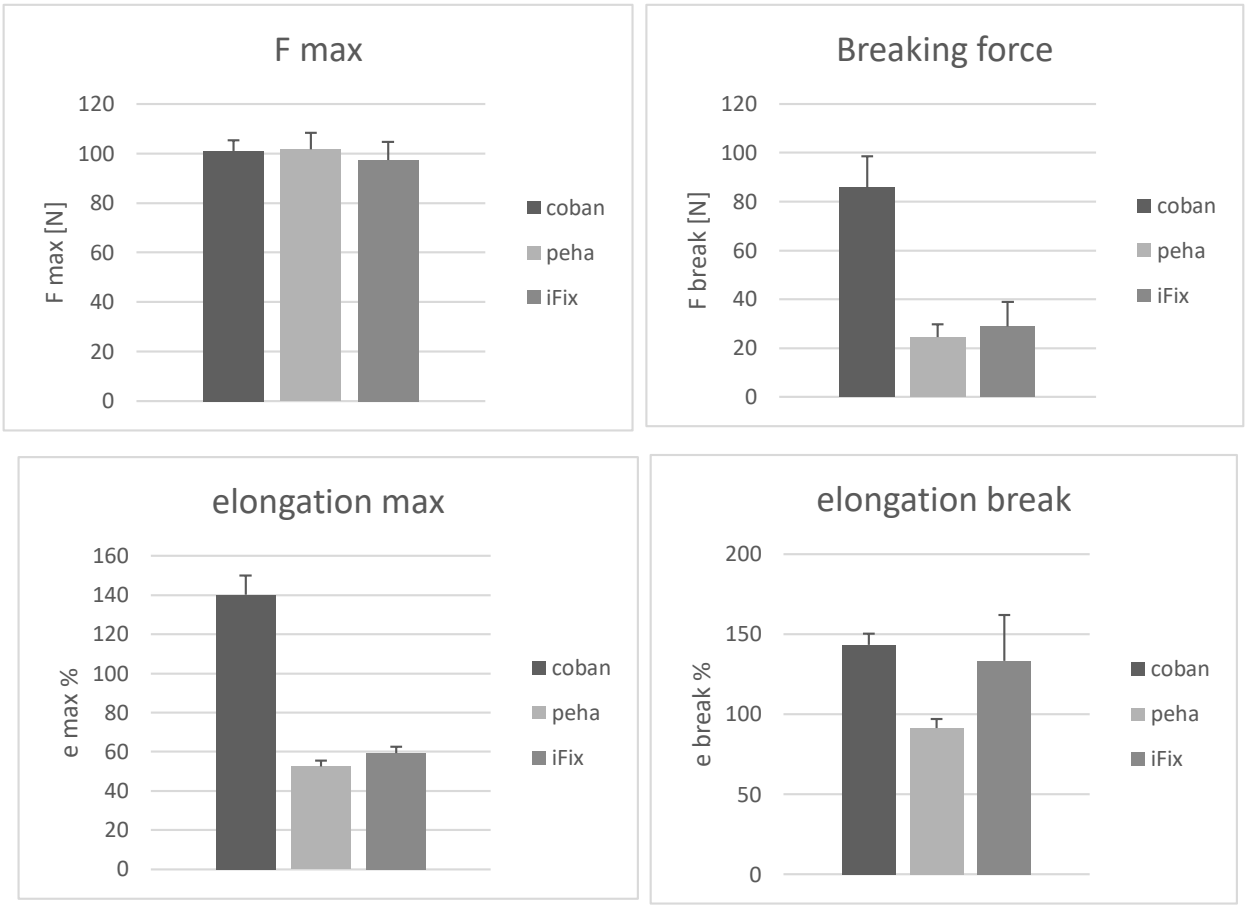

***Figure 2.21**: Histograms of the values of iFix,Coban and Peha-haft in the longitudinal orientation*

With the mean values of the force maximum and the elongation, the dynamic modulus is calculated.

***Table 2-9**: Dinamic modulus for each bandages*

	Coban	**Peha-haft**	**iFix**
Dinamic modulus	0,72	1,94	1,64

Table 2.9 shows that: Peha-haft's dynamic modulus is higher than Coban and iFix. The Coban's dynamic modulus is 63 % lower than the Peha-haft, and the iFix's dynamic modulus is 15 % lower than the Peha-haft. So the Peha-haft and the iFix are more rigid than the Coban, because of their high dynamic modulus.

***Table 2-10**: results test ANOVA*

ANOVA table	SS	DF	MS	F (DFn, DFd)	P value
F max					
Treatment	108,1	2	54,05	F (2, 27) = 1,381	P=0,2684
Residual	1056	27	39,12		
Total	1164	29			
E% max					
Treatment	55412	2	27706	F (2, 27) = 720,9	P<0,0001
Residual	1038	27	38,43		
Total	56449	29			
Breaking force					
Treatment	23319	2	11659	F (3,36) =5,684	P=0,0027
Residual	2644	27	97,91		
Total	25962	29			
E% break					
Treatment	1353	3	451	F (2, 27) = 119,1	P<0,0001
Residual	7725	36	214,6		
Total	9078	39			

Table 2.11 shows the results of the Turkey's test: for the maximum force, the three bandages present values that are not many different (according to the histograms in *Figure 2.21*), they are in the same range (100 N), the maximum peak is in the same range, and between this three bandages there is no difference (only for the maximum force); about the breaking force the Coban bandage is statistical significant different from the other two (same result of the histogram), the p value is less than 0,0001; for the maximum elongation the three bandages are significant (all the p values are less than 0,0001); finally, about the elongation to break, the iFix is similar to the Peha-haft but different from the Coban (that is the same result of the breaking force, and is linked to the process of breaking).

***Table 2-11**: Results of Turkey test for the tensile test (Coba, Peha-haft,iFix)*

Turkey's test	Mean 1	Mean 2	Mean Diff.	95% CI of diff.	Adj. P value
F max					
I-Fix vs. Coban	97,3	101	-3,666	-10,6 to 3,27	0,4017
I-Fix vs. PeHA	97,3	101,6	-4,31	-11,25 to 2,626	0,2884
Coban vs. PeHA	101	101,6	-0,644	-7,58 to 6,292	0,9712
E% max					
I-Fix vs. Coban	50,27	150,9	-100,7	-107,5 to -93,79	<0,0001
I-Fix vs. PeHA	50,27	73,92	-23,65	-30,52 to -16,77	<0,0001
Coban vs. PeHA	150,9	73,92	77,01	70,14 to 83,89	<0,0001
Breaking force					
I-Fix vs. Coban	28,93	85,77	-56,84	-67,82 to -45,87	<0,0001
I-Fix vs. PeHA	28,93	24,57	4,356	-6,616 to 15,33	0,5928
Coban vs. PeHA	85,77	24,57	61,2	50,23 to 72,17	<0,0001
E% break					
I-Fix vs. Coban	113,2	157,3	-44,13	-61,99 to -26,28	<0,0001
I-Fix vs. PeHA	113,2	129,4	-16,23	-34,09 to 1,628	0,0802
Coban vs. PeHA	157,3	129,4	27,9	10,05 to 45,76	0,0017

2.1.2.4.2 Grab test

The two curves have different shapes: for the Coban, the curve has only one peak, which corresponds to the maximum force, while the Peha-haft has a lot of peaks. The feature of the last one is seen also for the tensile test and it is caused by the presence of wires, which break in different moments. The Coban doesn't have the same structure, so it has only one big peak, and sometimes others, when the bandage doesn't break suddenly. The first part of the curves is similar because they are elastic materials, and much different from the iFix, in fact this one has a first stroke, which is linear. The other two have a tract like an exponential curve.

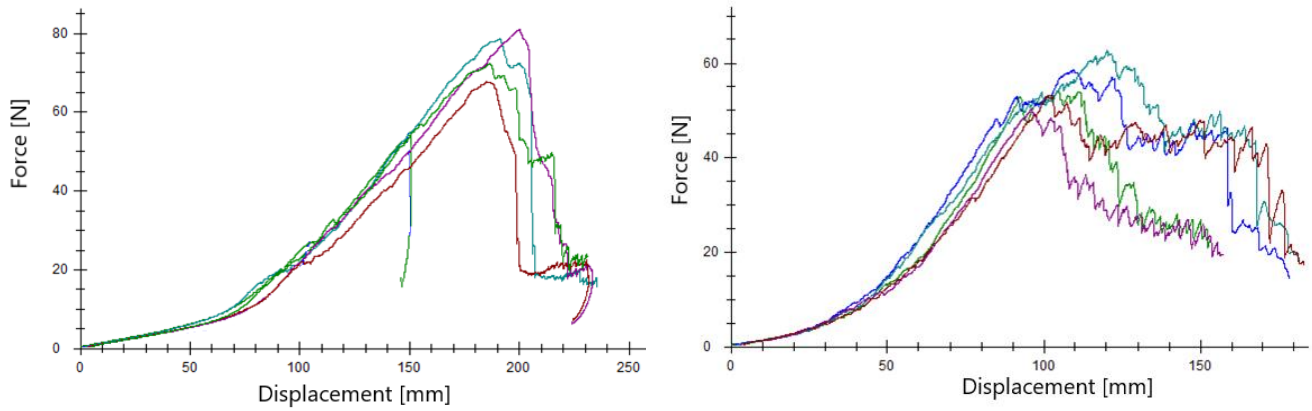

***Figure 2.22**: A) Coban's force displacement curve; B) Peha-haft's force displacement curve. Graphs are shown on different scales*

For the Coban, this stroke is longer than the Peha-haft. The Coban has also a breaking length higher than the Peha-haft: the first one breaks over 200 mm while the second at 180 mm maximum. The same behaviour can be seen also in *Graph 2.23* where the elongation is statistical significant higher for Coban than Peha-haft (p = 0,0116, *Table 2.13*)

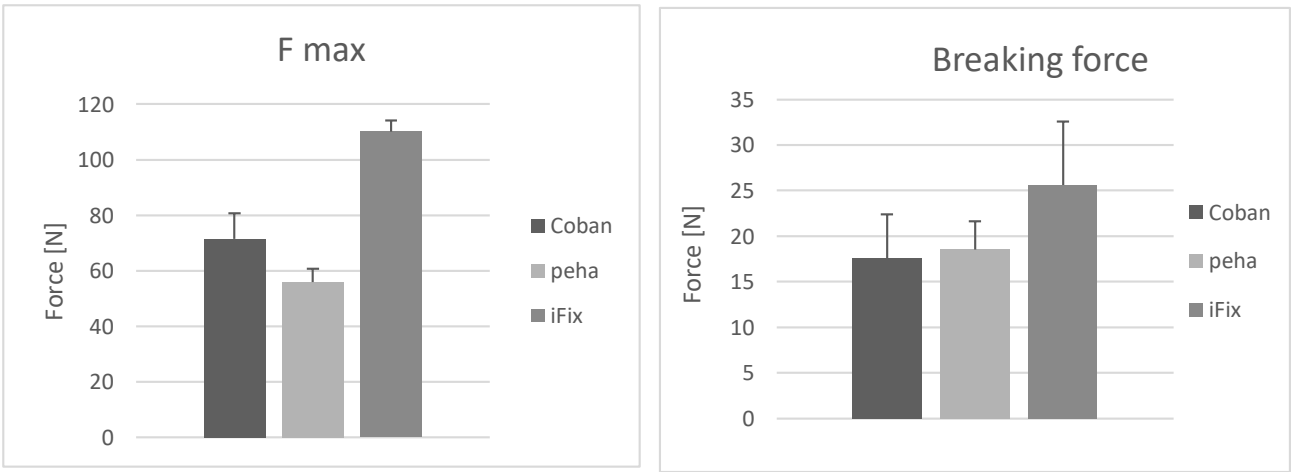

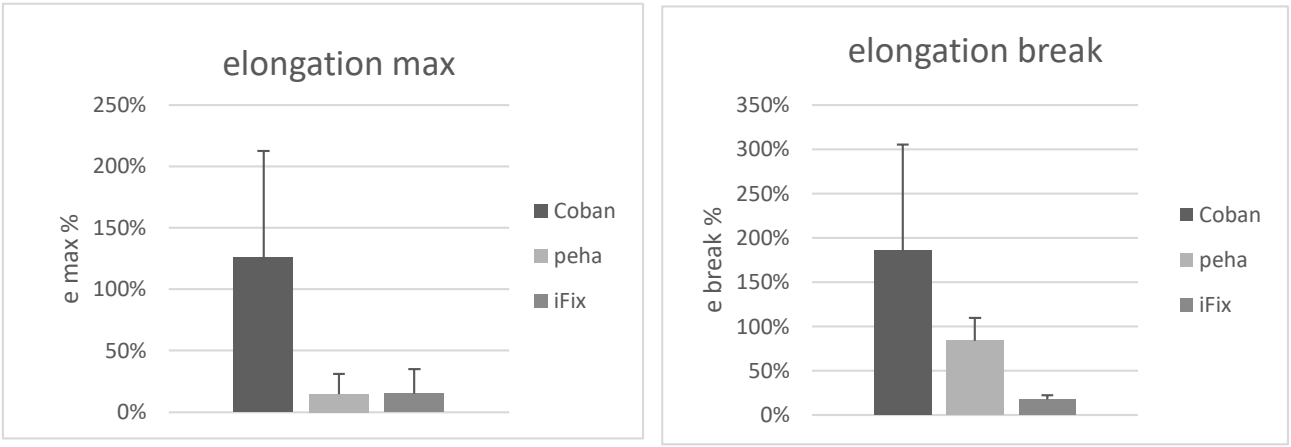

***Figure 2.23**: The four histograms show the comparison between the three bandages*

The four histograms show that: about the forces, the Peha-haft and the Coban have similar values that are different to the iFix, which has higher forces. About the elongations, the Coban reaches high elongations (three times of its initial length), while the iFix has the lower length (over the 50 %).

The different groups are analysed with ANOVA. No difference could be found for the breaking force, while for the maximum force, there is a statistical significance difference between the groups ($p<0,0001$). About the elongation: the maximum and the breaking have a statistical significance difference; in fact, the p value for the maximum is 0,0045, and for the breaking 0,0317. This behaviour is shown also in the histograms (*Figure 2.23*).

***Table 2-12**: results test ANOVA for the Grab test*

ANOVA table	SS	DF	MS	F (DFn, DFd)	P value
F max					
Treatment	8788	2	4394	F (2, 14) = 102,3	P<0,0001
Residual	601,1	14	42,93		
Total	9389	16			
E% max					
Treatment	47626	2	23813	F (2, 14) = 8,135	P=0,0045
Residual	40982	14	2927		
Total	88608	16			
Breaking force					
Treatment	123,7	2	61,83	F (2, 8) = 2,726	P=0,1251
Residual	181,5	8	22,69		
Total	305,1	10			
E% break					
Treatment	43346	2	21673	F (2, 8) = 5,481	P=0,0317
Residual	31636	8	3954		
Total	74982	10			

The ANOVA table shows that only for the breaking force there is a similitude between the bandages.

The Turkey test shows which bandage has significant difference from the others. In this case:

- The maximum force is different for both the bandages. The same behaviour is shown in the histograms; the iFix presents a maximum force, which is higher than the values of the other two bandages.
- The maximum elongation doesn't have a significant difference only for the couple iFix-Coban, which has a p value higher than 0,9999.
- The breaking force is similar for both the bandages. The couple Peha-haft vs Coban presents a p value near the unit; this similarity is clear in the histogram.
- The couple iFix – Peha-haft is the only that is different for the elongation at break, with a p value of 0,0271.

***Table 2-13**: results of Turkey's test*

Turkey's test	Mean 1	Mean 2	Mean Diff.	95% CI of diff.	Adj. P value
F max					
iFix vs. PeHA	110,1	55,89	54,22	43,84 to 64,61	<0,0001
iFix vs. Coban	110,1	71,38	38,73	28,83 to 48,63	<0,0001
PeHA vs. Coban	55,89	71,38	-15,49	-25,88 to -5,109	0,0042
E% max					
I-Fix vs. Coban	15	14,8	0,2	-85,55 to 85,95	>0,9999
I-Fix vs. PeHA	15	125,7	-110,7	-192,4 to -28,91	0,0085
Coban vs. PeHA	14,8	125,7	-110,.9	-196,6 to -25,12	0,0116
F break					
I-Fix vs. Coban	25,64	17,58	8,053	-3,059 to 19,17	0,1576
I-Fix vs. PeHA	25,64	18,5	7,137	-2,803 to 17,08	0,1620
Coban vs. PeHA	17,58	18,5	-0,9167	-10,86 to 9,023	0,9626
E% break					
I-Fix vs. Coban	17	83,6	-66,6	-197,8 to 64,63	0,3626
I-Fix vs. PeHA	17	185,3	-168,3	-315 to -21,62	0,0271
Coban vs. PeHA	83,6	185,3	-101,7	-233 to 29,49	0,1281

2.1.2.4.3 Tear resistance test

During the test, the Coban didn't reach the maximum force, because the tensile machine had a small range of elongation for this test. So it is measured only the maximum force and elongation for the iFix and the Peha-haft. The first stroke of the two curves shows a different behaviour: the Peha-haft starts to break its wires, so it has a lot of peaks at low forces (near 20 N) and its trend is lower than the iFix. This isn't elastic, and at low elongation it has a high force. Only for Peha-haft there is an initial break near the cut.

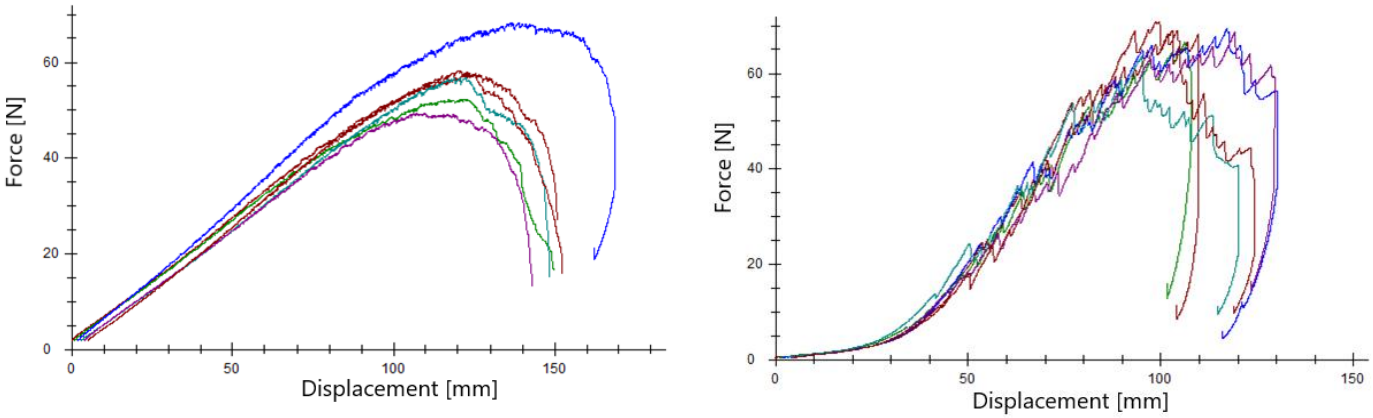

***Figure 2.24**: A) iFix's force displacement curve; B) Peha-haft's force displacement curve. Graphs are shown on different scales*

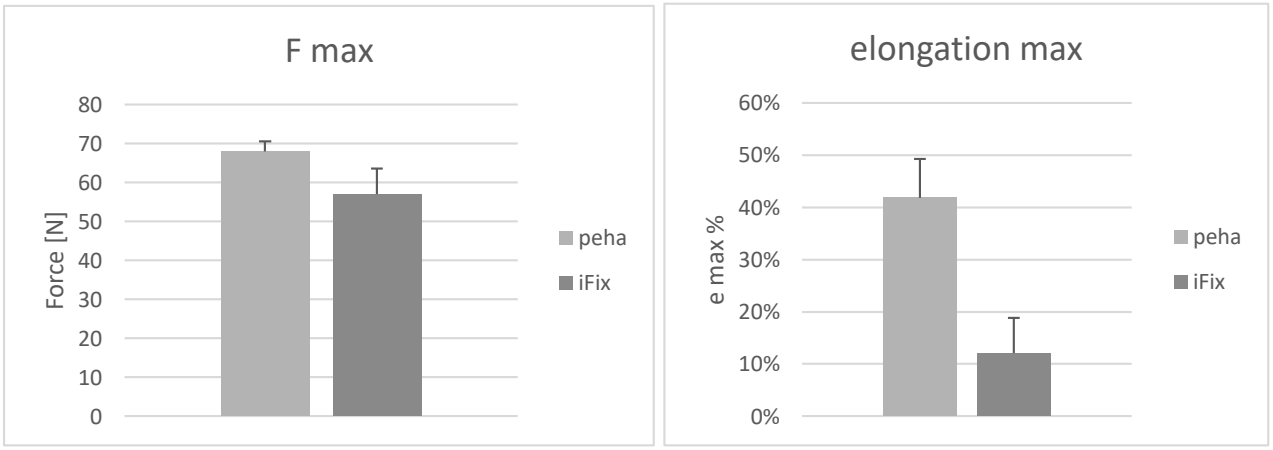

***Figure 2.25**: The two histograms show the comparison only between the Peha-haft and the iFix*

The two histograms show that the Peha-haft has a force and elongation higher than the other bandages: the maximum force is 19 % higher than the iFix, and the elongation is 250 % higher than the iFix. The iFix's values are lower than the Peha-haft, and it is caused by the elastic property of the last one.

***Table 2-14**: Results of the t test for the tear resistance*

t test table	P value	Mean 1	Mean 2	Mean Diff.	95% CI of diff.
F max	0,0073	57,11 ± 2.637	68,01 ± 1,054	10,9 ± 2,89	4,086 to 17,7
e max	<0,0001	12 ± 2,708	41,83 ± 3,016	20,79 ± 4,053	20,79 to 38,88

The t test shows that this two bandages have a statistical significant difference for the maximum force and elongation: for the second one the difference is more significant (less than 0,0001); the same behaviour is shown by the histogram.

2.1.2.4.4 Adhesive test

In the material and method section, it is told that this kind of test is qualitative.

During the test, it was observed that the samples followed two behaviours:

- If the adhesion was good, the maximum force was near 100 N and after the break the sample stretched for a force of 70 N;
- If some part was not well fixed, the maximum force was near 30 N or less and suddenly it broke.

This particular behaviour was explained right after. In fact, it was told from the factory that made iFix, that this particular bandage shows different properties for each of its sides, so the test was lead with not considering this.

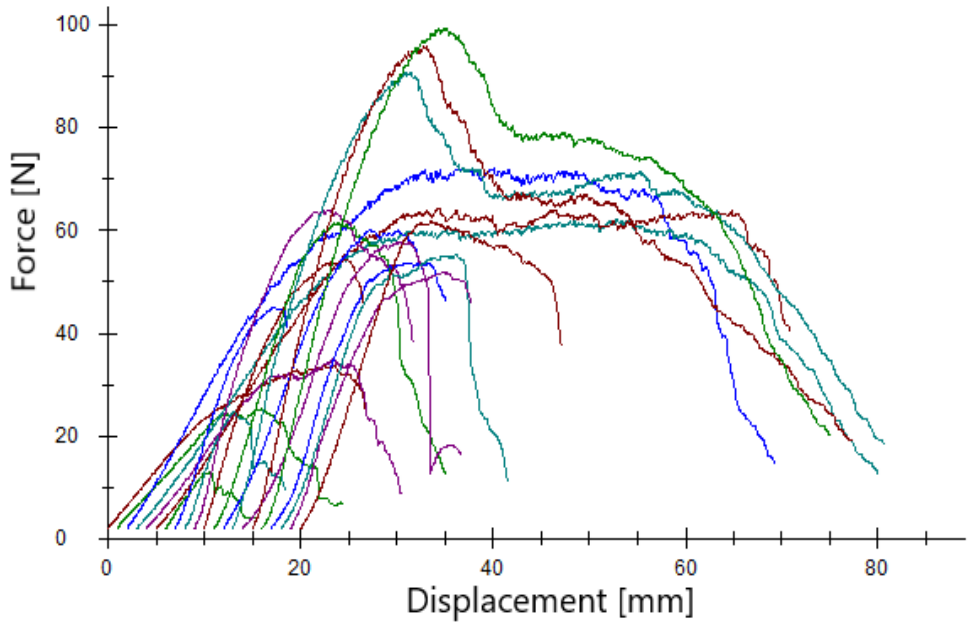

***Figure 2.26**: Force displacement curve for the adhesive test*

So it is possible to determine the interval of adhesion for:

- The maximum force: from 13,04 N to 99,34 N.
- The maximum elongation: from -95 % to -43 %.
- The force at break: from 3.79 N to 51.83 N.
- The elongation at break: from 11 % to 89 %.

From those data, it is possible to say that a good adhesion is given for kind of forces like the ones obtained in the tensile test for fleece sample.

The following histograms report the averages for the four measured values with the standard deviations, which are very high for the motivations explained before.

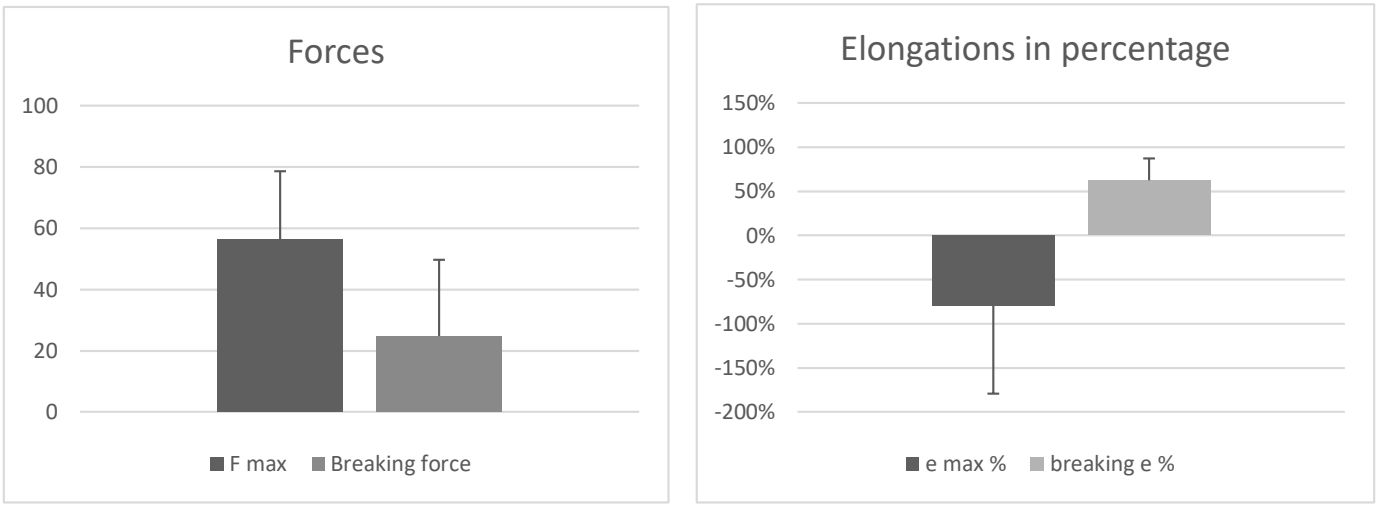

***Figure 2.27**: Histograms for the adhesive test*

The histograms show lower values than those obtained with the tensile test of the iFix. The maximum force is 44 % lower and the breaking force is 20 % lower than that of iFix in the tensile test. Also the elongations changes, that is caused by the presence of two materials. The breaking elongation is 54 % lower than that of the iFix in the tensile test. This behaviour could be caused by the force of adhesion between the two materials.

2.2 Discussion

In this chapter, the mechanical properties of the iFix bandage are measured and compared with other two bandages: the Coban and the Peha-haft. These two are the most used, in particular the Coban is used in the operation room because it is sterile.
The analysis began with the SEM imaging, which is a method to investigate the material's structure. The iFix showed a different conformation between the Coban and Peha-haft. These two are similar; they present curly fibres in the transverse and longitudinal orientation. This is important for their mechanical behaviour, in fact, their wires provide elastic properties to the material. Instead, the iFix has straight fibres in all the directions, that are melted together in regular points. These points are as nodes, they give rigidity and they are gripping points for the adhesion between the patch and the fleece iFix. Indeed, this behaviour could be observed also in the mechanical tests showing a higher/lower elasticity than the other two, also under wet conditions (grab test).
The straight wires are predominant in the longitudinal directions, so the structure is anisotropic. This behaviour is clear in the mechanical tests. The material shows higher forces (maximum and breaking) in the longitudinal orientations than the others, and for wet samples the longitudinal orientation shows a higher maximum force, but the breaking force becomes similar to the transverse. The sample has the same elongation at breaking point for all the orientations, though has a different maximum elongation, which is higher for the transverse.
The material changes its mechanical properties if there is a cut on the surface: the two forces become similar for the two orientations (longitudinal and transverse), but the elongations are different.

Observing the test, the samples haven't the same behaviour: the transverse starts to break near the cut, while the longitudinal behaves as if there it isn't.
The iFix's structure doesn't show an elastic behaviour of the material, because its curve force – displacement doesn't show an initial tract where for low forces there is high displacement. The results of tensile test evidenced that the forces of all these materials are similar. So the iFix is able to resist at the same force, but its rigidity prevents it to have the same elongation. If the literature's data are considered, they show different values compared to those measured: in literature the Peha-haft could have a percentage of elongation of 85 %, which is specified if it refers to the maximum force or to the breaking force. For the Peha-haft the two measured percentage are 52 % (maximum force) and 91 % (breaking force). The data, referred to the iFix, shows a maximum force of 120 N, while the measured force is 97 N. With the measured values (from the tensile test) it is possible to classify the three bandages; in *Paragraph 2.1.1* three classification are shown, and the first one is used because it considered data that are obtained in vitro. According to the standard DIN 61632, the iFix for the longitudinal and the two diagonal orientations is Short Stretch, but for the transverse it is Long Stretch; the Peha-haft is Short Stretch; the Coban is Long Stretch. Instead, if it is considered the dynamic modulus, all the bandages are classified as Short Stretch because their modulus are over 0,3 but less than 30, so all the bandages aren't rigid, but there isn't a distinction between the Coban (which is more elastic than the others) and the other two bandages.
The features of Peha-haft and Coban change if they are wet: in this case the maximum force for all the materials are different, though it is the opposite for the breaking force. This happens also if there is a cut on the sample: the maximum force and elongation aren't similar for these materials. In fact, the Peha-haft starts to break its fibres near the cut, but this process needs time and high forces; the iFix (in the longitudinal directions) breaks near one of the extremities.
The measured data suggest that the iFix system could be the best of these three bandages to be used. This consideration is given by the mechanical properties of the bandages in the tests; in fact, the iFix didn't change its properties in wet condition and also in presence of cuts. Besides the tensile test's results suggest that the iFix is more rigid than the other two bandages: this behaviour could give a stable fixation of the patient on the operative table, but also it could generate high compression on the human body.

Chapter 3

3 Measurement of the pressure under bandage

The aim of this chapter is to describe how to estimate the pressure under a bandage, applied on human body. So this initial chapter describes the mathematical model to estimate this pressure, the commercial sensors and their properties.

3.1. Bandage pressure and stiffness measurement

3.1.1. Mathematical Model to Estimate the Sub-Bandage Interface Pressure

In order to design effective compression systems, to improve practice and help nurses to achieve the optimum pressure gradient, many researchers attempted to describe or to predict the interface pressure theoretically[42]. Thomas [49] used Laplace's law, which sets out that the pressure (P in N/m^2) of a compression applied onto a skin surface is proportional to the tension (T in N/m) of the compression material and inversely proportional to the radius of curvature (R in m) of a limb surface to which it is applied:

$$P \propto (T/R)$$

In clinical practice, the used bandage is multilayers, so Thomas [49] extended his model for multilayer bandage:

$$P = \frac{nT}{Rw}$$

Where *n* is the number of bandage layers and *w* is the bandage width in meters.
The problem of this relation is that it doesn't regard the increase of the radius caused by additional layers of the bandage. Al Khaburi[39] derived two mathematical expressions to calculate the interface pressure applied by multi-layer bandage to a limb with known radii of curvature.
The first one is:

$$P_n = \sum_{i=1}^{n} \frac{2T_i}{w_i D_i} \times 0{,}0075$$

The second is:

$$P_n = \sum_{i=1}^{n} \frac{T_i(D_i + t_i)}{0{,}5 \times w_i D_i^2 + w_i t_i (D_i + t_i)} \times 0{,}0075$$

Where $D_i = D + \sum_{i=1}^{n} 2t_{i-1}$
Where *i* is the bandage layer, t_i is the thickness of extended and compressed bandage layer in meter, T_i is the tension in Newton, w_i is the extended bandage width in meter, *D* is the limb diameter in meter, D_i is the combined limb diameter and previous bandage layers thickness in meter, and P_n is the pressure induced by *n* number of bandage layers in mmHg.
In his work Al Khaburi [50] compared this two models and the Thomas' equation. He found that the predict pressures of the two models were similar to the pressure measured by the FlexiForce sensor; this didn't agree with the mathematical model proposed by Thomas.

3.1.1 Measured pressure

To measure the level of pressure, several methods exist. Interface pressure is exerted by the device, which, in clinical practice, is the limb of skin under the compression device [51].

A group of medical experts and representatives from the industry formulated a paper in January 2005[52], with the aim to provide methods for measuring the interface pressure and for assessing the stiffness of a compression device in an individual patient. The stiffness is defined by the increasing of compression per centimetre in the circumference of the leg. This parameter characterizes the compliance of textile, which has an important role for the performance of the compression device. To quantify the pressure under a bandage, there is a variety of different transducers. The ideal measurement system, defined by these experts, should satisfy some specifications[52]:

- be thin (< 0,5 mm) and flexible;
- Its sensitive area should be optimized for different applications;
- be able to be in contact with the skin without skin irritation;
- be easy to calibrate;
- have a computer for measurements with high signal sampling rate;
- be low cost;
- have low hysteresis;
- be insensitive to force concentrations;
- be insensitive to bending;
- be durable;
- have a simple electronics;
- be reliable;
- be insensitive to temperature and humidity change;
- have linear response to applied pressure;
- have an operative range consistent with biological parameters
- be accurate;
- have a resolution time less than 0,1 s and amplitude less than 0,1 mmHg.

The type sensors used are: pneumatic, pneumatic-electric or pneumatic-piezoelectric; fluid-filled-resistive; resistive and strain gauge; capacitive.

3.1.2.1. Pneumatic pressure measurement system

This system is the most common type of pressure transducer; it uses air to transfer the forces applied by air compression. This force is converted in an electrical signal by electrical or piezoelectrical pressure transducers. The features of this system are: it has thin and flexible probes and it is cheap, easy and handy. However, its limitations are that it is sensitive for temperature and hysteresis.
In the following points a rundown of the pneumatic pressure measurement transducers is reported:

- *PicoPress*® (Microlab Electronica, Ponte S. Nicolo PD, Italy)(*Figure 3.1*[53]) is the best commercial transducers because of its high accuracy and precision. It is a portable digital device that can measures the pressure of a bandage. This device uses a thin (200 μm) circular sensor made by a biocompatible material, in which there is a known volume of air. The felt pressure is measured by a digital manometer and shown by a display. The PicoPress device incorporates a micro pump that works when the air flows in the sensor. Its features are: range from 0 to 189 mmHg, precision of ± 3 mmHg and maximum admissible pressure of 300 mmHg. The precision gets worse if the temperature is out of the range from 10 ºC to 30 ºC. In a study made by Rimaud et al.[51], they measured the pressure of a bandage with the patient in three positions: supine, sitting and standing. They used a PicoPress system and positioned three sensors at three reference points.

***Figure 3.1**: PicoPress system*[52]

***Figure 3.2**: Position of the sensors in the study made by D. Rimaud*[46]

- *Kikuhime*® (Meditrade, Soro, Denmark) (*Figure 3.3*) is a portable transducer, its sensors work with air filled flexible probe which is connected to the transducer. The sensor consists of an air-filled flexible probe which is connected to a pressure transducer. The probe is small and flexible, under filled conditions this is thicker than 5 mm. Pressure is shown at the screen, and continuous dynamic measurements are not possible.
  Partsch [54] measured linearity, variability and accuracy for this system in vivo (on a human leg, applied to the distal lower leg B1 point, where there is the transition of the muscular part into the tendinous part) and in vitro (fixed on a rigid cylinder). About linearity (between the pressure measured by sphygmomanometer and the device) the correlation coefficients revealed a Pearson $r > 0{,}99$. The variation coefficients showed acceptable values in the range between 20 and 40 mmHg interface pressure. This device showed a high variation in the low pressure range (< 20 mmHg). The accuracy is the maximal deviation for each pressure level from the reference, the Kikuhime overestimated the true values in the range between 10 and 70 mmHg.

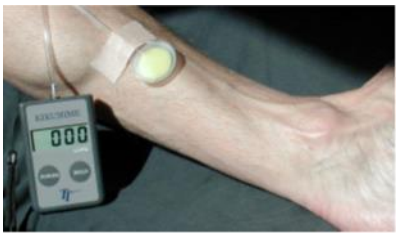

***Figure 3.3**: Position of the sensor in the study made by Kikuhime[53]*

- *The Sigvaris Interface-Pressure Gauge Advanced Tester* (*SIGaT* ®) is a pneumatic transducer, which is composed by a 7,5x5 cm wide plastic bladder and a pressure evaluation unit, connected by plastic tubes. The air is injected into the system by an external syringe; this causes a linear increase of pressure which tends to flatten as soon as the compression device is lifted by the filling bladder. Pressure changes are registered by a special software. Partsch [54] measured the variability in the range between 20 and 40 mmHg interface pressure, above 40 mmHg this device had high variation, it was accurate in the pressure region around 40 mmHg. Gaied et al.[55] used this device for measuring the mechanical compression stocking, they calibrated the sensors by immerging them into a water container at a known depth. They had an apparatus with an electric circuit that detected the pressure's change. (*Figure 3.4*)

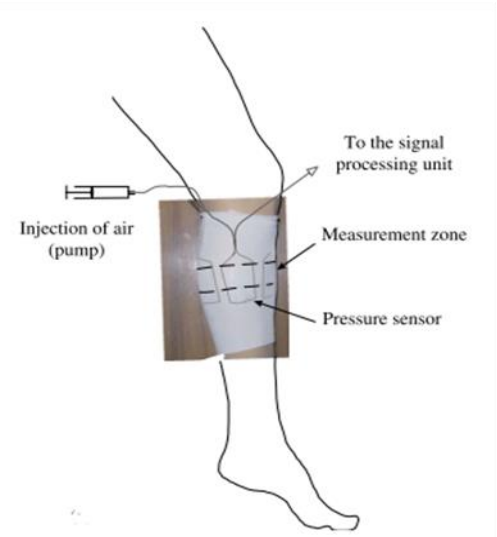

***Figure 3.4**: SIGAT system[54]*

3.1.2.2. Fluid – filled resistive pressure measurement system

This pressure measurement system uses oil or water to transfer the forces applied by compression products to a pressure that is converted to an electrical signal using electrical or piezo electrical transducers. These transducers are flexible, and they can do dynamic measurements; they have the limitation of becoming thick when they are filled, besides they have problems during motion. In the following few paragraphs some of them are summarized:

- *Strathclyde Pressure Monitor* (University of Strathclyde, Scotland), it is developed by Barbenel and Sockalingham[56]. The system is composed by PVC probes, the dimensions of which are 14 mm in diameter and 1,5 mm in thickness. The probes are filled with vegetable oil connected to a nylon casing, where it is located a piezo-resistive pressure transducer. This is connected to a processing circuit and a LCD screen to display the output. The system is tested using a water column for the pressure range of 0 – 37 mmHg, it has a linearity error, hysteresis error and drift for values less than 0,23 mmHg.

- *FlexiForce*® (Tekscan, South Boston, MA, USA) sensors are ultra-thin (0,203 mm) and flexible, they are composed by two layers of substrate film with silver conductive material applied over the substrates and a layer of pressure sensitive link (*Figure 3.6*[57]). The strength of the sensor decreases when a force is applied to the sensitive area, while the conductance increases. The sensor can be used with the lowest range of force 0 – 4,4 N, and so it can measure pressures of 0 – 57,7 kN/m^2. The sensor has a nonlinearity error of 8.07 ± 1,62 %FS, where the sensor FS is defined as 14,1 kN/m^2. Al Khaburi et al.[50] studied a system to map the pressure applied by compression at multiple points. They used a pressure-mapping mannequin leg embedded with force sensors for the preliminary experimental validation. Before the measure, they calibrated the system using an aneroid sphygmomanometer for the pressure range 0−16 kN/m^2 (0−120 mmHg). The calibration was carried out on a cylinder with 0,114 m in diameter. The aneroid sphygmomanometer cuff was inflated by 1,3 kN/m^2 (10 mmHg) increments from 0 kN/m^2 to 16 kN/m^2 and then deflated by 1,3 kN/m^2 decrements to 0 kN/m^2. The process was replicated ten times for each sensor. After the measures, the system was connected to the program LabView 8.6 to recorde the signals, display them, and convert them to pressure values using calibration fitting lines.

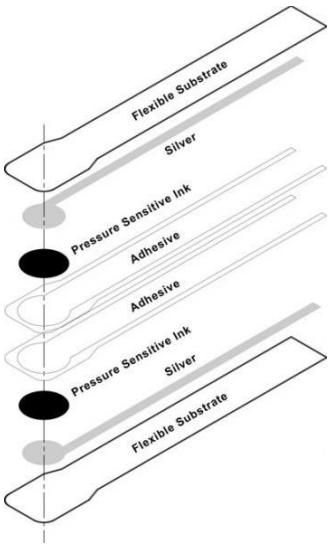

***Figure 3.5**: composition FlexiForce sensor[56]*

***Figure 3.6**: mapping system with multiple sensors[49]*

3.1.2.3. <u>Resistive and strain gauge pressure measurement system</u>

The principle of this system is based on the strength's change of a special piezo resistive layer when a force or a pressure is applied. Every commercial sensor has its own technology; the most common technology uses two thin flexible polymer sheets with a deposited or printed conductive film. This is

applied to one sheet or to both sheets. A special ink (sensitive to pressure and semi conductive) is put between the sheets. Generally, the resistance decreases with increasing force, though it is also possible that the resistivity of a polymer matrix-conductive filler composite decreases [39]. Some examples:

- *Force Sensing resistor* (FSR®) (Interlink Electronics, Camarillo, USA) is a device with a polymer film. The sensor's minimum dimensions are: 0,3 mm for thickness, 7,6 mm for diameter and 5 mm for active diameter. The sensor's pressure sensitivity range is 1 – 100 N.

- *FSA* (Vista Medical Ltd., Manitoba, Canada) is a piezo-resistive semi conductive polymer sandwiched between two layers of highly conductive rip stop nylon fabric. The conductive polymer is placed between the conductive layers which, according to the manufacturer, allow comfortability of the compound over curved surfaces. Some of the arrays sensing systems developed by Vista Medical Ltd are for the pressure range of 0 – 100 mmHg. However, the mentioned systems are about 4 mm thick.

- *Fontanometer* (Gaeltec Ltd, Dunvegan, Isle of Skye, Scotland). Its dimensions are 12,6 mm diameter and 3 mm thick. It has a sensor with a metal diaphragm with deposited resistive strain gauges directly. The metal diaphragm is made with a metal plate which is between two air pockets with the same pressure; when a pressure is applied in the upper air pocket, there is a strain in the metal plate and a change in the resistance of the strain gauge. The nominal resistance is 1,5 kΩ, the linear pressure range is 0 – 100 mmHg, the sensitivity is 5μV/V/mmHg, the linearity and hysteresis error is lower than ± 1% FS.

3.1.2.4. Capacitive pressure measurement system

The capacitive method is based on the principle that capacity between two parallel plates changes when a force or a pressure is applied. The plates are placed on a non-conducting elastomer sheet, and this moves closer when pressure is applied.
The capacity of flat capacitor with parallel faces is:

$$C = S \times {}^{\varepsilon}/_{d}$$

Where S is the capacitor's surface, d is the distance between the two plates and ε is the permittivity of the dielectric[58].

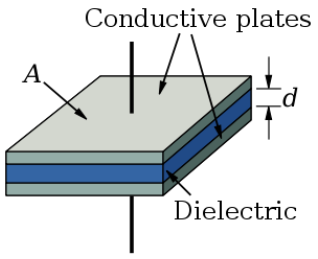

***Figure 3.7**: Capacitor*[57]

This system has the advantage to be less sensitive to temperature and humidity. The capacitive measurement gives a lower output value than the resistive one, because the output is the average

pressure over the sensing area[59]. The capacitive sensors use a similar three layers' structure. The conductive rows and columns enclose the pressure-sensing layer. The sensing layer is a non-conducting elastomer with high dielectric constant. The measured capacitance, that changes, is generally in the order of pF or even lower, so this makes it crucial to use highly sensitive, precise and stable read-out electronics.
Some of these sensors are:

- *Xsensor* (Crown Therapeutics, Belleville, IL, USA)[60] is made up of two grids of parallel conductive stripes separated by a thin compressible elastomer layer. The sensors are only in matrix form as pad, the smallest one has the dimensions of 2,50 - 120 -1 mm. The pad has 2500 sensing element points, with three pressure calibration ranges: 5-50 mmHg, 5-100 mmHg and 10-200 mmHg. This sensor architecture and construction method have two distinct advantages. First, the used materials and the way they are assembled, create a very pliable and conformable sensor pad. This minimizes any distortion of the true interface pressure by the presence of the sensor pad. Second, the sensor pad is extremely hard. Fergenbaum et al.[61] compared this sensor with the FSA system, and results showed that XSENSOR® had better accuracy compared to the FSA, since the XSENSOR® measured a force that was 64% of the peak force applied to the sensor; whereas the FSA measure a force that was 49% of the actual applied force. The XSENSOR® has a low coefficient of variation.

- *Novel sensors* (Novel GmbH, Munich, Germany) are constructed as a closed condenser with an elastic dielectric. The capacity of the sensor changes when the dielectric modifies its geometry; the operative force over the area of the sensor results as pressure. There is also an electronic circuit, which converts the capacity into electrical voltage: a change of external force causes a change in the sensor capacity and so the output voltage. The resulting voltage can be shown on the computer. This kind of sensor is flexible, it is 1 mm in height but with coating material, it becomes 1,6 mm. The Novel technology is currently used for external measurements such as pressure distribution under the foot. Rikli et al.[62] used this technology to define the amount and distribution of forces transmitted across the human radioulnocarpal joint under physiologic conditions in vivo. They adapted the device for intra-articular pressure measurement: to determine the shape in vivo, anatomic studies on cadavers are performed. They applied five different values of force; between 29,6 N and 149,5 N, they validated the sensor: about the hysteresis it did not exceed 7%, about the temperature, the values decreased with increasing temperature by -0,06 N/°C, about the sterilization, the calibration curve of the sensor was the same before and after gas sterilization. The results showed that the sensor's physical characteristics are appropriated. Compared with the gold standard in the field (by Fujifilm), this technology has some advantages: data are quantitative, static and dynamic measurements can be performed, the sensor doesn't damage the joint, the device is multiusable and the data can be digitalized.

***Figure 3.8**: s2011 single sensor[61]*

It is clear that any system doesn't satisfy the features of the ideal measurement technology. Nonetheless some of the new measurements have great potential, like PicoPress. Though, it has a problem of reliability, because it changes its thickness the bandage. The capacitive sensors are less effected by systematic errors but they are more expensive and their thickness is over 0,5 mm; nevertheless, the resistive sensors are cheap and thin but their systematic error are very large.

3.1.3. Sites of Pressure Measurement Under a Compression Device

The pressure device is positioned between the skin and the bandage, but the specific location of the sensor is matter of controversy. The main guideline is to not measure pressure over bony prominences or tendons because the hardness of the structure can influence the measurement. We must consider the curvature of the leg at the position of the sensor and how circumference changes during movement.
It is recommended that the identification of anatomical locations, described in the European document on standardization, is used to define the position upon the leg, along with recording the exact position of each sensor[52].

- B: ankle at point of minimum girth.
- B1: area at which the Achilles tendon changes into the calf muscles (*B*10–15 cm proximal to the medial malleolus).
- C: calf at its maximum girth.
- D: just below the tibial tuberosity.
- E: centre of the patella and over the back of the knee.
- F: between K and E (mid-thigh, between patella and groin).
- G: 5 cm below the centre point of the crotch.
- H: greatest lateral trochanteric projections of the buttock.
- K: centre point of the crotch.

Chapter 4

4 Sensors' Properties

This chapter describes the characteristics of the Pedar sensor, which is selected to measure the pressure under a bandage during a knee, hip, shoulder, or elbow arthroplasty. The measurements are done in a static way, in fact, during the operation the patients are still and the surgeon moves them. So the sensor characteristics are measured by calibration, which is defined as the relationship between the applied input and the output signal. The calibration is made by application of a known input, and measuring the recorded output. So the nonlinearity, hysteresis, repeatability, calibration fitting line errors are calculated and also the accuracy, response time and drift.

The Pedar system is a pressure distribution measurement system for monitoring local loads between feet and the shoes. So the sensors are placed into insole of various dimensions (it depends on the shoe's size), their number is between 85 and 99[63]. The insoles are linked to a control unit with cables, which is connected to the computer by bluetooth. A battery charges the control unit.

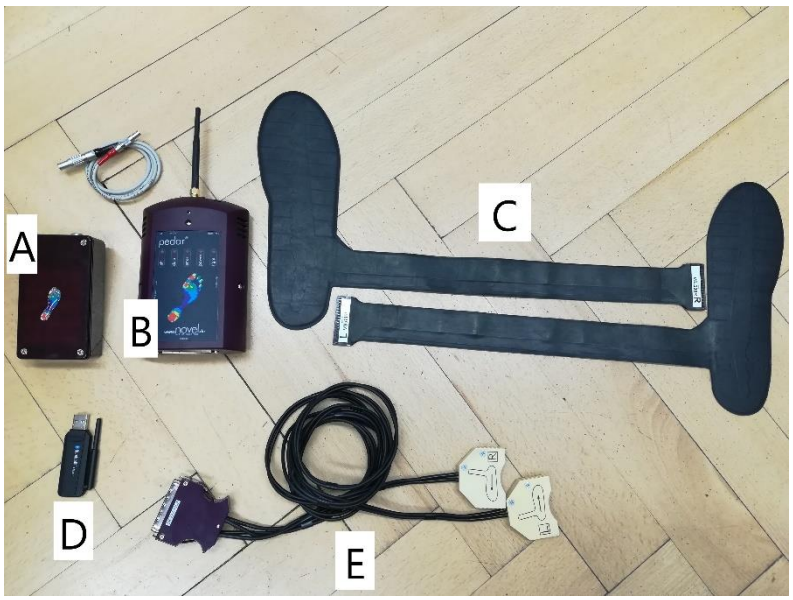

***Figure 4.1**: A) Battery; B) Control unit; C) Insoles; D) usb key for the Bluetooth connection; E) Cables*

The Novel calibrates the device, but this process has a limit: it is only valid for planar surface, and not for curve. So the aim of this chapter is the calibration of the device for curve surface but firstly, all type of errors for a measurement device are defined.

4.1. Background Information

The main concept[64] is that no measurement system is perfect, because always, the real value of the measurand (the unknown values that we want to obtain for certain physical variables) diverts from the measurement system output. To specify the validity of the measurement, standard terms are used.

4.1.1. Measurement Error

The error of a measurement[64] is defined as the difference between the measured value and the true value of the measurand:

$$error = measured\ value - true\ value$$

Generally, the true value is unknown, so it is possible to estimate the uncertainty interval of the measure, which provides the limits of error.
Errors are divided into two categories: *systematic errors* and *random errors;* they are distinguished by their causes.
The first ones are consistent and repeatable, so doing the same measurement of the same values in the same conditions, these errors will be the same every time. The systematic error can be estimated by the equation:

$$systematic\ error = average\ of\ reading - true\ value$$

The second ones are caused by a lack of repeatability in the output of the measuring system. They can be estimated as the difference between the single reading and the average of all reading of the same measurand:

$$random\ error = reading - average\ of\ reading$$

Random errors can be caused by the measurement system, the experimental system or the environment, but usually they are caused by uncontrolled variables. One environmental cause can be the electrical noise, generated by electric or magnetic fields.

By removing uncontrolled variables, these errors may decrease. Residual random errors may be amenable to statistical analysis; for example, a large number of readings can be averaged.

4.1.1.1. Nonlinearity Error

The major cause of systematic errors is the calibration process, in fact if this process has some errors, they will be brought into the measure. The calibration can also reduce and detect these errors. One source of calibration's systematic error is nonlinearity; in fact, it is considered that measurement system has a linear relationship between the input and the output, so the real nonlinearity causes errors. The linearity error is the maximum deviation between the straight line and the device output.

It is shown as a percentage of range or a percentage of span (difference between the upper and lower values of the range, which represents these values that produce useful output).

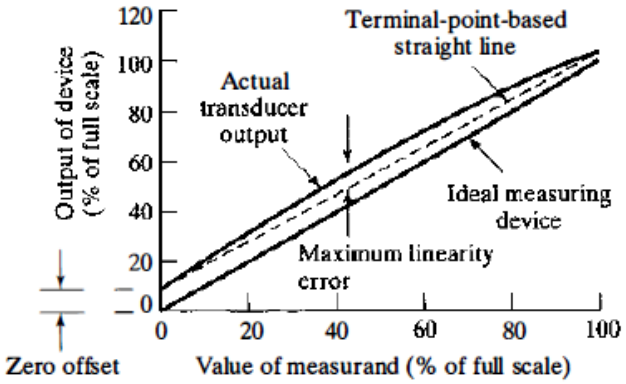

***Figure 4.2**: Non linearity error*[63]

The *Figure 4.2* shows that this error is often quantified in terms of maximum nonlinearity, its equation is:

$$\max nonlinearity = max\left(\frac{actual\ output - ideal\ output}{FS\ output}\right) \times 100$$

Where *FS output* is the full scale output, the highest possible output value.

4.1.1.2. Loading Error

The second main source of systematic error is the use of a measurement system; when the device is inserted into the environment of the measurand, this can be alterated. The devices, which cause this error, are called intrusive. For example, the thermometer is an intrusive measurement device, connecting the same to a surface may change the local temperature of that.

4.1.1.3. Environment causes

The third major systematic error is caused by other factors which don't include the measurand. For example, the spatial error: if the measurand changes in spatial region and yet a single measurement or a limited number of measurements is used to determine the average value of the region, there will be a spatial error. To measure the air temperature in a room, the used thermometer can measure low values. This is because the thermal radiation effects and if the walls are cooler than the air.

4.1.1.4. Accuracy

Accuracy is the difference between the measured value and the true value when a device is being properly adjusted and calibrated, so it defines the residual uncertainty which characterizes the device. The accuracy can be given for the entire device, or for a part of it (as a sensor), and it is specified as

a percentage of full scale output. If a measurement is done with multiple components, combined uncertainty must be determined. The *Figure 4.3* shows a measuring device, characterized by accuracy of ± 5% of full scale. At readings[64] toward the lower end of the range, the percent uncertainty might be completely unsatisfactory. This problem, with high uncertainty at the low end of the range, represent the main problem for the selection of a measurement system. To minimize uncertainty, the experimenter should select measurement systems, where important readings are included in the middle of the upper range.

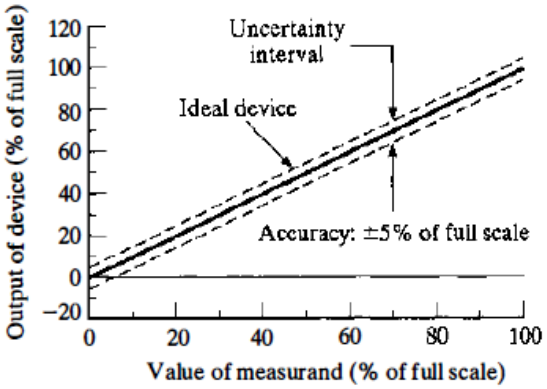

***Figure 4.3**: Accuracy as a percentage of the full scale[63]*

4.1.1.5. Hysteresis Error

Accuracy is corrupted by hysteresis; this phenomenon gives two different values for the same measurand, when the input increases and when it decreases. The hysteresis error is quantified in terms of maximum hysteresis and expressed as percentage of full scale value:

$$\max hysteresis = max\left(\frac{|loading\ output - unloading\ output|}{FS\ output} \times 100\right)$$

It is due to the effects of friction, mechanical flexure and electrical capacitance. The hysteresis errors are repeatable if the measurement conditions are the same. This kind of error would be considered a systematic error, but the experimenter doesn't know if the measurand increases or decreases, so the effect of hysteresis is random, and it is one of the instrument manufacturers' features of accuracy.

4.1.1.6. Repeatability Error

Repeatability is the ability of a device to produce the same output reading when the same measurand is applied, using the same procedure. When it doesn't happen, there is a random error called repeatability error, which is one of the manufacturers' specification of instrument accuracy.
Repeatability error is often quantified in terms of maximum differences between two calibration cycles and expressed as a percentage of full scale.

$$\max repeatabily = max\left(\frac{output\ run\ 1 - output\ run\ 2}{FS\ output} \times 100\right)$$

4.1.1.7. Zero Error

When no input signal is applied, the measurement device doesn't measure anything; but this doesn't happen for all the device, so they have a zero offset. If the zero offset is not considered using the device, the offset can produce a systematic error in all the readings, which is called zero error. When the null point doesn't agree to the zero value for the output, the device should be first adjusted. The software pedar-x, which is used with the insole, can identify the point of zero.

4.1.1.8. Drift

The drift is an unintended effect and it describes the change of the output for a fixed measurand over a period of time. It can be expressed in terms of full scale or relative to the output at time where firstly, the load is applied.

$$Drift = \frac{output(t = T) - output(t = 0)}{output\ (t = 0)} \times 100$$

Many measuring systems[64] are also sensitive to environmental temperature, the thermal stability of the device, which is a known characteristic. The drift and thermal stability can affect the features of the measuring system and cause additional errors of zero, linearity, hysteresis, and sensitivity. These drift and thermal stability-caused errors are not usually defined in manufacturers' specifications of accuracy. However, manufacturers give additional information about the drift and the thermal stability of instruments, which can estimate the random uncertainty.

4.1.1.9. Dynamic Response

The dynamic term is used for the process, where the measurand is changing in time and the measurement system doesn't show instantaneous response. The dynamic response is divided into three categories: zero order, first order and second order. The zero order replies instantly to measurand. The features of the dynamic response are: the transient response, which characterizes the response of the measurement system when the input changes as step, and the frequency response, which characterizes the response to sinusoidal inputs. The expressions of these systems are characterized by a value: the time constant, τ. It is a numerical specific of transient response of the instrument and defined when the response, y/y_e (y_e is the equilibrium change in the output system), is $1 - 1/e = 0{,}632$.

4.2. Novel's Calibration

Novel.de, the company that made the Pedar sensor, calibrated these devices with the trublu calibration systhem [65]. This device uses an assisted computer procedure, and it calibrates the sensors using a known air pressure. The software shows the calibration curves for each sensor in a short time.

***Figure 4.4**: Trublu calibration device[64]*

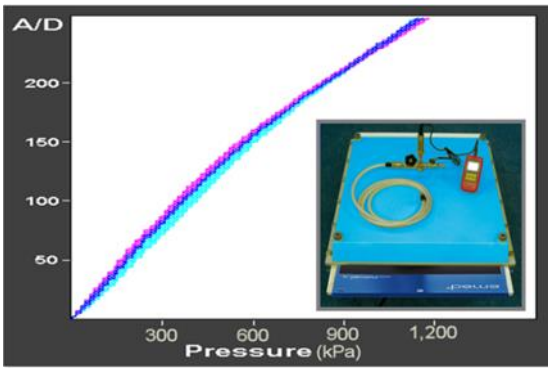

***Figure 4.5**: Example of the relationship between input and output[64]*

The calibration check, for each sensor, consists in putting the insoles in the trublu airbladder system, then applying a homogenous pressure across the entire area[66]. The result has to be the same, within the specified accuracy, for each sensor.
In 2006 Giacomozzi[67] was working for a two-year approved project to design, validate and implement dedicated testing methods and instruments for a pressure measurement device (PMD), and technical assessment with respect to accuracy and reliability of measured pressure, hysteresis, accuracy and precision of center of pressure (COP) estimation. She tested five PMDs: three had resistive sensors (TEKSCAN, RSSCAN, MEDILOGIC), one had capacitive elastomer sensors (NOVEL), one had capacitive air sensors (AM CUBE). The performances of Novel device showed a high linearity, low creep, low hysteresis and high correlation under slow sinusoidal loading, high accuracy and precision in COP estimation, low variability of all performances over the whole sensor matrix.

The technical data[63] given by the Novel company are:

***Table 4-1**: pedar technical data[62]*

shoe size	22 to 49
thickness (mm)	1,9
number of sensors	85 - 99
pressure range (kPa)	15 - 600
hysteresis (%)	< 7
resolution (kPa)	2,5
offset temperature drift (kPa /K)	< 0,5
minimal bending radius (mm)	20

4.2.1. Evaluation of Novel Sensor's Errors in Planar Surface

Objective

The aim of this paragraph is the measurement of the systematic, random, nonlinearity, repeatability, hysteresis, the maximum and minimum errors for each insole (right and left).

4.2.1.1. Systematic, random, repeatability, maximum and minimum error

Materials and Methods

The sensors of each insole, which are 99 for the model 695l-696r, are tested on a rigid plane and are loaded with 0,974 kg (*Figure 4.6*). This load had a support with a spike, so it didn't stress the sensors all over their surface. To define the application surface of this load on the insole, it is used a cylindrical support with a diameter of 1 cm (*Figure 4.6*). The application area was 0,785 cm^2, calculated by the equation:

$$A = \pi \times (d/2)^2$$

The known pressure is 121,719 kPa, it is calculated by:

$$P = (g \times m)/A$$

Where g is the constant value of 9,81 m/s^2, m is the load in kg and A is the application area in m^2. Then all the sensors of each insole are stressed. The acquisition system recorded a matrix with 99 colons (which corresponds to the sensors) for each insole and as many rows as the samples for the acquisition times. This matrix had the values of pressure expressed in kPa and it was in ASCII extension. The sample frequency was 50 samples for second, and we measured the sensors' answer for 6 s.
The recorded data are analyzed using Matlab R2017b and Excel 2016. To calculate the errors, it is used the equations described in the section *Background Information*.

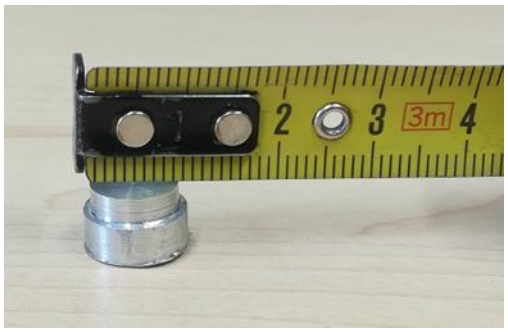

***Figure 4.7**: Cylindrical support with diameter of 1 cm*

***Figure 4.6**: Position of the load*

Results, Analysis and Discussion

The maximum error for each sensor is reported in the *Figure 4.8* section A; in the section B it is showed the minimum error; in section C the repeatability error, and in *Figure 4.9* the systematic and random errors. The maximum and the minimum error show that the right insole has positive values, while they are negative for the left; the magnitude of the left's errors are higher than the right. Also, the repeatability error is higher for the left than for the right, in fact, the left has a maximum of 27,5 % while for the right is 20 %. These errors are high and they are caused by the sensor's characteristics, for the examples the resolution (2,5 kPa), which doesn't allow to have precise values. All of these errors are expressed in percentage, and the full scale is the known pressure (121,719 kPa).

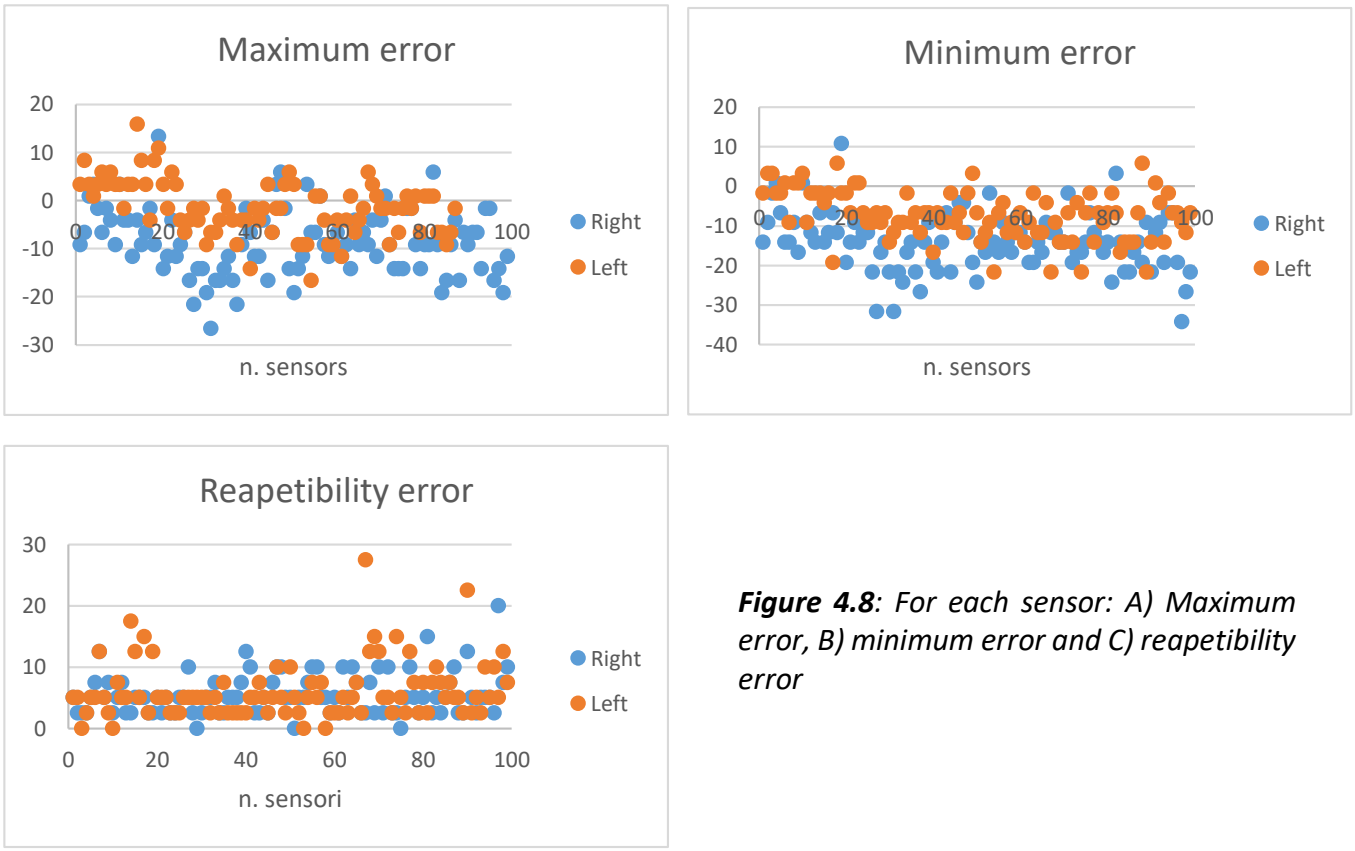

***Figure 4.8**: For each sensor: A) Maximum error, B) minimum error and C) reapetibility error*

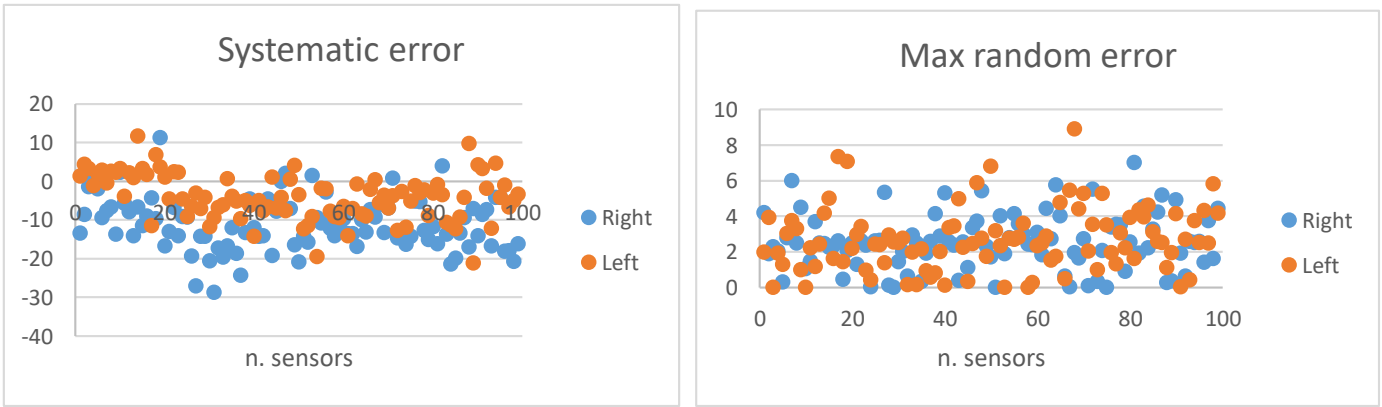

***Figure 4.9**:A) Systematic error and B)Random error*

For each error it was calculated the maximum and the mean value, and they are reported in *Table 4.2.*

***Table 4-2**: Summary of the Novel sensors' statistic characteristics*

Statistics	Maximum error	minimum error	Repeatability error	Systematic error	Random error
max right	15%	13%	14%	15%	9%
mean right	6%	3%	3%	4%	2%
max left	17%	15%	15%	17%	18%
mean left	7%	3%	3%	5%	3%

Also, this table shows higher values for the left insole than the right; in particular, for the random error.

4.2.1.2. Non linearity Error

Materials and Method

For this test, two cylindrical steel weights are designed to apply pressure between 121,719 kPa and 186,607 kPa on one sensor. Following the instruction of the study by Bonnaire et al.[68], the weights are randomly applied in sensors 1, 16, 32, 34, 51,67,69,86 and 98 for the right and left insole (*Figure 4.8*). Thirty measurements are recorded for each sensor. The dispersion, the standard deviation and the equation of the trend line (linear) are calculated. The dispersion is defined as the difference between the maximum and the minimum pressure measured for each applied pressure; it is expressed as a percentage, dividing the result for the value of the applied pressure. The standard deviation s_p of the measured pressure is defined by the following formula:

$$s_p = \sqrt{\frac{1}{(n-1)}\sum_{i=1}^{n}(P_i - \bar{P})^2}$$

With n is the size of the measured sample and P is the measured pressure value for each applied pressure in kPa.
The non-linearity error is calculated as the difference between the value of the trend line and the measured value; it is expressed as a percentage, dividing the result for the value of the applied pressure.

Results, Analysis and Discussion

The *Table 4.3* shows the standard deviation, the upper value of the dispersion and the mean value of the non-linearity errors. The left insole shows higher standard deviation than the right, but the other values are the same for the two insoles. The values are high for the dispersion. It is low for the non-

linearity error. These values are calculated when two loads are applied; they can be more accurate if more loads are applied.

***Table 4-3**: standard deviation, maximum dispersion and non-linearity error*

Insole	S_p	Max dispersion	non linearity error
Right	3,68	11%	3%
Left	4,15	11%	3%

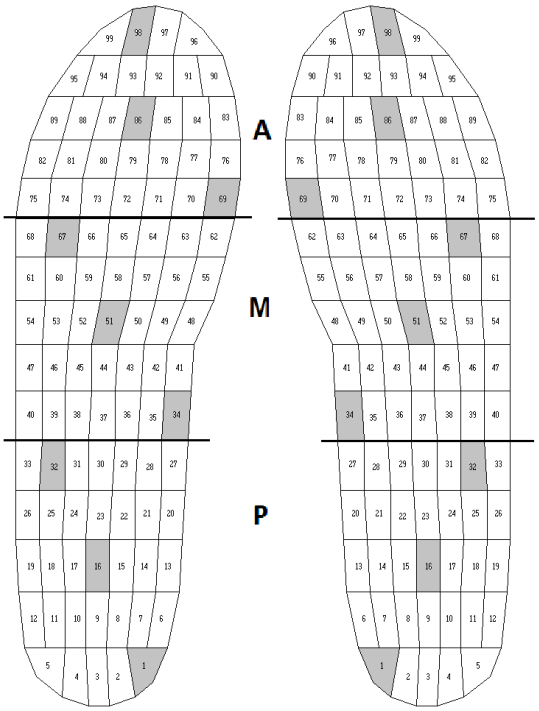

***Figure 4.10**: Position of the nine sensors for each insole, there are three sensors for each insole's zone: A as anterior, P as posterior and m as medial*

4.2.1.3. Hysteresis Error

Materials and Method

Two types of hysteresis tests are performed[68]: an hysteresis test in only one sensor, and an hysteresis test in all sensors at the same time. For the first test, the same weights as for the linearity test are increasingly and decreasingly applied on the nine sensors for each insole (as for the linearity test). For the second test, the insoles are tested when it is applied a distributed human weight of 60 kg. The pressure of each insole is recorded without loads, with and then without again (*Figure 4.9*). So it is possible to calculate the hysteresis.

Results, Analysis and Discussion

The *Table 4.4* shows that the first test has higher values than the second, this because in the first test not all the sensors are stressed and also, the applied weights are different. For the second test each insole has a hysteresis error lower than the value declared by the Novel Company. The maximum value is calculated because it shows the worst situation.

***Table 4-4**: Hysteresis errors*

Insole	First test	Second test
Right	12%	6%
Left	16%	6%

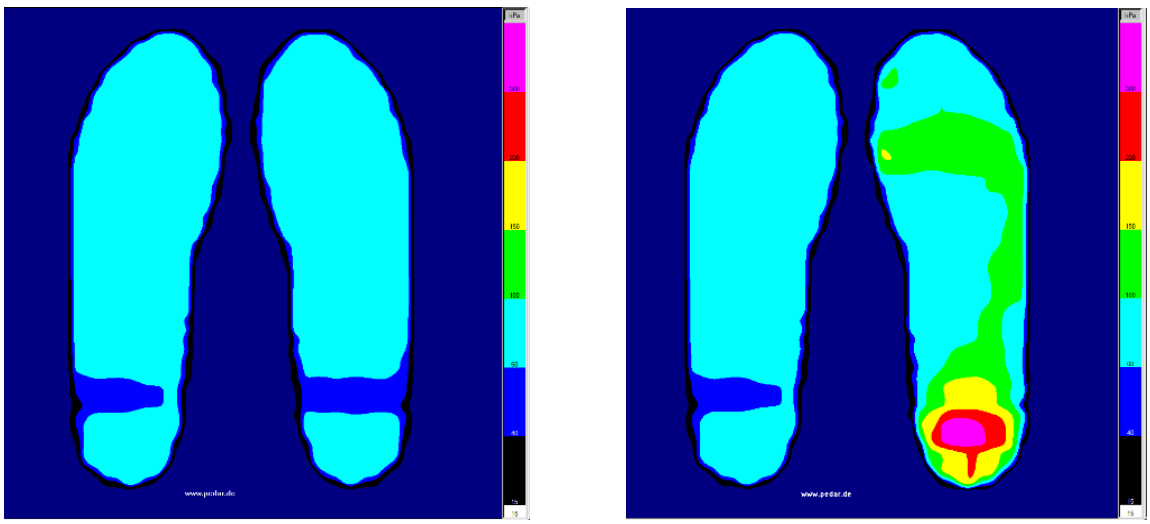

***Figure 4.11:** A) Insole without loads, B) with loads*

4.2.1.4. Zero Error

The *Figure 4.12* shows the values of pressure that the sensors have without loads. In the section *Background Information,* it is described this phenomenon as Zero Error, and it is fixed by the software *pedar-x*. In fact, it is possible to record the values without loads and then considered as zero's values. In *Figure 4.12* the values for each sensor are shown, they are not all the same: the lower value is about 40 kPa, and the upper 90 kPa.

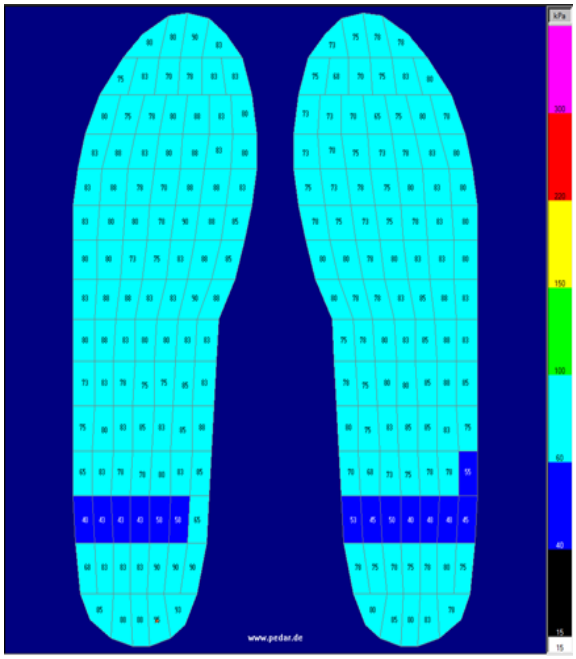

***Figure 4.12**: Zero's values: in each insole there is a sensors' tract (blue) with values between 40 kPa and 60 kPa, the others are over 60 kPa*

4.2.2. Evaluation of Novel Sensor's Errors in Curved Surface

Objective

The aim is to evaluate the systematic, random, nonlinearity, repeatability, hysteresis, the standard deviation for each insole (right and left), when it is applied to two cylinders with different diameters.

Materials and Method

The 99 sensors of each insole (model 695l-696r) are tested on a curved plane, two cylinders of steel; one with a diameter of 10 cm and the other of 12 cm (*Figure 4.13*). The insole is placed on the cylinder's surface and over that, the sphygmomanometer is applied (*Figure 4.14*). The sensors are calibrated using the sphygmomanometer for pressure range of 80-260 mmHg (10,66- 34,66 kPa), to reduce[42] the errors introduced by the curved nature of the used cylinders. The aneroid sphygmomanometer cuff is inflated by 20 mmHg increments from 80 mmHg to 260 mmHg. The inflating and deflating processes are used to measure the hysteresis errors of these sensors. The process is reproduced 30 times to overcome the repeatability error associated to the sensors and the aneroid sphygmomanometer. So 30 measures are done for each insole and for each cylinder. The data are processed using MATLAB 2017b. A linear fitting line (first order) is used to describe the pressure (mmHg) relative of the measured pressure (kPa).

***Figure 4.13**: Two used cylinders with diameter of: 10 cm and 12 cm*

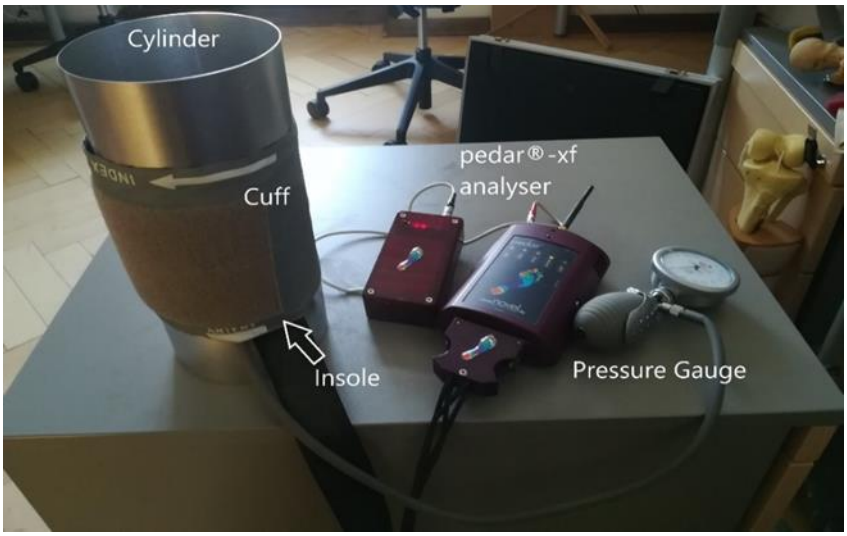

***Figure 4.14**: Instruments for the measures of calibration*

Results, Analysis and Discussion

The *Table 4.5* shows the results of the insoles on the first cylinder (diameter of 10 cm). The two insoles have similar results for the standard deviation, the repeatability, random and hysteresis errors; but for the systematic and non-linearity error the right insole is worst. The errors of the table are given in percentage, and they are divided for the Full Scale, in this case 260 mmHg (34,66 kPa).

In the *Table 4.6* there are the results of the insoles applied to the second cylinder. The errors are similar to those of the first cylinder: the non-linearity error is lower for each insole and also the random error. The standard deviation is not the same for the two insoles, in fact, for the left insole is lower than the right.

The calculated errors for the planar surface are lower than these of curved surface.

***Table 4-5**: Results for the cylinder with diameter of 10 cm*

Statistics	S_p	Repeatability	Systematic	Random	non linearity	Hysteresis
mean right	1,07	7%	13%	3%	18%	6%
mean left	1,17	7%	6%	4%	9%	5%

Table 4-6: *Results for the cylinder with diameter of 12 cm*

Statistics	S_p	Repeatability	Systematic	Random	non linearity	Hysteresis
mean right	1,42	7%	14%	2%	12%	7%
mean left	0,42	7%	7%	2%	6%	5%

The fitted lines are calculated for each insole; they are showed in *Figure 4.15*.

The letter D means right and S means left; the number 10 means the diameter of 10 cm and 12 the diameter of 12 cm.

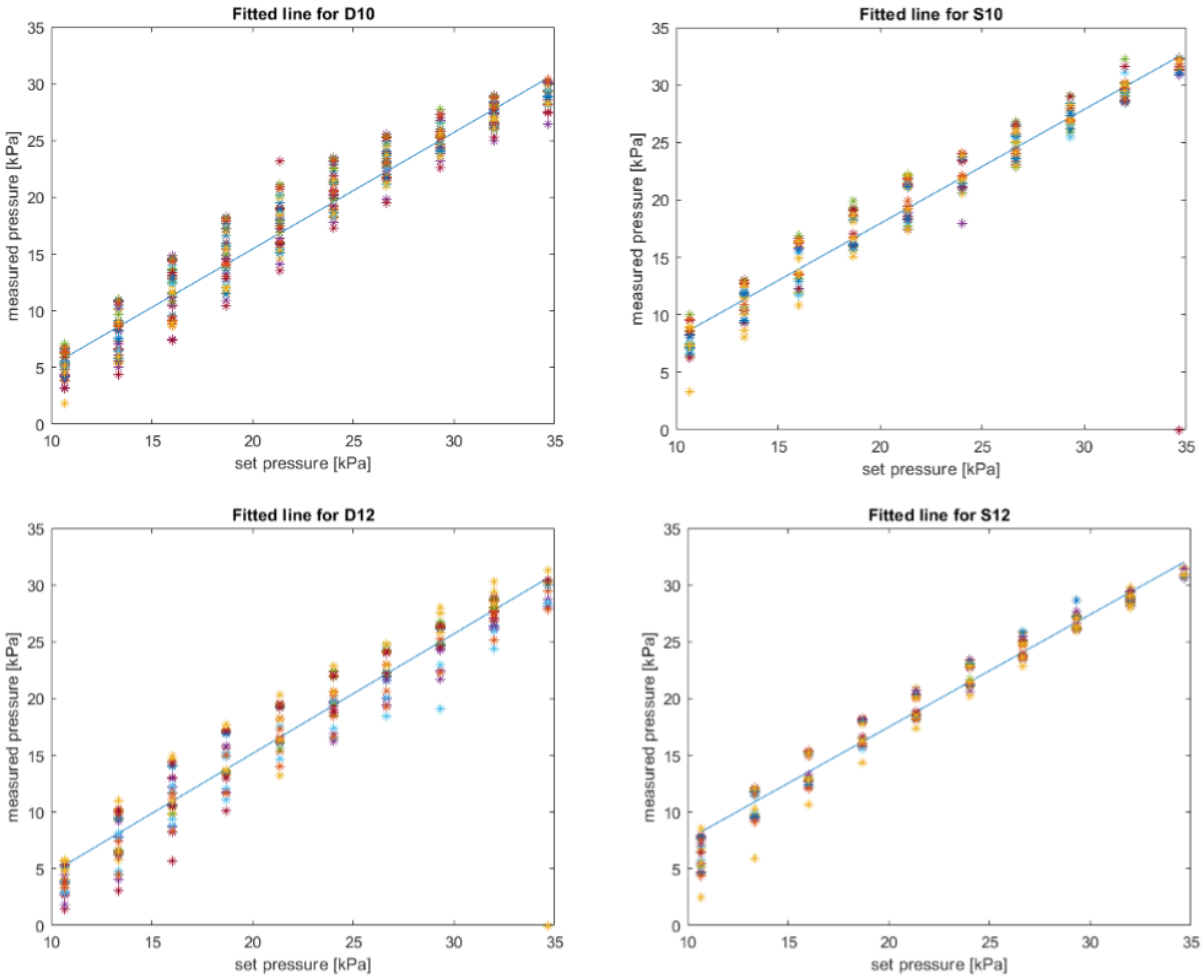

Figure 4.15: *Fitted line for each insole; S is for left, D for right, 10 and 12 for the diameter of the cylinders*

In the following table it is showed the angular coefficient of each fitted lines: we can see that for each case this value fits to the unit value, so the measurement tool measures the value showed by the sphygmomanometer.

***Table 4-7**: Angular coefficient of the fitted lines*

	Angular Coefficient	
Diameter	**10**	**12**
Right	1,03	1,06
Left	0,99	0,99

The graphs with the fitted lines show a dispersion of the points referring to the line, in particular for the right insole with both the cylinders, so the measured pressure is not exactly the same of set pressure for the right insole. The angular coefficients show that: the right insole is more accurate than the right, but it gives an approximation for default and the right for excess.

The cylinder with diameter of 12 cm gives a higher angular coefficient (for the right insole) than the others. About the left insole there isn't difference between the two kinds of cylinders.

Chapter 5

5 Sub bandage pressure's measures in vivo

This chapter presents the description of a method to measure in vivo (with cadavers) the pressure applied by two kind of bandage: iFix and Coban. The second one is the most used in the operation of arthroplasty to fix the limbs. The aim of this chapter is to define if the iFix bandage applies more or less pressure on the human leg than the Coban, and the potential causes of its behaviour.

5.1. Material and method

These measures were made in the section of Anatomy in Innsbruck's Medicine University. The measures' subject was the cadaver number 8076 with the following features: it was of female gender, with a leg's length of 78 cm. The subject's foot was placed in a rigid positioner with the shape of the foot (*Figure 5.1*), under the heel it had a metal peak, where a dynamometer was hooked up.

The test consisted in the application of increased traction loads at the lower end of the left leg, and in the measure of the pressure under a bandage applied on the leg. The forces were: 40 N, 80 N, 120 N, 160 N and 200 N. To identify the hysteresis' effect, these loads were also applied in decreasing way. The loads were applied by an operator, who controlled the force using a dynamometer (*Figure 5.2*)

The used bandages were: iFix system (the fleece and the patch) and the Coban 3M. To measure the pressure, it was employed the Pedar system (described in the chapter 4), which was linked to a program to display the values of pressure. The recorded data were analysed with two programs: *Excel 2016* and *Matlab R2017b*.

***Figure 5.2**: System of the traction made by an operator*

***Figure 5.1**: Foot's positioner*

The adopted procedure for the placement of the bandage and the sensors was: the two insoles were applied on the left leg as *Figure 5.3*, then it was bandaged in different ways for the Coban and iFix. The zone covered with the right insole is called 'R' and that covered by the left 'L'.

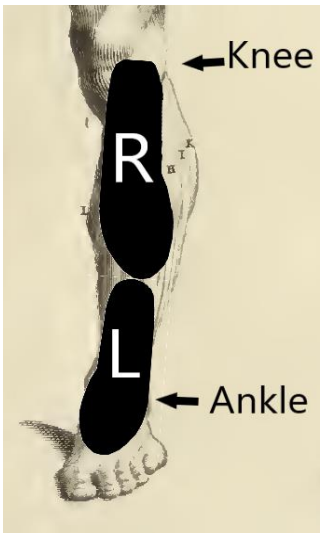

***Figure 5.3:** Position of the two insoles on the left leg*

The iFix system is not an elastic bandage with adhesive property, so for its application and fixing of the two extremities, the patch is required. It is cut in three pieces with the dimensions of (*Figure 5.5*): 20 x 50 cm for the foot (1), 16 x 50 cm for lower part (2) of the leg, 12 x 50 cm for the higher part (3); each part is fixed by the iFix patch. The Coban is coadhesive (it doesn't need the patch), therefore the operator used a shape of 10 cm x 4,5 cm and held up the leg with the bandages; he made two rounds for each zone (*Figure 5.4*).

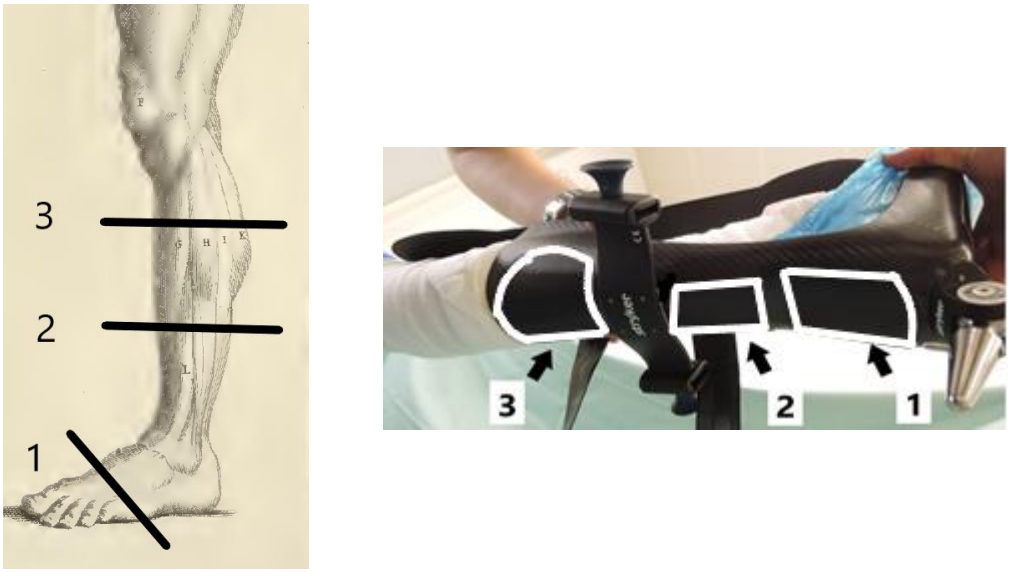

***Figure 5.4**: Three zones for the position of the iFix patch (second image) and for the bandages*

After this preparation, pressure was measured using the program linked with the insole, *pedar x-Recorder*, that recorded the measured pressure in time for each insole's sensor. The program front panel showed each insoles' sensor, and which of that was activated (the square with the number) and the value of the pressure. It showed also the time like curves of pressure (kPa), force (N) and activated area (cm^2).

With the same bandage the operator applied nine forces (40 N, 80 N, 120 N, 160 N, 200 N, 160 N, 120 N, 80 N and 40 N). Then the bandage was changed and a new measure was done; this was repeated for 10 times.

The data, which were pressures in kPa, were saved in ASCII format for the reading in Matlab. A script was developed (the flow chart is reported in *Appendix C)*; the steps are:

1. Reading the data for the two bandages, which are written in matrix with dimensions of n° time x 198 x 90, 198 is the sensors' number, and 90 all the measures.
2. Determining start and end times for all the measures, in this way the number of zero in the matrix is reduced.
3. Plotting the trends of the maximum and average (of the 99 sensors) in time, and saving these values for each measure. Then, these were analysed in Excel and plotted with histograms.
4. Calculating the mean and maximum value for each sensor and plotting these values in colour maps.

This analysis was done for the Coban and iFix bandages, so the results for each one were compared: first it was valuated the normal distribution of the data for each load and for each bandage. This data didn't have a normal distribution; so, for the comparison, it was used the independent samples Mann-Whitney U test (it is used to compare differences between two independent groups when the dependent variable is either ordinal or continuous, but not normally distributed).

5.2. Results

Firstly, the Matlab's script displays two kinds of colour maps (that show the most exposed areas qualitatively): the first one takes the mean value on time of the sensors for each repetition, so each sensor has 10 values, which are mediated; the second one takes the mean value on time, and from the 10 values, it takes the maximum one. Each colour map is linked with a colour bar that indicates the values of pressure for each colour. The *Figure 5.5* shows the area of the leg which corresponds to the colour map's area: the knee's position is at 46 cm and the ankle is at 13,5 cm.

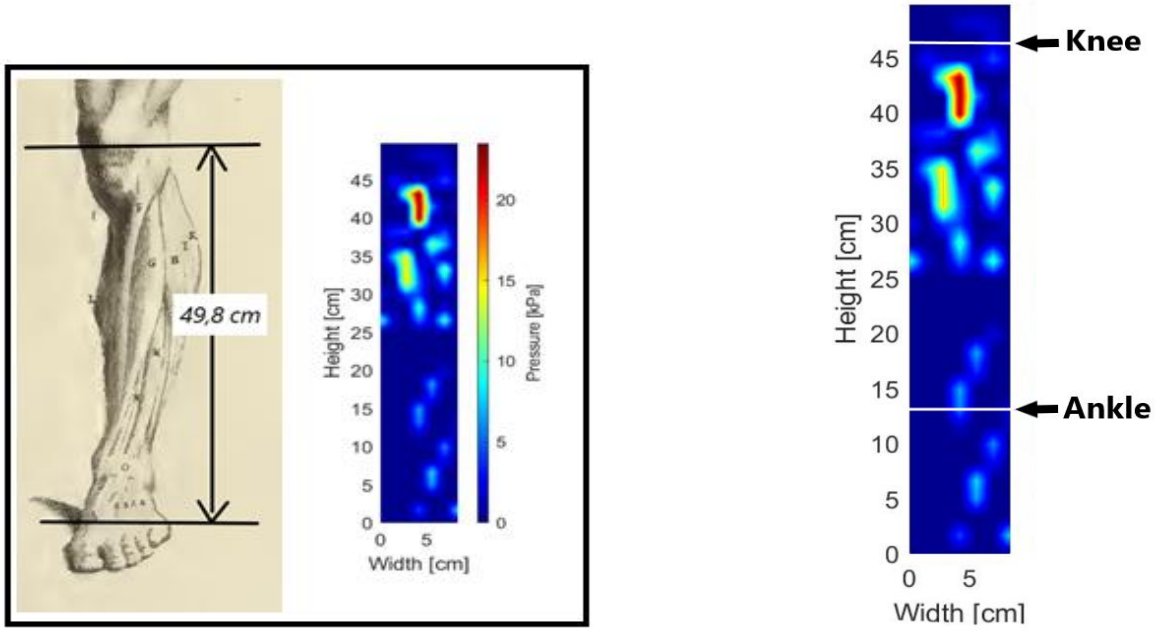

***Figure 5.5**: Colour map refers to the left leg. The second image shows the zone of the colour map*

The map with the maximum value shows the worst behaviour of the bandage. The two kinds of maps show different values of pressure; with the maximum the values are higher (all the colour maps are reported in *Appendix D)*.

The stressed areas are different for the kind of pressure and for the bandage; the two most significant examples are those at 40 N and that at 200 N.

For the maps with the means values, at 40 N the iFix shows three stressed points: one near the ankle, one in the middle of the shank and the last one near the knee; these are axial and the second point is the higher with a value of 4 kPa. About the Coban, it shows only one point with a values higher (5,5 kPa) than that of the iFix, which is near the ankle.

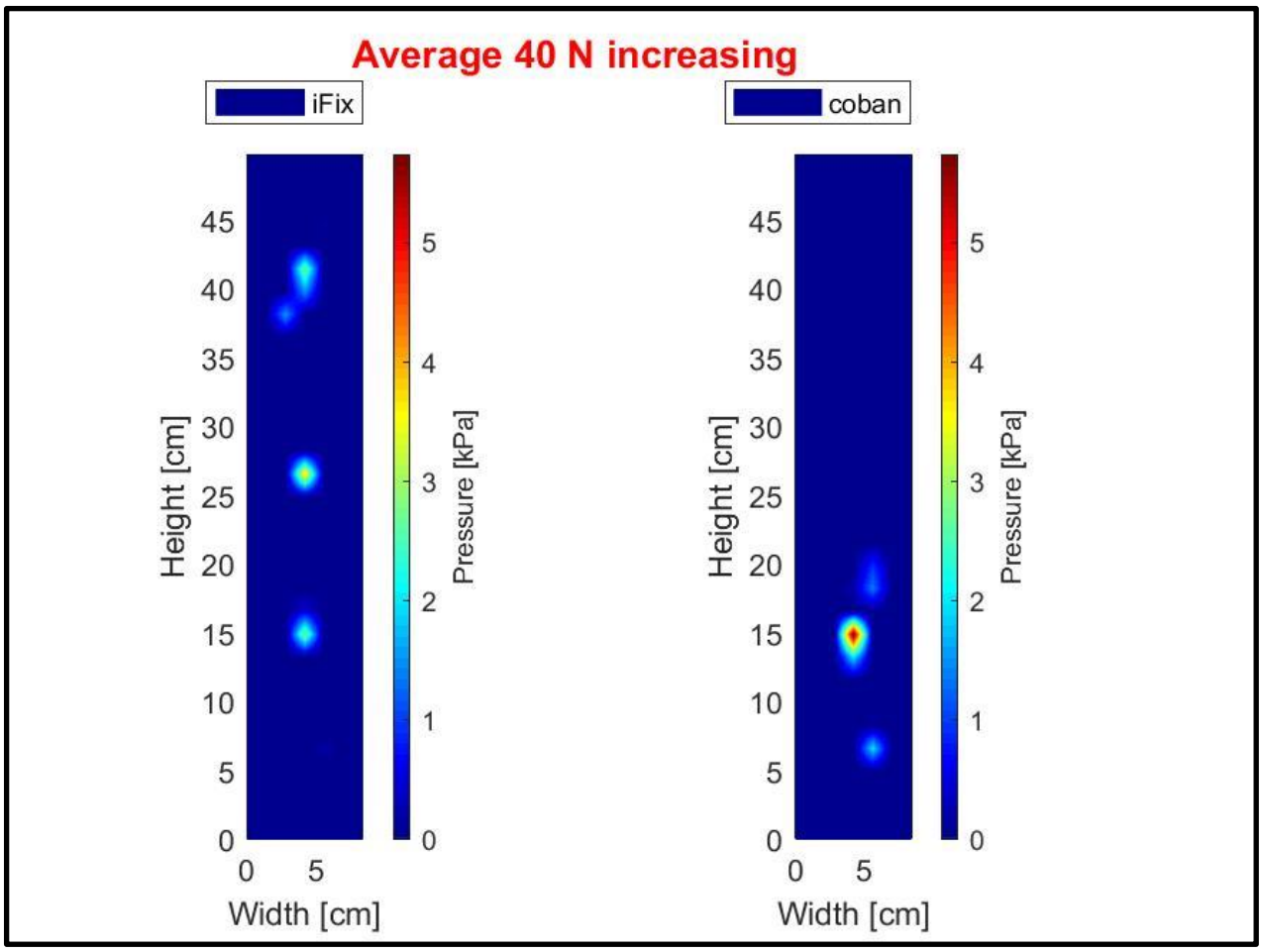

***Figure 5.6**: Colour map which describes the bahaviour of the two bandages for small external forces: the iFix shows three stressed points on the same y-axis, the Coban only one point near the ankle but with a higher value (red)*

At 200 N the stressed areas are the same for the two bandages: one large zone (of 20 cm) that extends from the knee to the middle of the shank, and two small, one near the ankle and the other in the middle of the foot. The iFix has the higher values for the first zone: over 50 kPa; while the Coban 40 kPa.

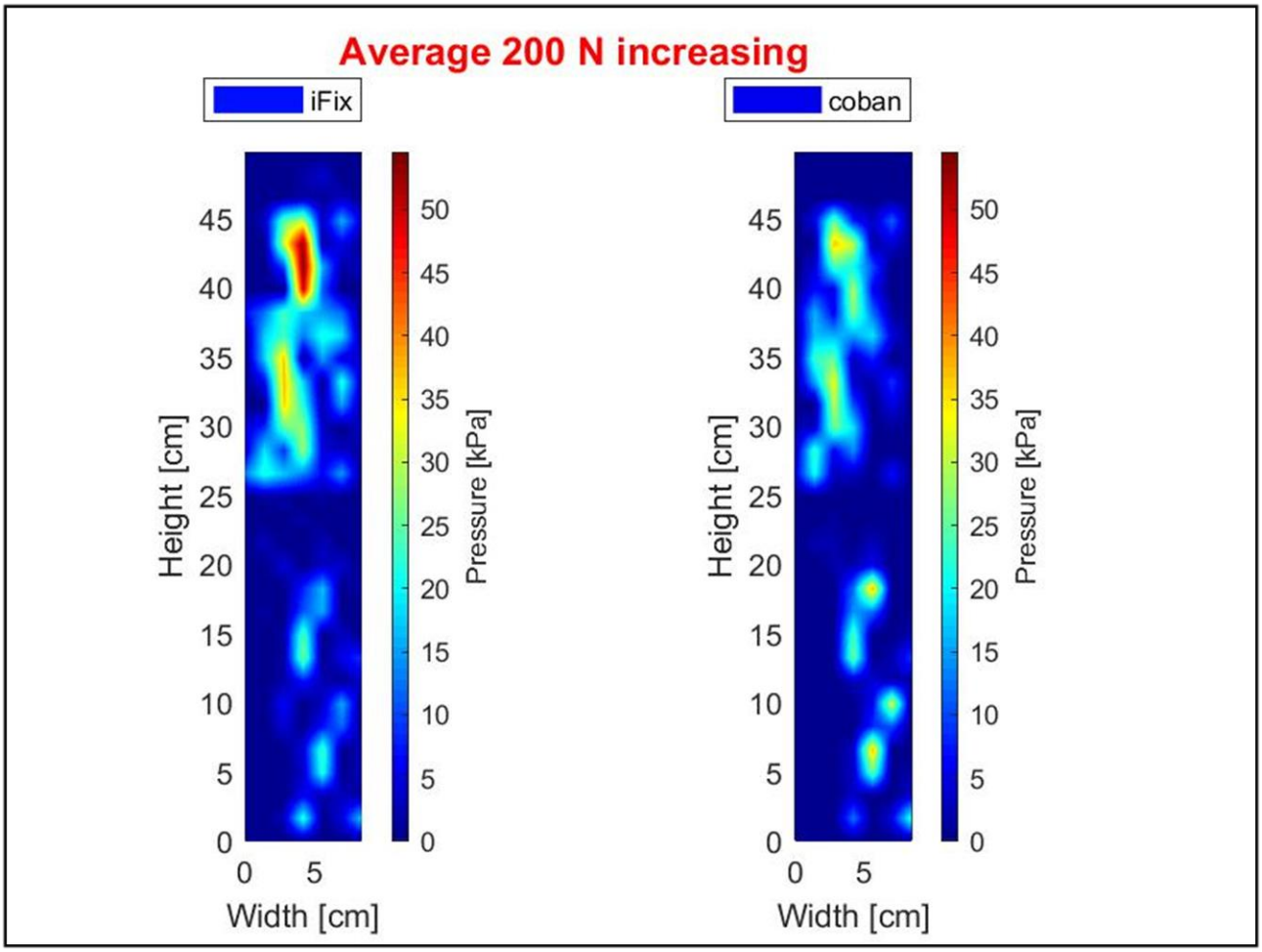

***Figure 5.7**: Colour map which shows the sub pressure when the bandages are exposed to higher forces (200 N). The stressed area is bigger than that for small loads, and it is the same for the two bandages. The iFix has center zones with values over 50 kPa (red)*

About the maps with the maximum values: at 40 N the iFix has the same three points, but the two external points are more stressed than that in the middle, in fact they have a pressure over 25 kPa. The Coban shows not one, but three points near the ankle (one in the middle of the foot) with the maximum value of 20 kPa.

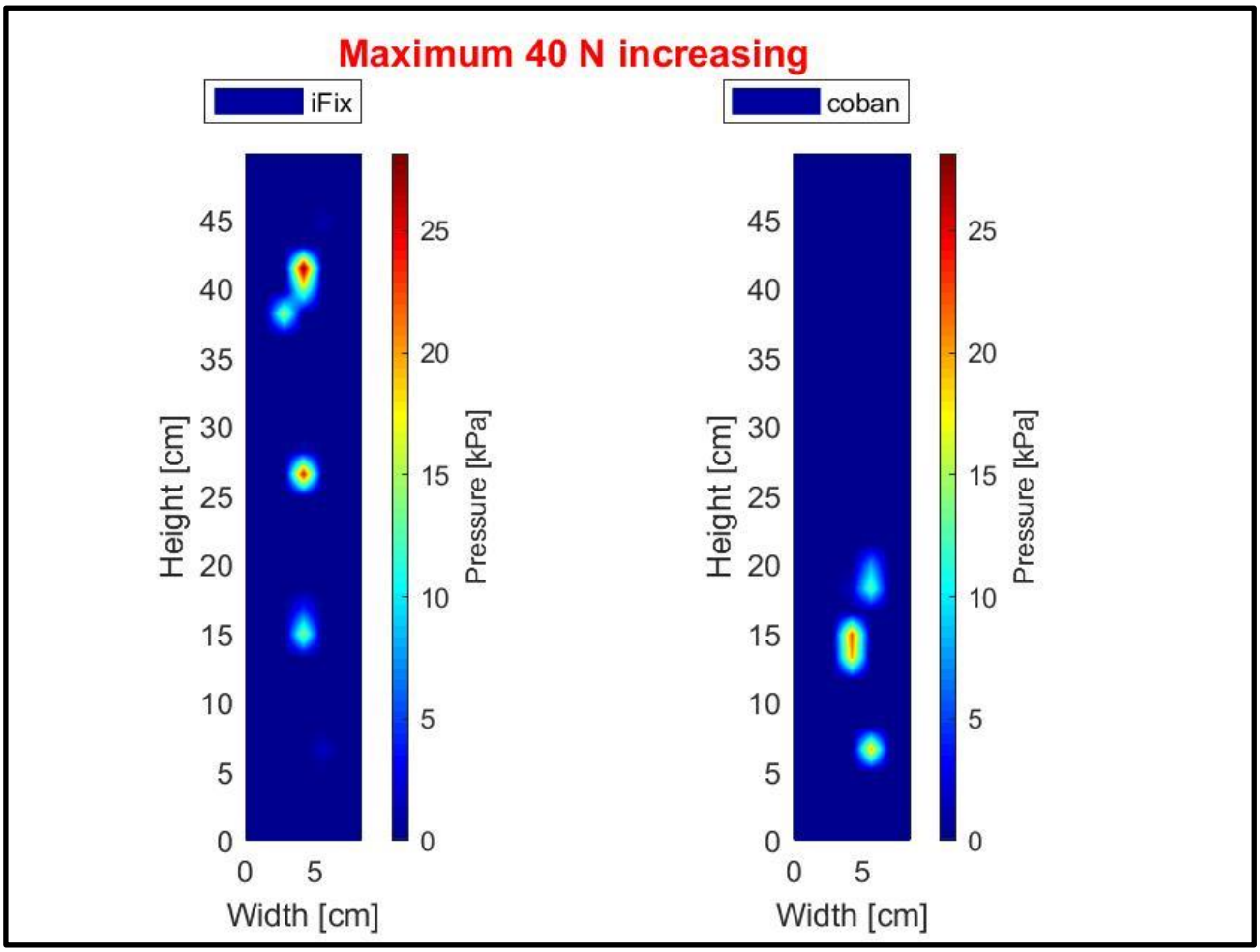

***Figure 5.8**: Colour map which shows the maximum values of the sensors for a force of 40 N. The two bandages have more stressed points; it is clear for the Coban, in fact it has two points. The pressure in the center of the three points of iFix is as high as the Coban*

At 200 N the stressed areas are larger than the first kind of map, the maximum of both is over 90 kPa, but for the iFix is near the knee, and for the Coban there are two maximums: one near the ankle and the other in the middle of the foot.

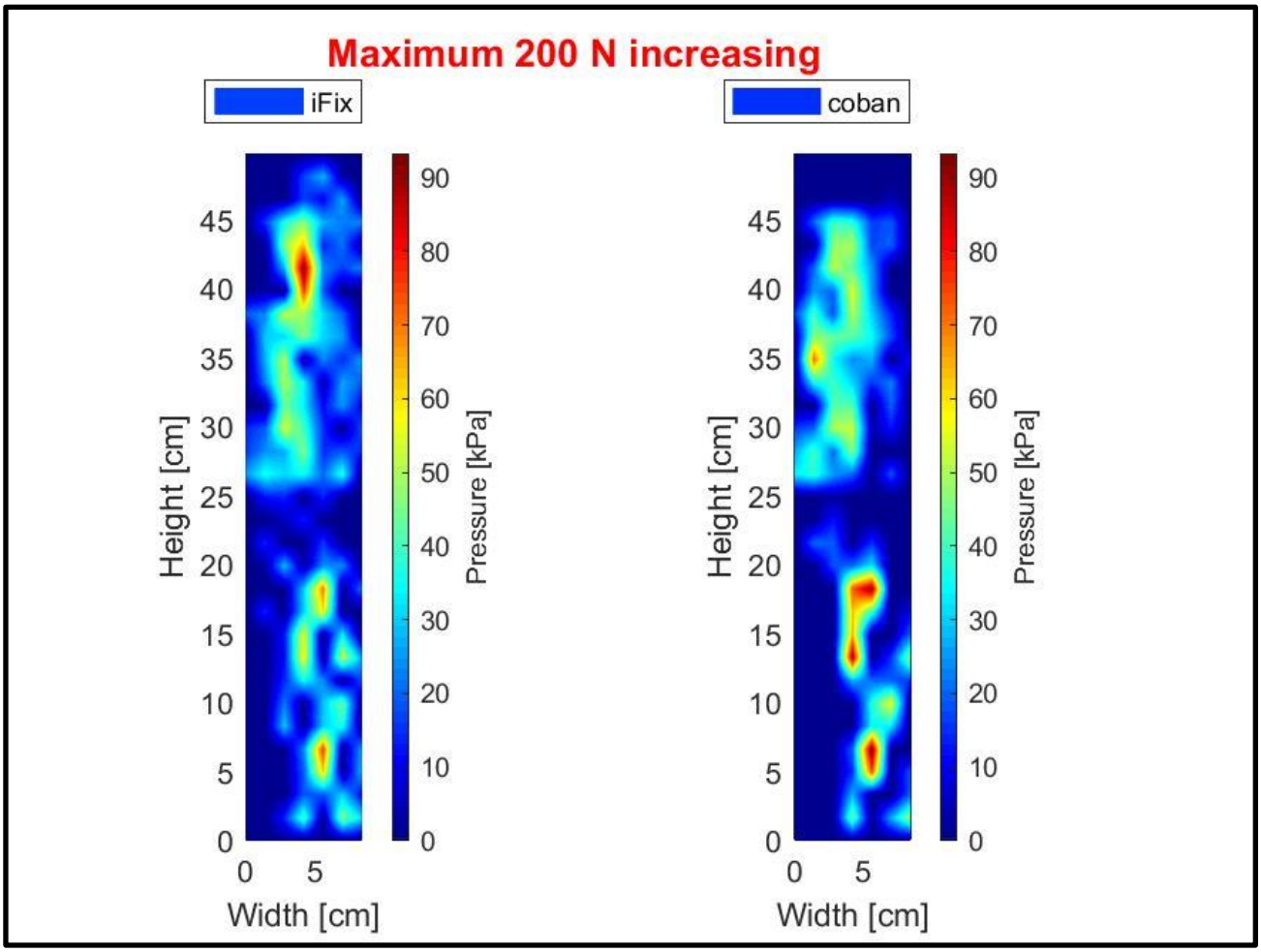

Figure 5.9: *Colour map for external force of 200 N. The stressed areas are similar for the two bandages, but the Coban shows a maximum value (in the central zone) of 40 kPa while the iFix is over 60 kPa*

Looking at these last maps, the iFix has a stressed area larger than the Coban, so it seems that the loads are more distributed, but it shows a big zone with higher pressures. This is not isolated, in fact, near this point there is lower pressure. The Coban has two regions with high pressures, but it doesn't have a near area with lower pressure (like iFix); the load is isolated. It seems that the Coban applies forces in some points but it doesn't distribute them.

This is not true if it is considered the map of the mean value on the 10 measures; in fact, the iFix shows areas with higher value than the Coban.

So, in both colour maps the iFix system has elevated pressures; it suggests that the iFix is more rigid than the Coban. This consideration can agree with the mechanical tests made in laboratory, where it is seen that the Coban has an elastic behaviour.

The comparison between these bandages is also done considering, for each repetition, the mean value on time for each sensor, and for all the insoles, two type of operations are done: do the maximum

value of that, and do the average value of that. To show the results by the histograms, it is calculated the average and the standard deviation on the repetitions for each loads, and this is also analysed with the statistic test (U test). For this analysis, the interest zone is divided in two parts: one superior, which corresponds to the right insole, called "Superior Tibia" (from 24,9 cm to 49,8 cm), and the other called 'Tibia' (from 0 cm to 24,9 cm), which corresponds to the left insole.

About the average:

- Tibia: the iFix has higher values for all the forces; at 40 N it shows a small pressure but for the Coban the pressure is zero, then at 200 N it has a value of 10 kPa while the other one is 7 kPa.
- Superior Tibia: the behaviour is the opposite of the Tibia, the Coban has slightly higher values than the iFix.

About the maximum: in the two zones, the behaviour of the two bandages is the same of the histograms with the mean values; though the values are higher, for example at 200 N in the Tibia's zone the iFix shows a value of 60 kPa.

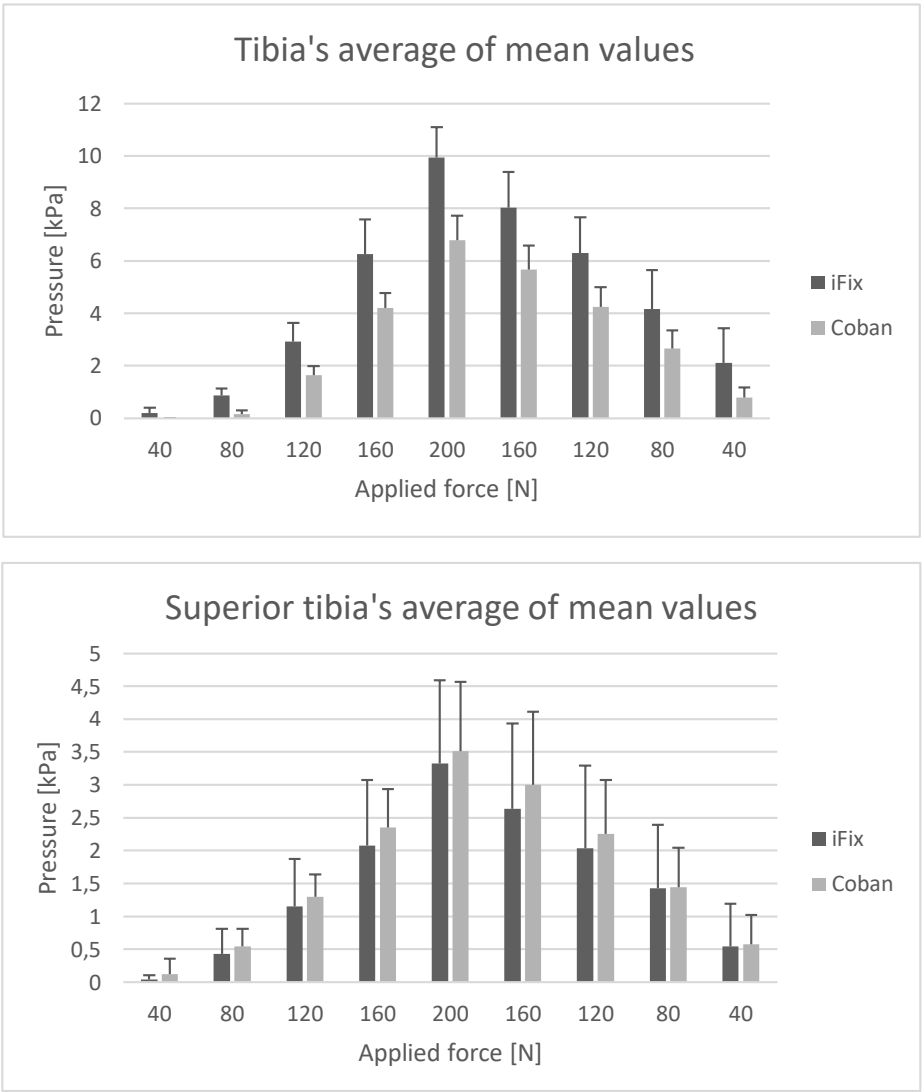

***Figure 5.10**: Two histograms, which show the average of mean pressure*

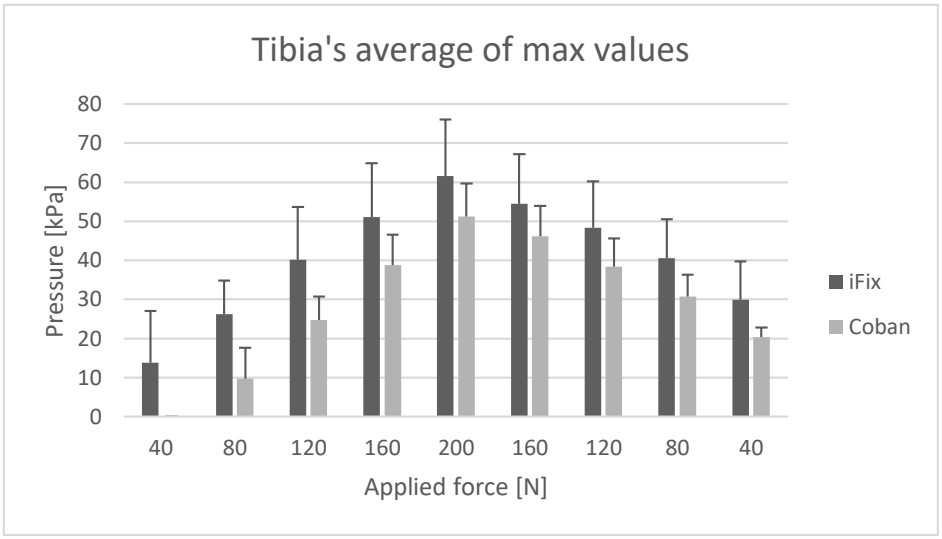

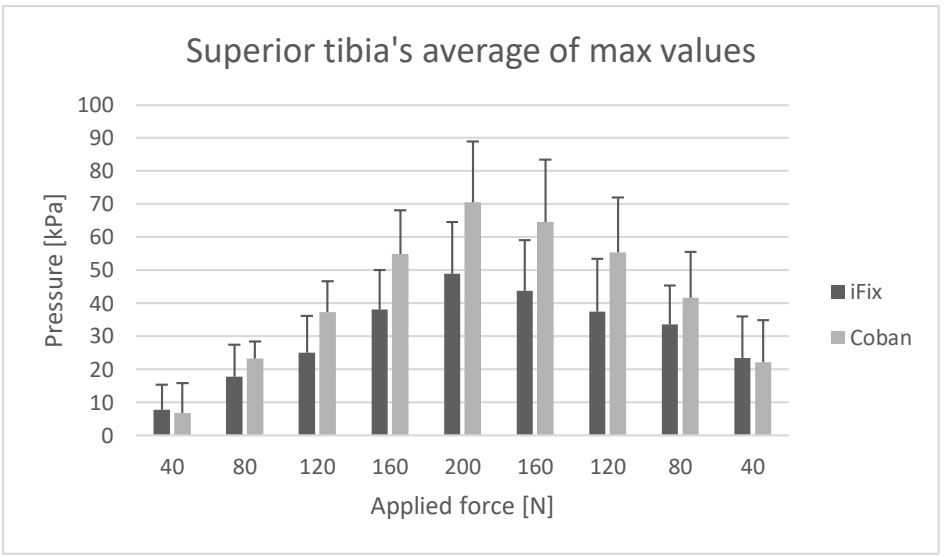

***Figure 5.11**:Two histograms, which show the average of maximum pressure*

***Table 5-1**: Mean pressure on the Tibia's zone and on the superior tibia.*

	Tibia			**Superior Tibia**		
	iFix	*Coban*	*%*	*iFix*	*Coban*	*%*
40	0,02 ± 0,191	0	inf	0,04 ± 0,071	0,12 ± 0,237	-70%
80	2,10 ± 1,319	0,78 ± 0,393	171%	0,54 ± 0,647	0,57 ± 0,453	-5%
120	0,87 ± 0,255	0,15 ± 0,140	472%	0,43 ± 0,385	0,54 ± 0,265	-22%
160	4,16 ± 1,493	2,67 ± 0,689	56%	1,42 ± 0,965	1,44 ± 0,602	-1%
200	2,92 ± 0,714	1,63 ± 0,354	78%	1,15 ± 0,721	1,30 ± 0,334	-11%
160	6,29 ± 1,363	4,24 ± 0,760	48%	2,04 ± 1,251	2,25 ± 0,820	-10%
120	6,26 ± 1,314	4,21 ± 0,63	49%	2,08 ± 1,000	2,35 ± 0,585	-12%
80	8,03 ± 1,362	5,68 ± 0,904	41%	2,64 ± 1,295	2,99 ± 1,115	-12%
40	9,93 ± 1,163	6,80 ± 0,935	46%	3,32 ± 1,272	3,51 ± 1,049	-5%

***Table 5-2**: Maximum pressure on the Tibia's zone and on the superior tibia's zone*

	Tibia			Superior Tibia		
	iFix	*Coban*	*%*	*iFix*	*Coban*	*%*
40	13,86 ± 13,231	0	inf	7,79 ± 7,516	6,89 ± 8,977	13%
80	29,91 ± 9,777	20,40 ± 2,426	47%	23,45 ± 12,535	22,08 ± 12,818	6%
120	26,17 ± 8,604	9,78 ± 7,892	167%	17,81 ± 9,582	23,28 ± 5,115	-23%
160	40,58 ± 9,897	30,74 ± 5,619	32%	33,55 ± 11,749	41,73 ± 13,741	-19%
200	40,11 ± 13,503	24,76 ± 5,977	62%	25,08 ± 11,044	37,35 ± 9,392	-33%
160	48,29 ± 11,875	38,38 ± 7,233	26%	37,52 ± 15,991	55,45 ± 16,559	-32%
120	51,01 ± 13,815	38,80 ± 7,692	31%	38,05 ± 11,950	54,97 ± 13,177	-31%
80	54,41 ± 12,744	46,21 ± 7,705	18%	43,70 ± 15,327	64,53 ± 18,931	-32%
40	61,64 ± 14,439	51,15 ± 8,548	20%	48,91 ± 15,731	70,57 ± 18,327	-31%

The histograms and the *Tables* (*5.1 and 5.2*) show the opposite situation described by the colour maps: in fact, if it is observed only the histograms, the iFix stresses more the Tibia's zone (the lower zone) and it is the opposite for the Coban. The two *Tables* (*5.1 and 5.2*) show the mean, the standard deviation and the percentage, which was calculated as the increment of iFix compared to the Coban. In the *Table 5.1* the percentage presented positive value for the Tibia's zone, but negative for the Superior tibia. There is the same behaviour in *Table 5.2*, which presents the maximum values.

This happens for the mean and for maximum values. This behaviour is possible because in the insole, for each loads, there are wide zone with no pressure, so when the values are mediated, also the zeros are included (the average decreases). So these histograms are not many relevant.

To understand if there are some similitude between the iFix's behaviour and Coban's, with the data of the histograms U test is done. A possible significant difference between the two bandages is looked for all the loads, and the maximum and mean value for the two zones (Tibia and Superior Tibia).

***Table 5-3:** Results of U test. For each external force it is possible to see if there is a significant difference or not*

		P values								
		40	*80*	*120*	*160*	*200*	*160*	*120*	*80*	*40*
Tibia	*Max*	0,001	0,0001	0,0001	0,0001	0,0001	0,0001	0,0001	0,009	0,001
	Mean	0,001	0,0001	0,0001	0,0001	0,0001	0,0001	0,0001	0,009	0,001
Sup. Tibia	*Max*	0,310	0,842	0,023	0,007	0,019	0,029	0,023	0,353	0,364
	Mean	0,353	0,579	1,000	0,739	0,853	0,684	0,796	0,971	0,579

The mean values give a more relevant indication than the maximums, which can describe the behaviour for just one repetition, and not for all.

If the mean values are considered, for the lower area (the Tibia), the difference of behaviour between the two bandages is significant, except when it is applied a load of 80 N after 120 N, because this measurement is disturbed by the hysteresis. In fact, near the ankle the stressed areas and pressure's values change for the iFix and Coban.

For the higher area, the behaviour is the same, and it is clear by the colour maps, which show the same large and stressed areas with similar modulus.

About maximums, the difference is always significant for high forces, though for some low values it can be not.

The load 40 N and 80 N shows that there is a statistical significant higher value ($p<0,001$) on the tibia for Coban comparing to iFix (see *Table 5.3* and *Fig. 5.11*).

5.3. Discussion

In the two kinds of colour maps, different values of pressure are plotted, depending on the applied force, on the bandage and on the application's zone. The values of the colour maps should be compared with those used for the medical compression hosiery. The *Table 5.4* shows the values of pressure which classifies the medical compression hosiery; these values are measured at the ankle, and for the RAL-GZ[41] this compression is higher than in other parts of the leg.

***Table 5-4**: Pressure value at the ankle. From the quality assurance RAL-GZ 387/1*

Compression class	Compression intensity	Compression in kPa
I	Low	2,4 to 2,8
II	Moderate	3,1 to 4,3
III	High	4,5 to 6,1
IV	very high	6,5 and higher

These compression's values set the security's limits, because they don't cause diseases on the vascular system. The colour maps show that:

- If the mean values are observed, the two bandages are under the limit for an applied force of 80 N, but the Coban has high compression near the ankle, while the iFix on the Tibia.

- If the maximums are considered, the limit force is 40 N.

These limits agree with the values given by the histograms; in fact, the mean values have a maximum of 10 kPa for the applied force of 200 N, and a maximum of 10 kPa for the maximum values.

The iFix stresses the tibia's zone, which is near the bone and it has the breaking limit of 133 MPa. If the ligaments are considered, in particular for the anterior cruciate, the maximum force is indicated

in the study made by Ryan and al. [69] The table with the structural properties of the ligament is reported below:

***Table 5-5**: Comparison of structural properties[59] of the anterior cruciate ligament*

	No. of Specimens	Stiffness (kN/m)	Linear force (kN)	Maximum force (kN)	Energy to Failure (N-m)
Older human (48-86 yrs.)	20	129 ± 39	0,62 ± 0,283	0,73 ± 0,266	4,89 ± 2,36
Younger human (16-26 yrs.)	6	182 ± 56	1,17 ± 0,75	1,73 ± 0,66	12,8 ± 5,5

For an old human being the maximum force is 0,73 kN, so below the applied force of 200 N.

The two bandages react in different ways: the iFix reacts with an inverse momentum on the opposite extremity; the Coban with an inverse momentum near the ankle and then with distributed forces. These behaviours should be given by their mechanical properties: the iFix is more rigid and it doesn't move, while for the Coban was observed a movement of 2 – 3 cm from the foot's positioner.

During an operation the maximum applied force could be 200 N just for short time, then the two tested bandages can resist, but if the force is applied for long time, the generated compression could cause disease for the tissues and the circulatory system in the human leg.

.

Chapter 6

6 Conclusion and Future developments

6.1. Conclusion

The aim of the project was to investigate a new bandage, which was able to immobilize the body's parts during the arthroplasty of knee. The investigated bandage is already sold, although for another application: to immobilize patient during MRI scans. In knee and hip surgery auxiliary systems are needed, which are mounted on the operation table in order to let the patient be moved in specific situations, and be fixated stable on the table during the surgery.

The forces, which are applied by the surgeon during the operation, aren't known so the bandages were tested with a large range of forces.

The first characterization was mechanical: the test demonstrated that the iFix wasn't isotropic, so its features changed with the direction. The bandage was less elastic than the Coban and peha haft. The bandages will be used during a surgery, but they could be in contact with human liquid so they are tested in wet conditions. The mechanical test showed that the iFix didn't change its features if it was wet. They were also tested with a cut on the sample. The peha haft and iFix had a maximum force (near 60 N) which is less than that obtained in normal condition (100 N). The peha haft showed the breaking of the wires; the iFix showed the same behaviour for the transversal direction but not for the longitudinal.

It was also made a characterization in vivo: in this test the sub bandage pressure was measured. The mechanical properties of iFix caused higher pressure near the knee because the bandage was rigid. This feature ensures a stability of the fixed part when it is applied a maximum force of 200 N. This didn't happen with the Coban, which showed a movement of the foot. This applied force could cause a high compression on the human body, and over 80 N it could generate diseases in the vascular system. This test presents some limitations: first of all, the sensors weren't applied on all the leg's surface, so in the posterior part of the leg the generated compression was unknown; the bandages weren't applied all the times in the same way and by the same operator. This last could be a limitation for the measurements but it was done intentionally, because it wanted to simulate a realistic condition.

It is possible to make some considerations for the usage: it is important to look at the cut's direction of the bandage, the presence of cut on the surface, the force of adhesion between the patch and the fleece parts. In wet condition the bandage didn't change its properties, so it could be used in vivo, in contact with blood or other liquid. All of these aspects are important for a stable fixation. Working in

vivo, the high forces have to be moderated because they could generate high values of pressure on the body.

6.2. Future developments

As future work, it will be significant to investigate the applied forces during an arthroplasty of knee and hip: the forces to move and to bandage patient's parts. Knowing the real range of forces, the measurement on cadavers should be done again. In this case the used sensors would have another shape to cover all the tibia's surface; besides it would be better to put sensors between the shank and the foot's support, because the pressure could be too high on that part. In *Chapter 3* some sensors were described, so some of them could be used:

- The PicoPress: this sensor has high accuracy and precision; then it is thin and biocompatible. The range of pressure is 0 – 189 mmHg, so 0 – 25,2 kPa. This could be good for measure the low pressures, that were not measured with the Pedar system; but this can't measure the high pressures. It is a single sensor, which could be applied in some specific points, but it doesn't cover all the surface.
- The FlexiForce: it is a small and ultrathin sensor. It is available in four configurations, to measure at maximum: 4 N, 111 N, 445 N, 4448 N. So the first one has a pressure range of 0 – 464 mmHg, in kPa from 0 to 61,86 kPa. If the maximum force, applied on the bandage, is 8 N, it would be perfect.
- Skiboot Tibia: it is a sensors' matrix made by the *Novel,* which has a range of pressure of 2 – 200 kPa. The matrix has 64 sensors and an area of 56 x 226 mm^2. It would be better if the range has the maximum of 100 kPa.

The choice depends on the applied forces and if the maximum interest pressure is high or low.

For the study in vivo constant forces were applied, while during an operation the forces are variable; so we could study the compression during a simulation of the operation. Furthermore, the bandage could be fixed in a way that considers the orientation of the fibres.

It would be important to investigate the effect of this compression on the epithelial tissue (for example the formation of hematoma) and on the circulatory system (for example the occlusion of small vases).

So there will be a complete view of the bandage's effect during an arthroplasty, which will be significant for the surgeon and the operators.

From our point of view, IFix can be used on lower extremities of the body, as the average pressure was constantly under 10 kPa, and the tests showed its resistance if wet or cut. Our study showed that the iFix gave a stable fixation, which depends on the orientation of the fibres, and it could generate high compressions near the bone. So these two points could limit the usage. Although, further investigation has to be done before clinical usage of IFix.

Appendix A: Mass of the samples

1. **Tensile test**

Longitudinal	i Fix
n°	Mass (g)
1	0,535
2	0,481
3	0,525
4	0,501
5	0,63
6	0,652
7	0,575
8	0,63
9	0,555
10	0,552

Transversal	i Fix
n°	Mass (g)
1	0,69
2	0,686
3	0,592
4	0,617
5	0,6
6	0,539
7	0,618
8	0,674
9	0,696
10	0,707

Diag. 45°	i Fix
n°	Mass (g)
1	0,552
2	0,578
3	0,627
4	0,639
5	0,646
6	0,628
7	0,659
8	0,611
9	0,619
10	0,594

Diag. 135°	i Fix
n°	Mass (g)
1	0,642
2	0,58
3	0,581
4	0,585
5	0,599
6	0,609
7	0,61
8	0,616
9	0,615
10	0,628

Longitudinal	Coban
n°	Mass (g)
1	1,141
2	1,212
3	1,191
4	1,212
5	1,129
6	1,192
7	0,329
8	1,191
9	1,182
10	1,232

Longitudinal	peha haft
n°	Mass (g)
1	0,528
2	0,547
3	0,528
4	0,54
5	0,496
6	0,513
7	0,608
8	0,615
9	0,51
10	0,535

2. Grab test

Longitudinal	i Fix
n°	Mass (g)
1	1,045
2	1,026
3	1,035
4	1,108
5	1,067

Transversal	i Fix
n°	Mass (g)
1	0,991
2	1,042
3	1,085
4	1,155
5	1,138

Longitudinal	Coban
n°	Mass (g)
1	2,376
2	2,41
3	2,416
4	2,344
5	2,396

Longitudinal	peha
n°	Mass (g)
1	1,045
2	1,036
3	1,03
4	1,022
5	1,046

3. Tear resistance test

Longitudinal	i Fix
n°	Mass (g)
1	0,771
2	0,749
3	0,892
4	0,83
5	0,791

Transversal	i Fix
n°	Mass (g)
1	0,809
2	0,747
3	0,748
4	0,753
5	0,81

Longitudinal	Coban
n°	Mass (g)
1	1,797
2	1,86
3	1,802
4	1,886
5	1,862

Longitudinal	peha
n°	Mass (g)
1	0,838
2	0,79
3	0,79
4	0,797
5	0,786

Appendix B: Tables

Fig.1

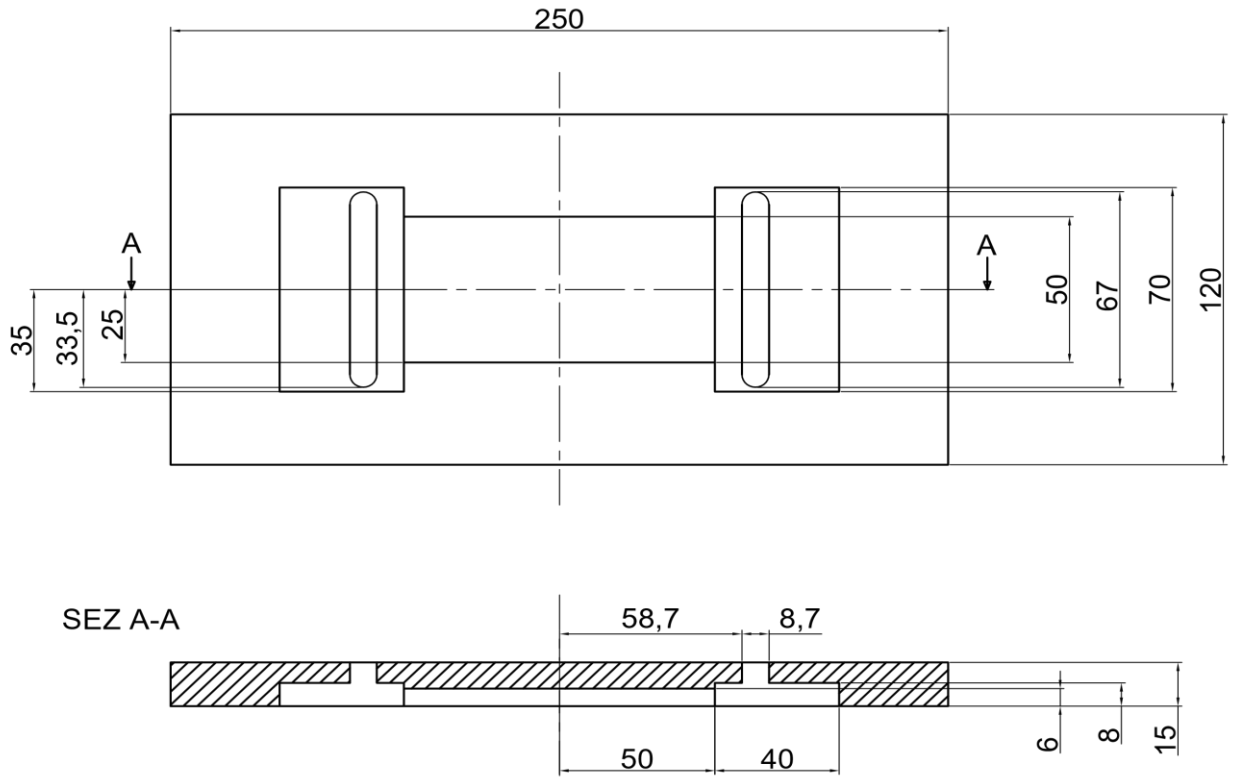

Raccordi non quotati R4,35

Fig. 2

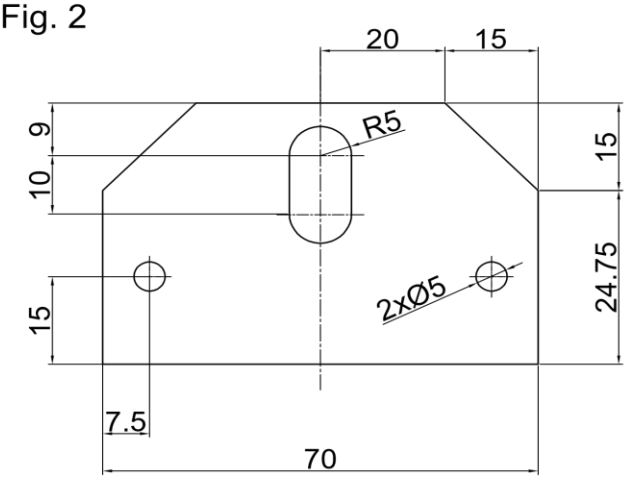

TAV n°1	
Fig. 1: Support	Scala 1:2
Fig. 2: Clamp	Scala 1:1
Tensile test	

Fig.1

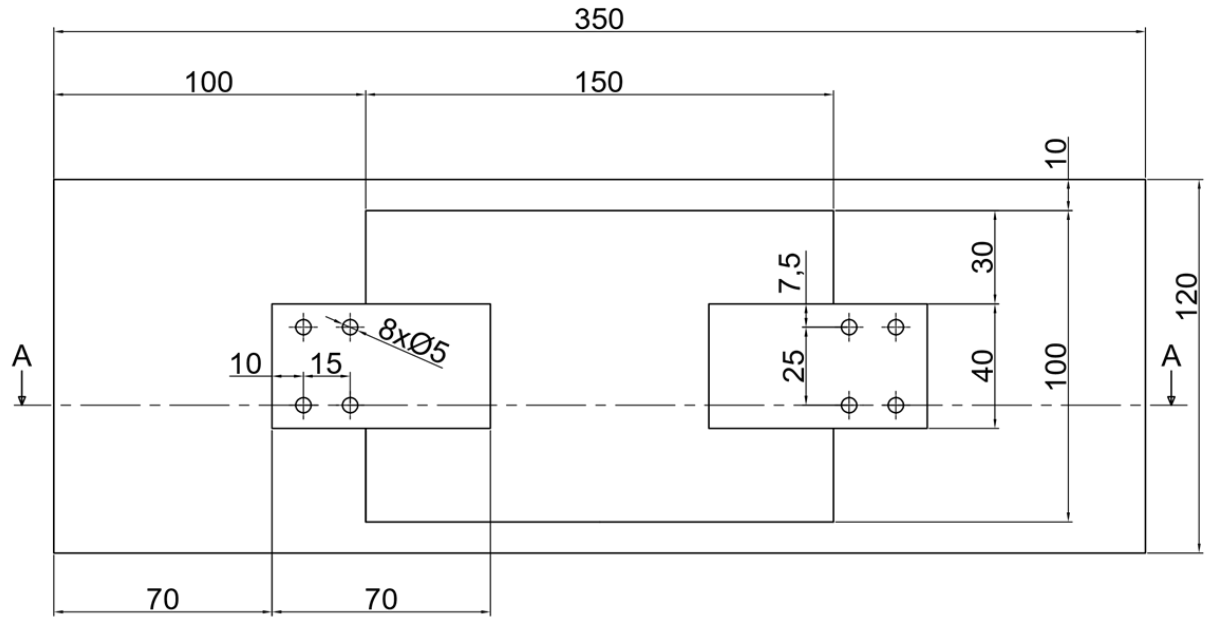

SEZ A-A

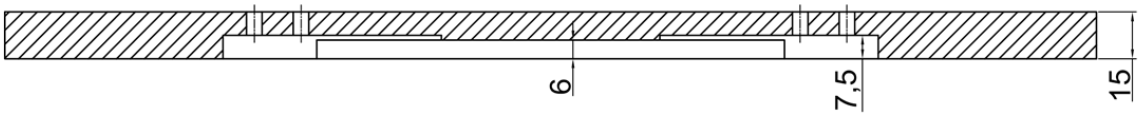

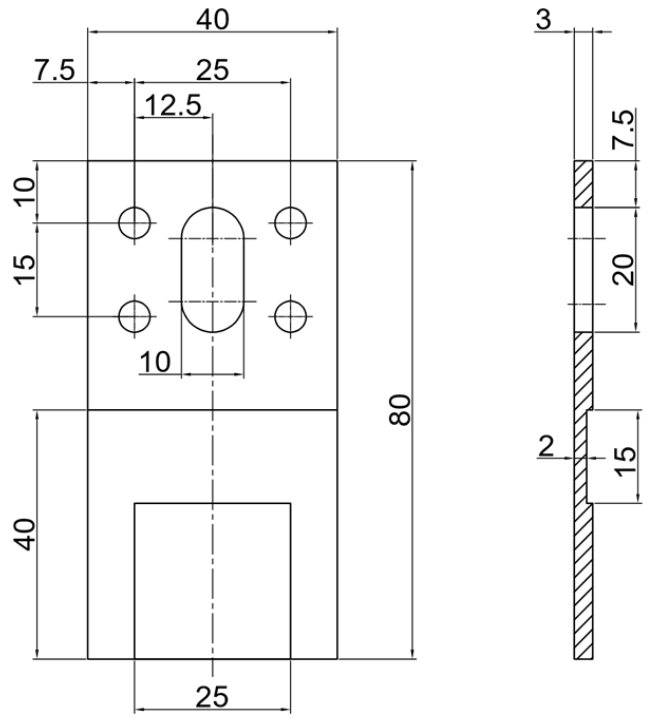

Fig.2

Fori non quotati 4xØ5

TAV n°2	
Fig. 1: Support	Scala 1:2
Fig. 2: Clamp	Scala 1:1
Grab test	

Fig.1

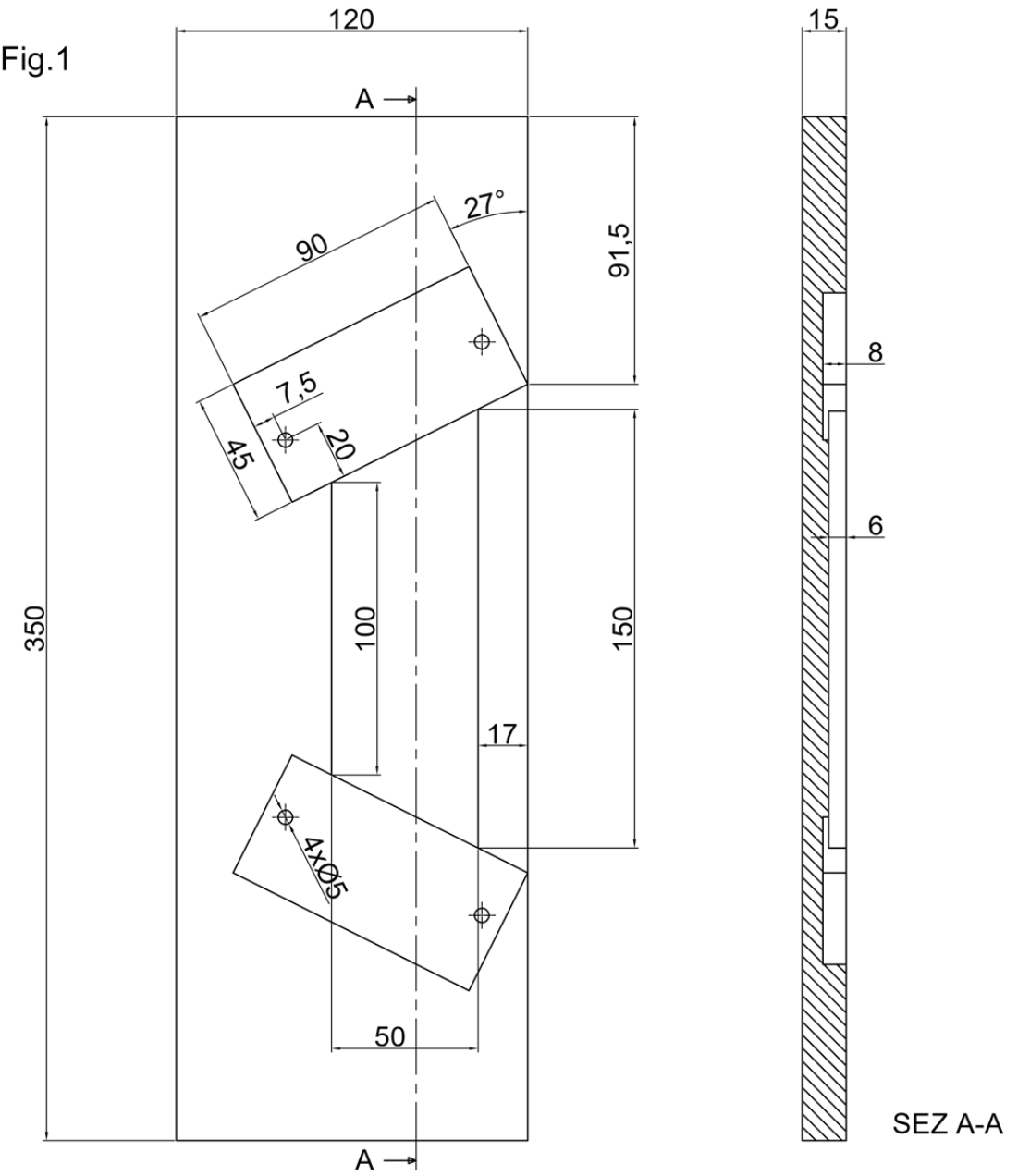

Fig.2

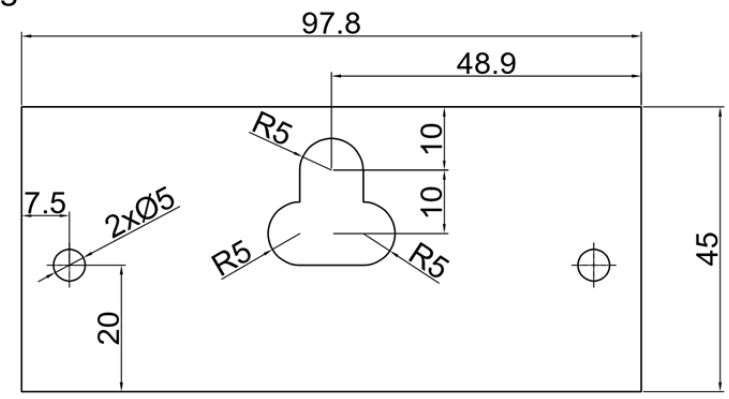

TAV n°3	
Fig. 1: Support	Scala 1:2
Fig. 2: Clamp	Scala 1:1
Tear test	

Appendix C: Flow chart

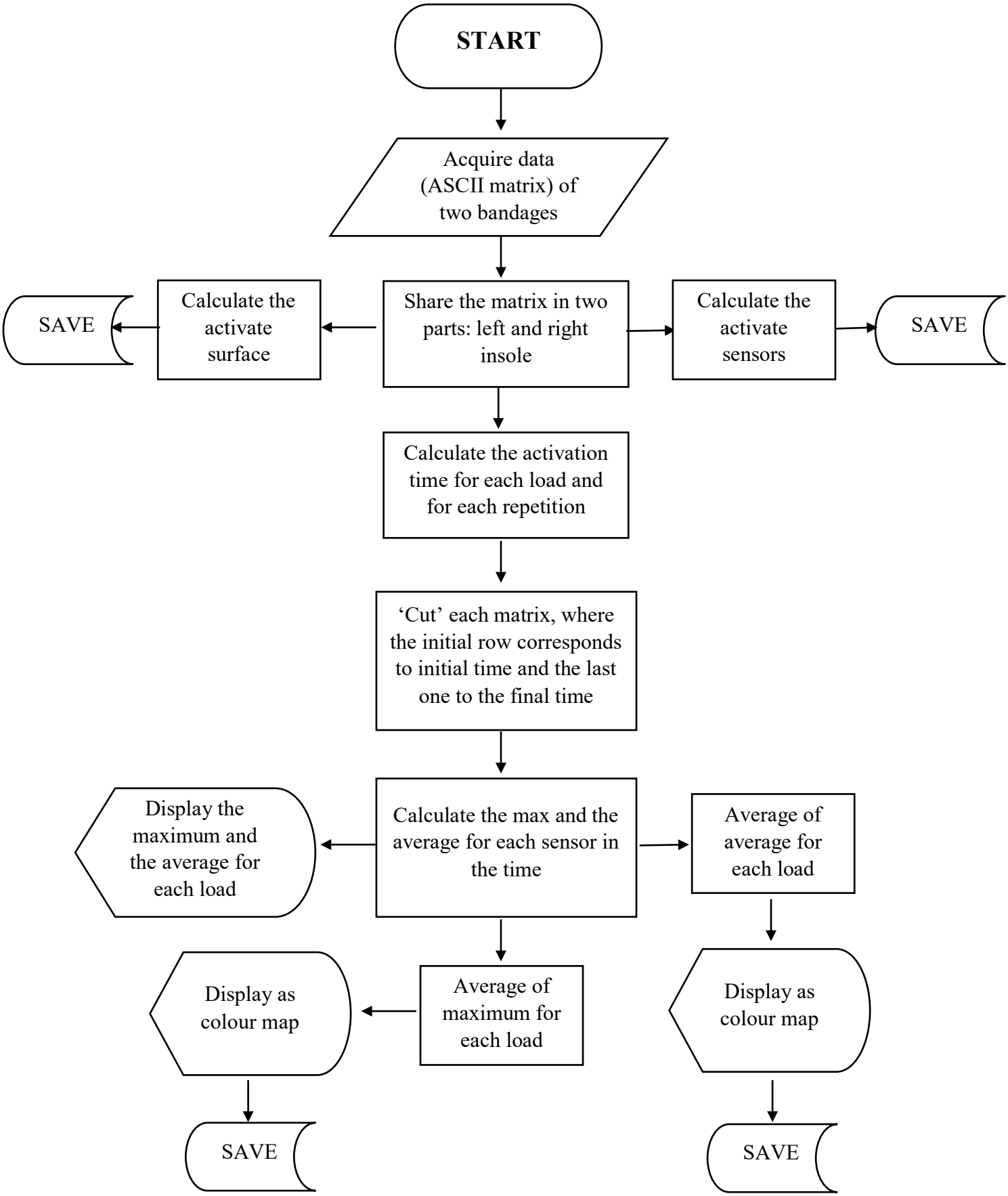

Appendix D: Colour Maps

1. Average colour maps

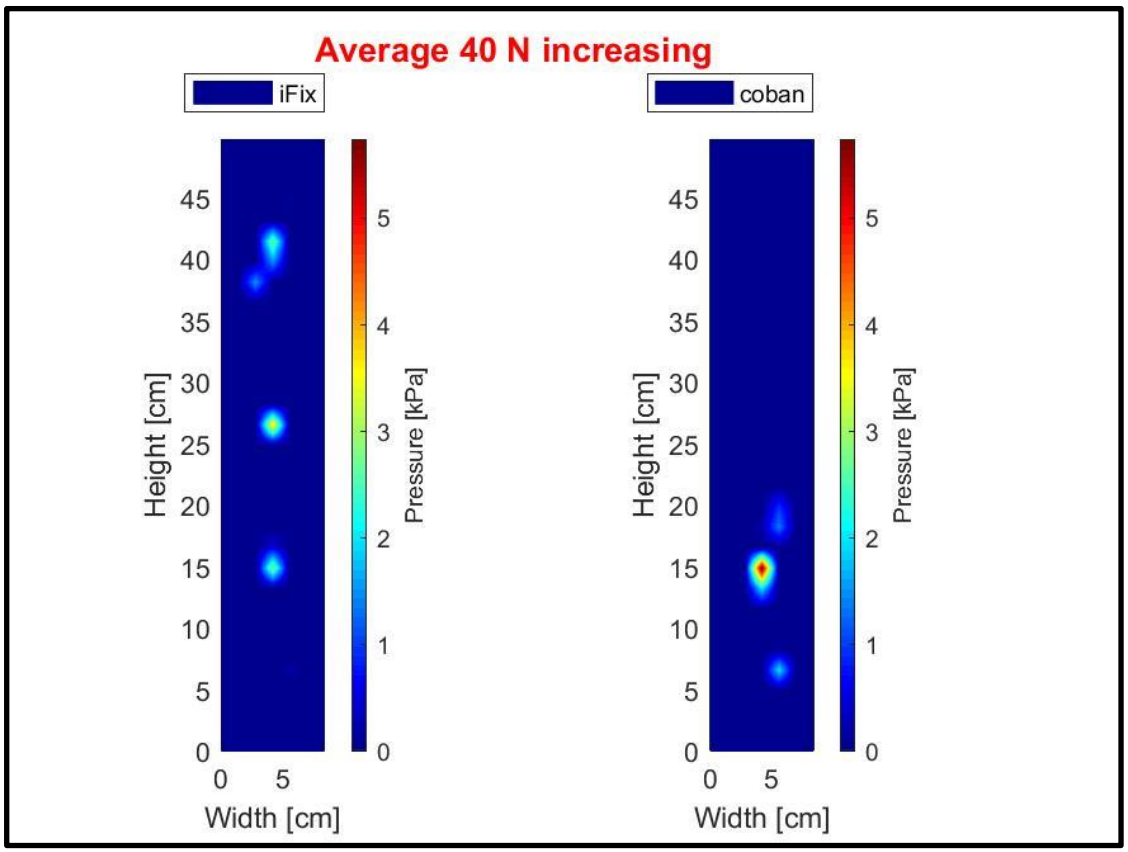

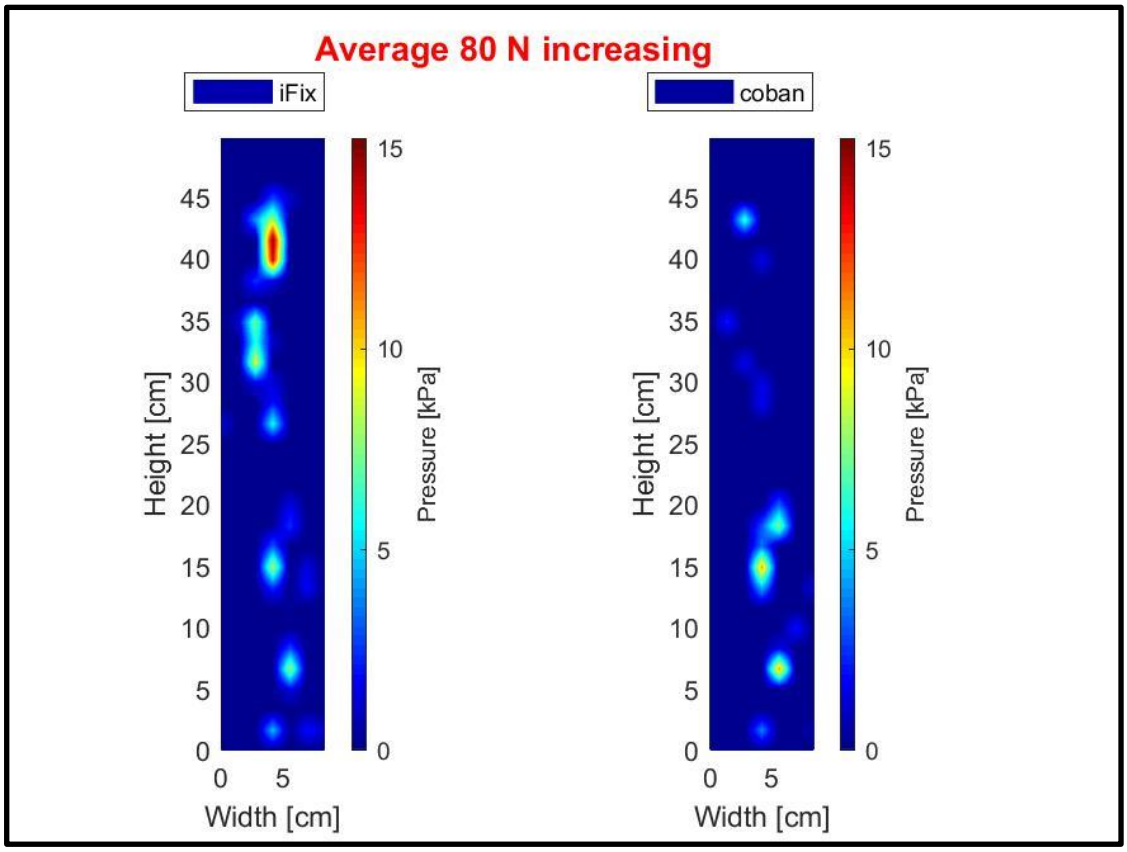
Average 80 N increasing
iFix
coban
Height [cm]
Width [cm]
Pressure [kPa]
0
5
10
15
20
25
30
35
40
45
0
5
10
15

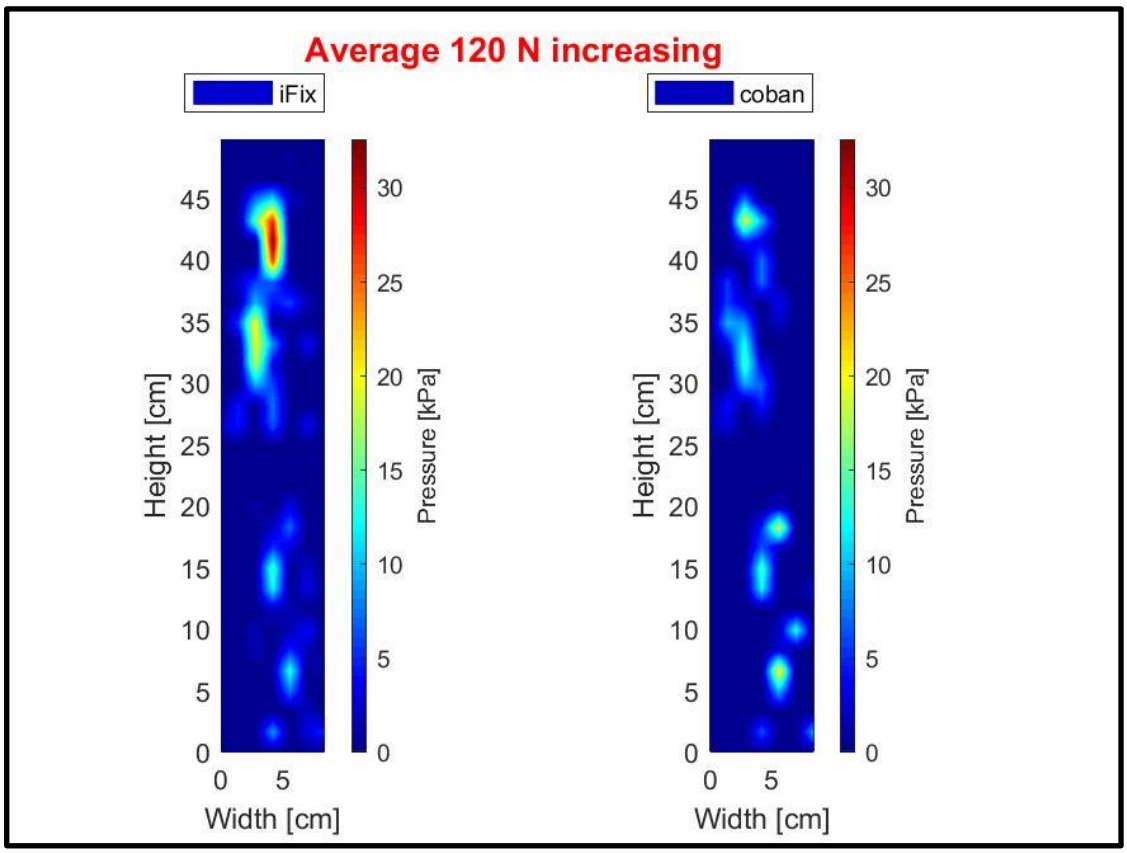
Average 120 N increasing
iFix
coban
Height [cm]
Width [cm]
Pressure [kPa]
0
5
10
15
20
25
30
35
40
45
0
5
10
15
20
25
30

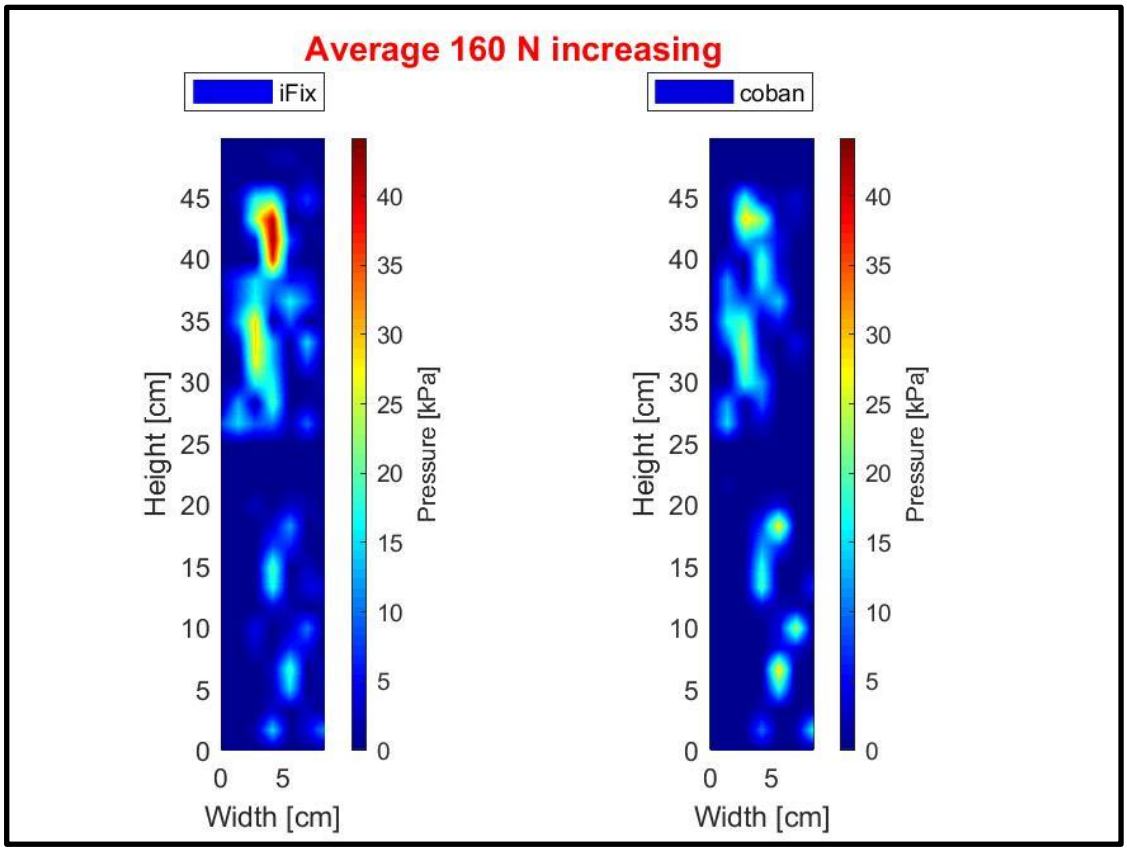
Average 160 N increasing
iFix
coban
Height [cm]
Width [cm]
Pressure [kPa]
0
5
10
15
20
25
30
35
40
45
0
5
10
15
20
25
30
35
40

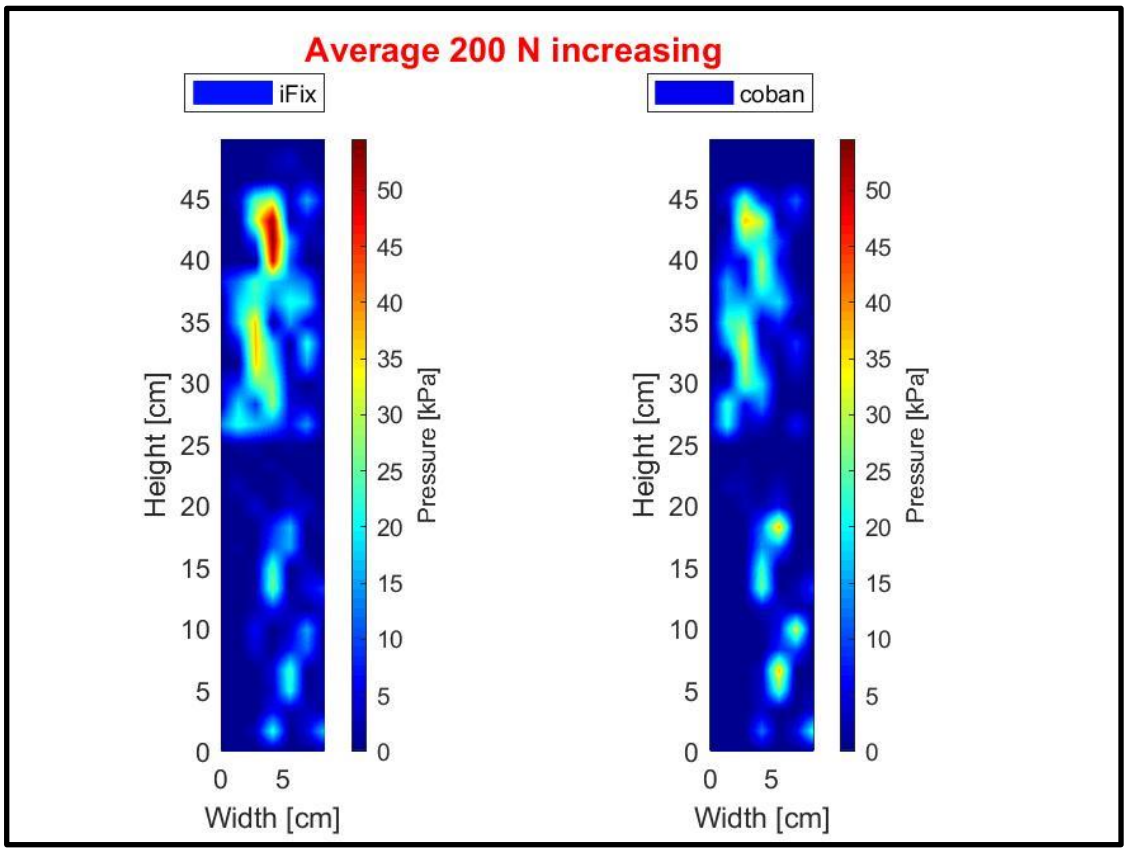
Average 200 N increasing
iFix
coban
Height [cm]
Width [cm]
Pressure [kPa]
0
5
10
15
20
25
30
35
40
45
0
5
10
15
20
25
30
35
40
45
50

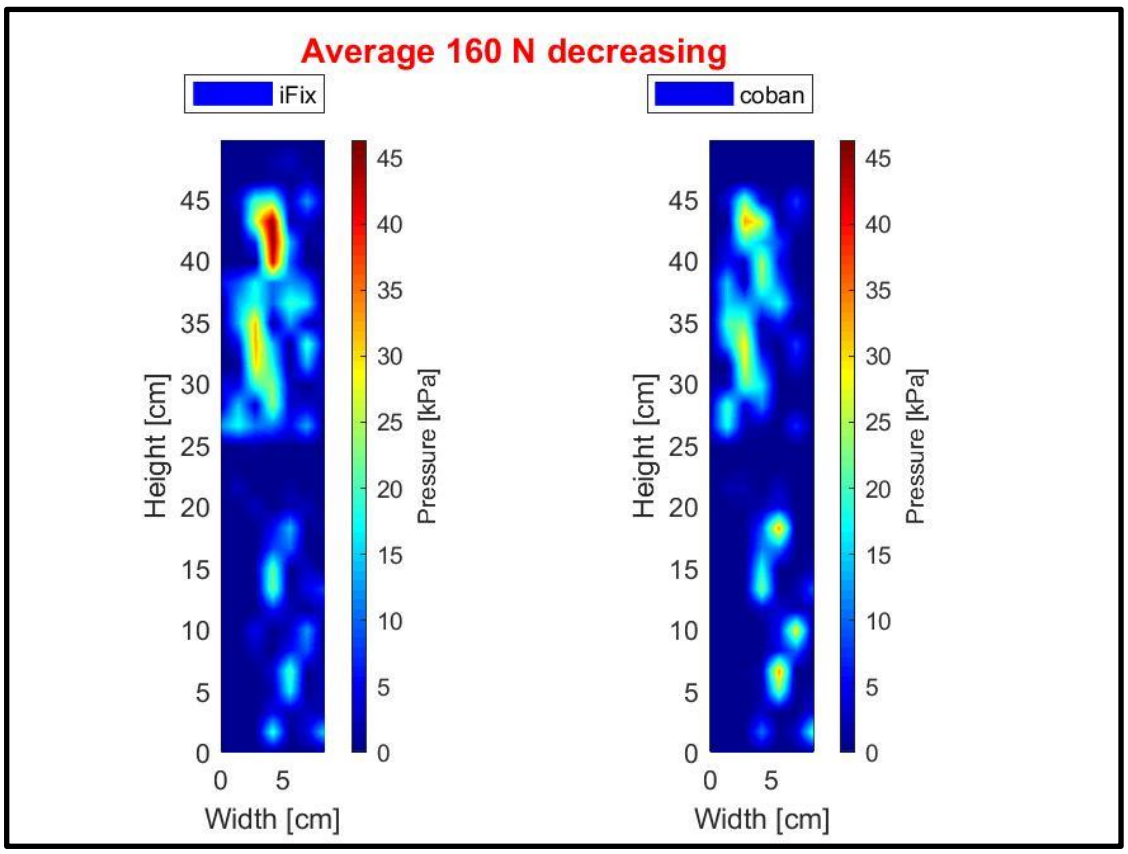
Average 160 N decreasing
iFix
coban
Height [cm]
Width [cm]
Pressure [kPa]
0
5
0
5
10
15
20
25
30
35
40
45

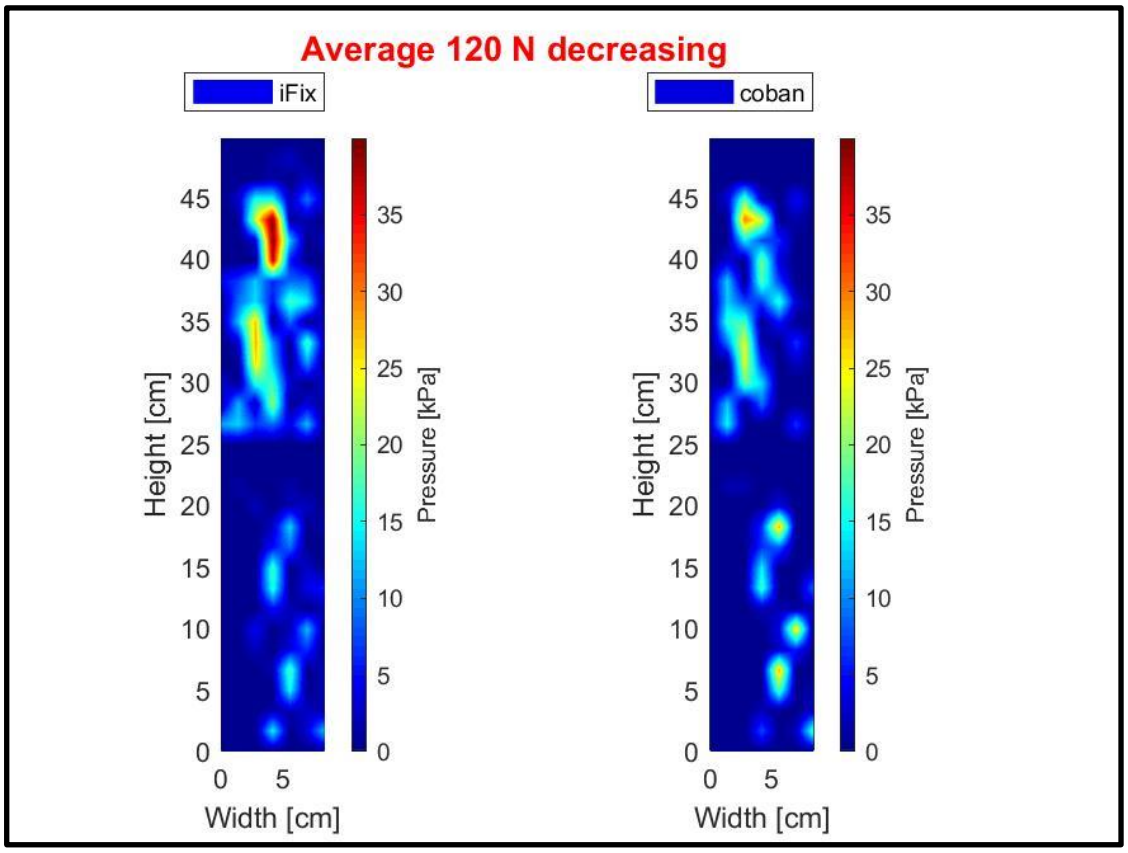
Average 120 N decreasing
iFix
coban
Height [cm]
Width [cm]
Pressure [kPa]
0
5
0
5
10
15
20
25
30
35
40
45

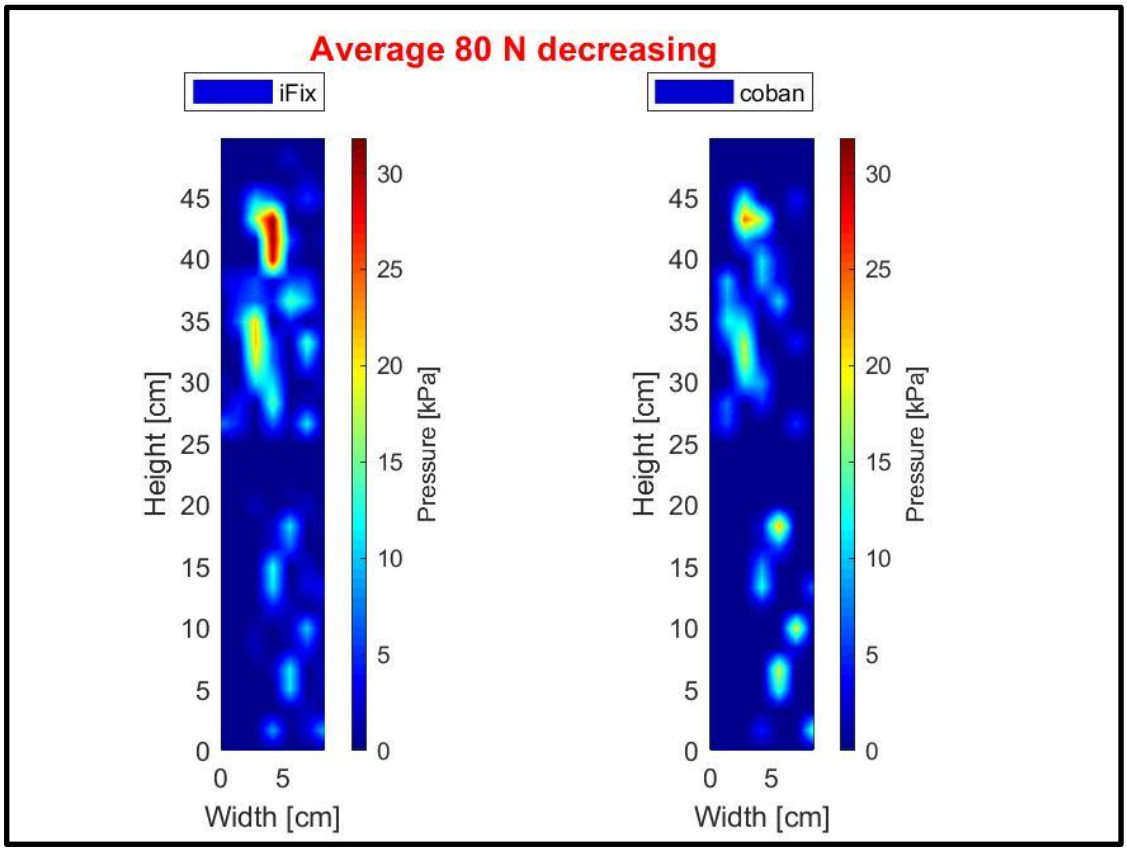
Average 80 N decreasing
iFix
coban
Height [cm]
Width [cm]
Pressure [kPa]
0
5
10
15
20
25
30
35
40
45
0
5
10
15
20
25
30

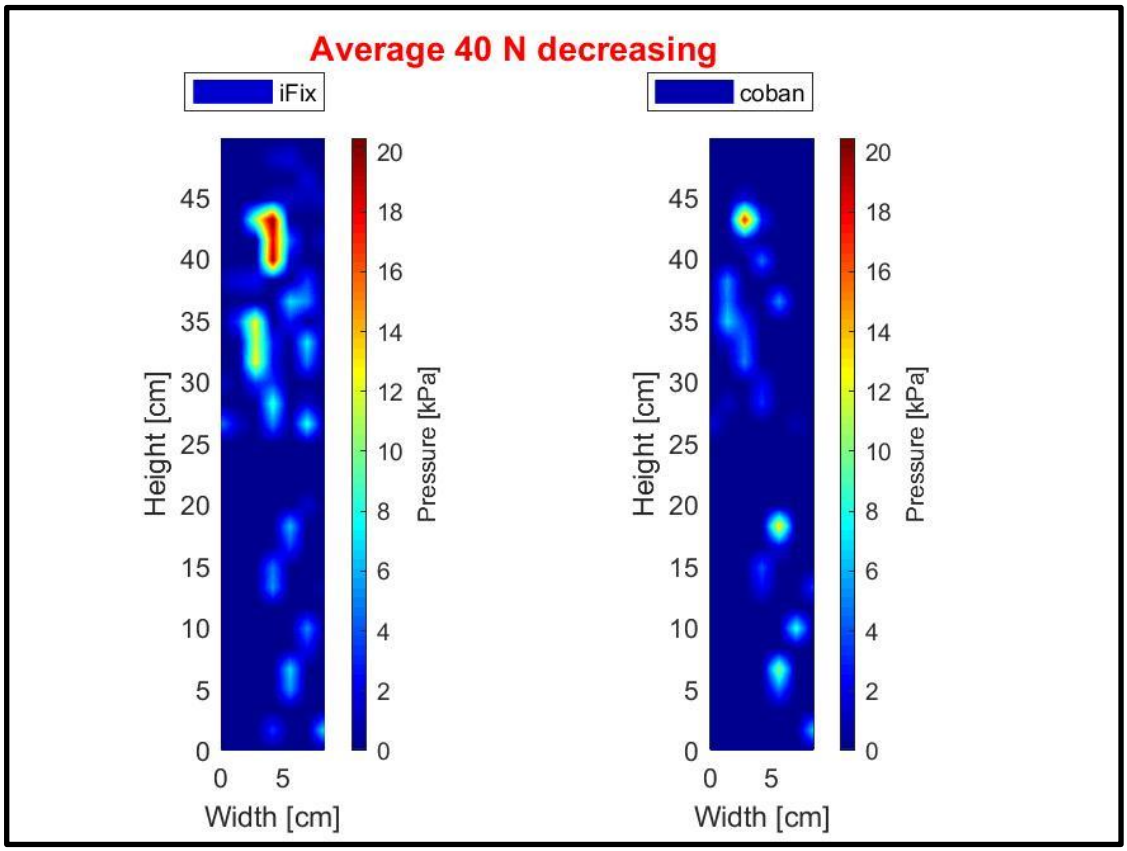
Average 40 N decreasing
iFix
coban
Height [cm]
Width [cm]
Pressure [kPa]
0
5
10
15
20
25
30
35
40
45
0
2
4
6
8
10
12
14
16
18
20

2. **Maximum colour maps**

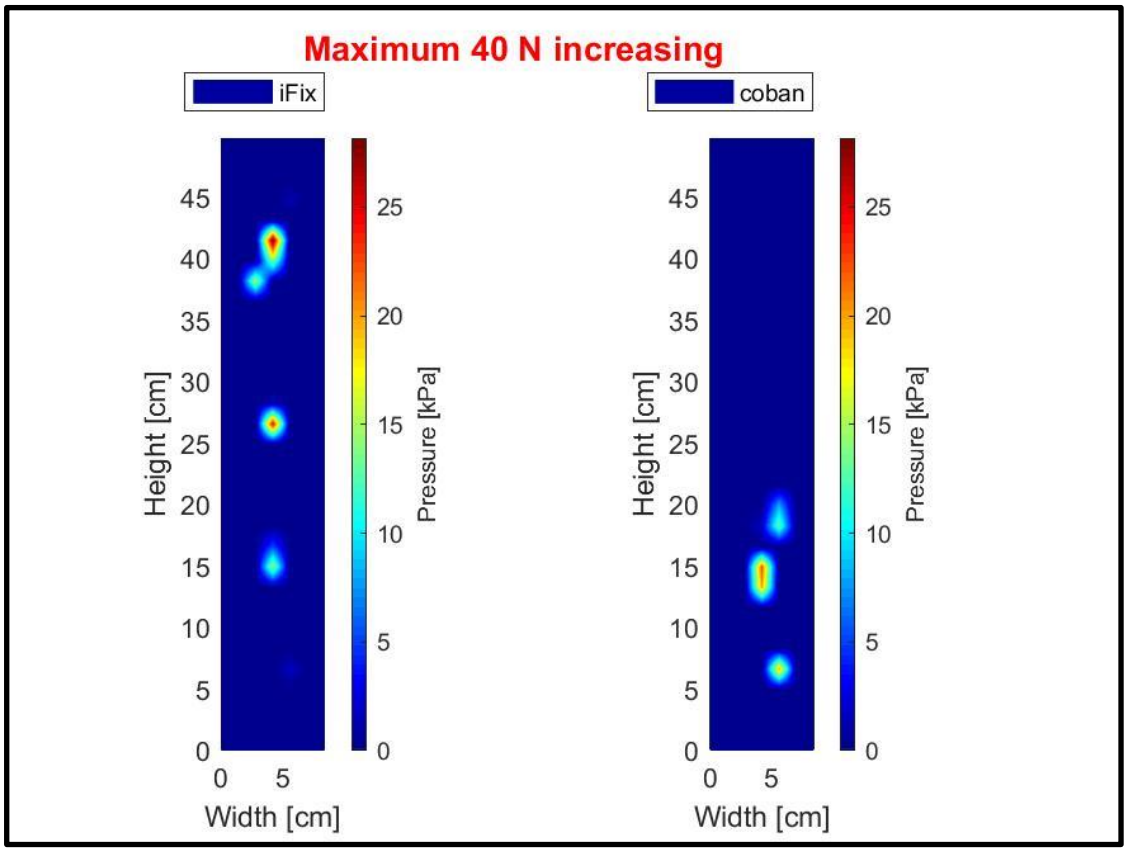

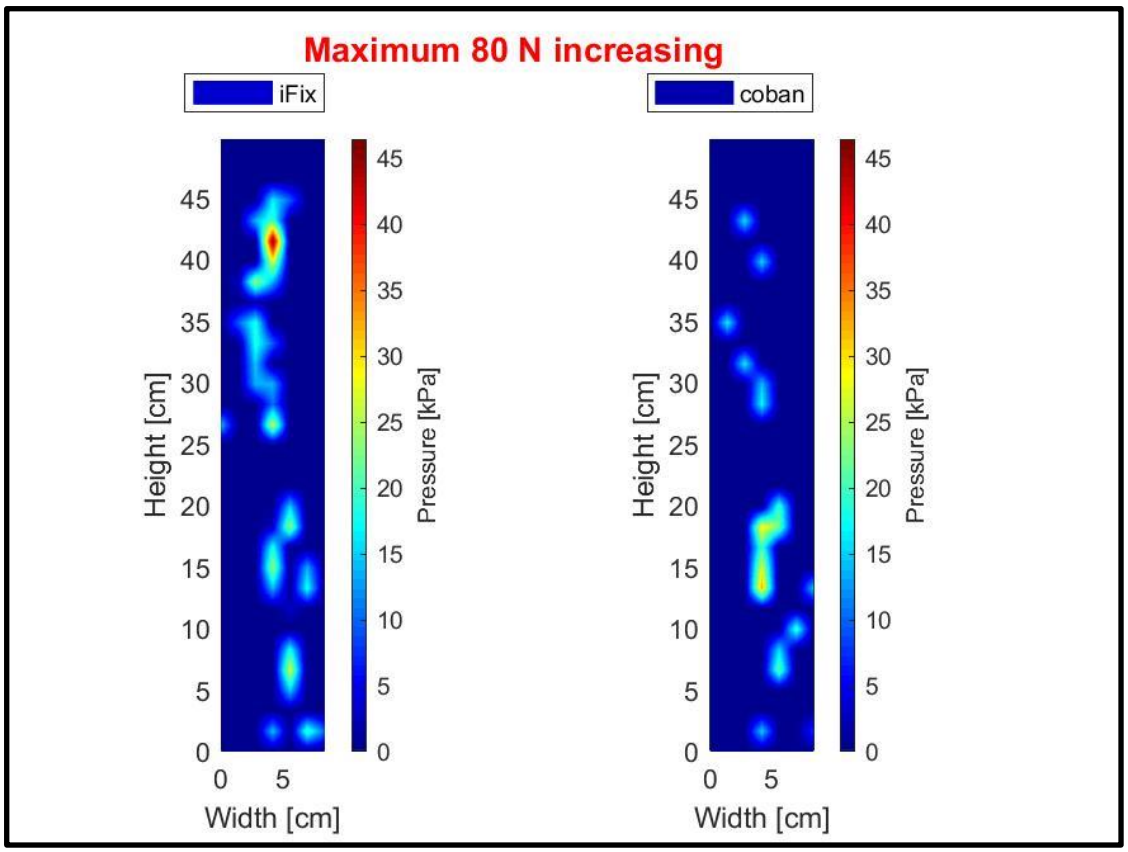

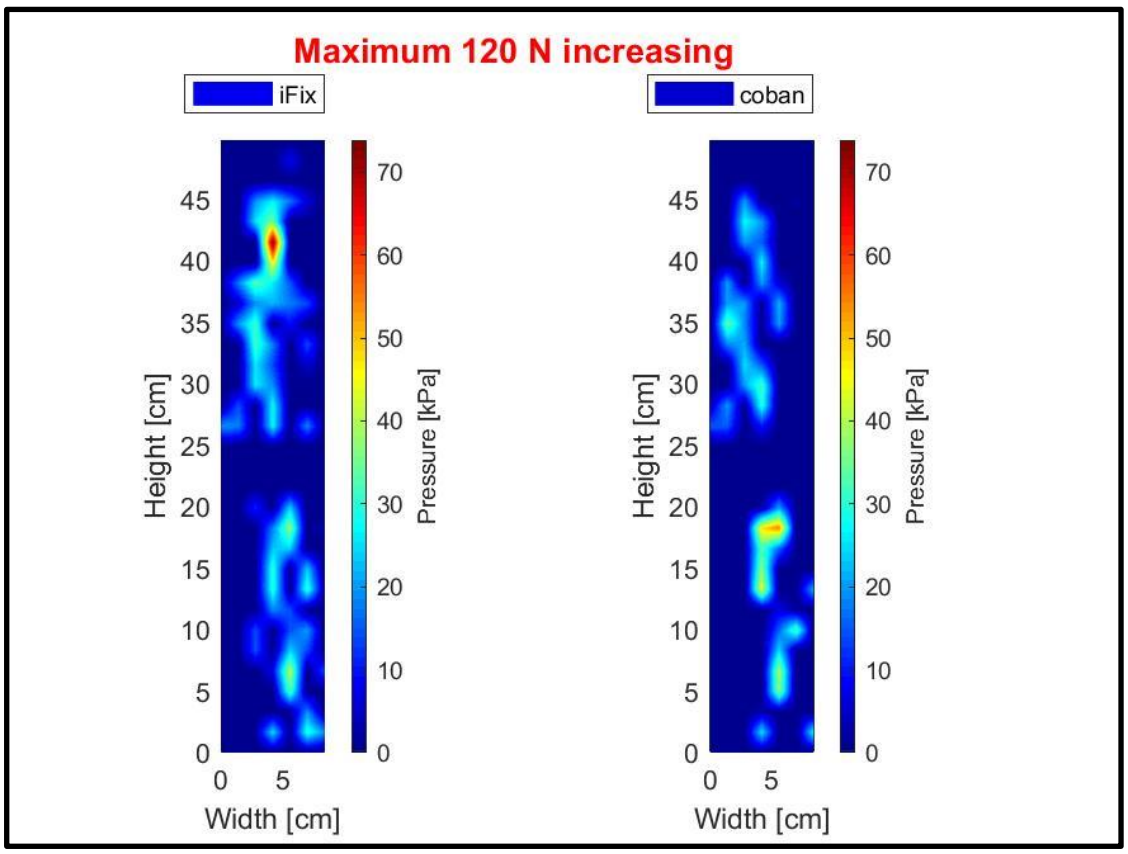
Maximum 120 N increasing
iFix
coban
Height [cm]
Width [cm]
Pressure [kPa]
0
5
10
15
20
25
30
35
40
45
0
10
20
30
40
50
60
70

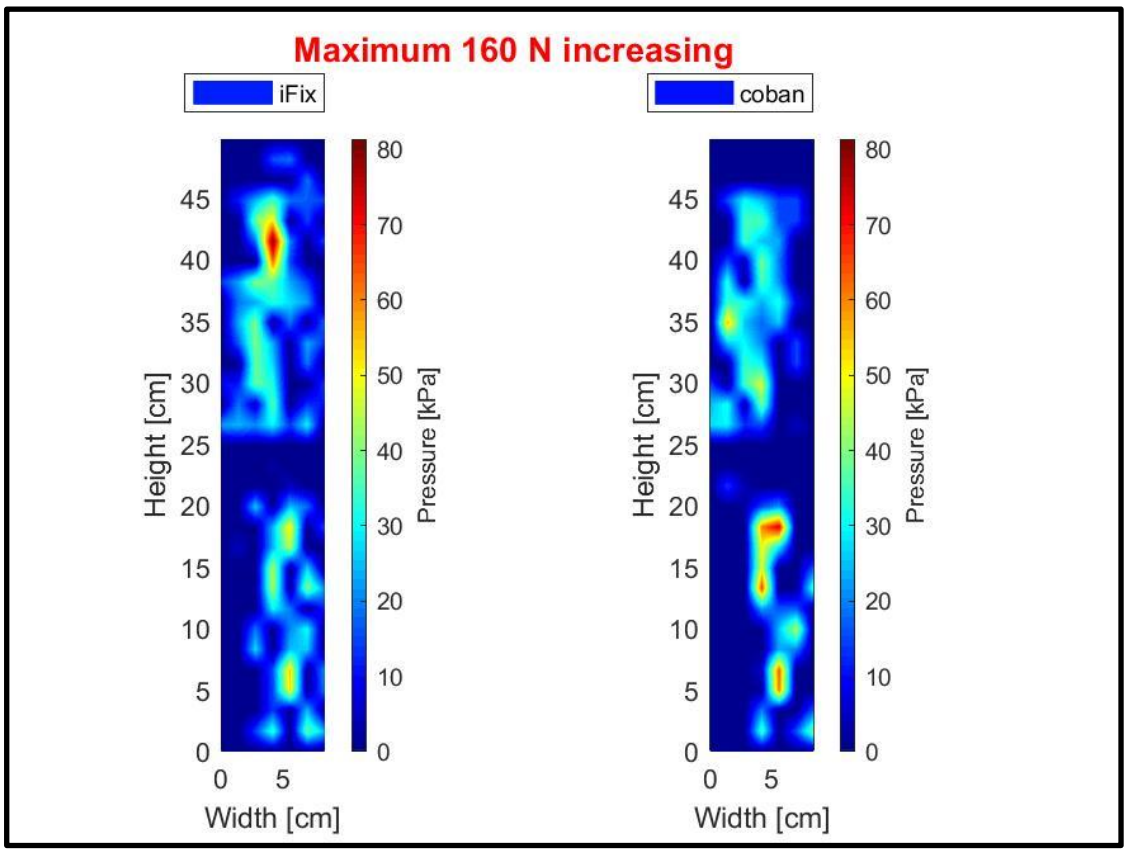
Maximum 160 N increasing
iFix
coban
Height [cm]
Width [cm]
Pressure [kPa]
0
5
10
15
20
25
30
35
40
45
0
10
20
30
40
50
60
70
80

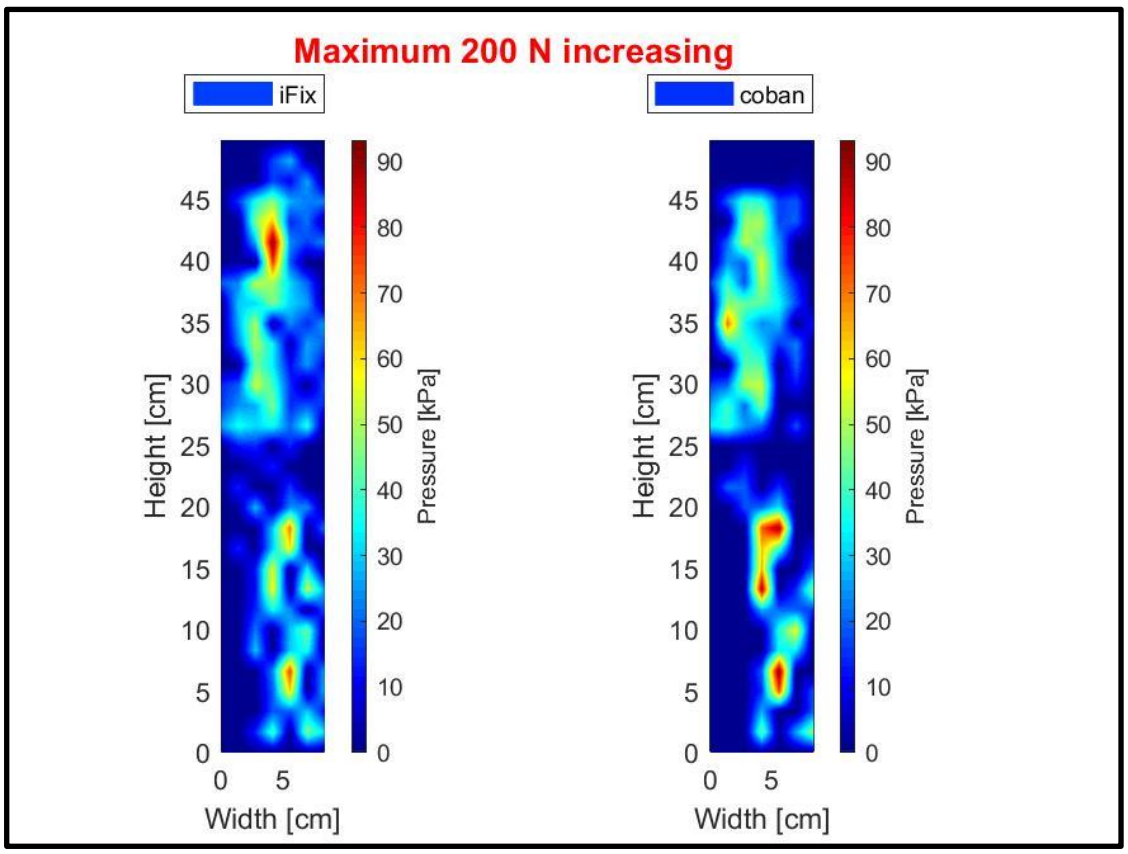
Maximum 200 N increasing
iFix
coban
Height [cm]
Width [cm]
Pressure [kPa]
0
5
0
5
10
15
20
25
30
35
40
45
0
10
20
30
40
50
60
70
80
90

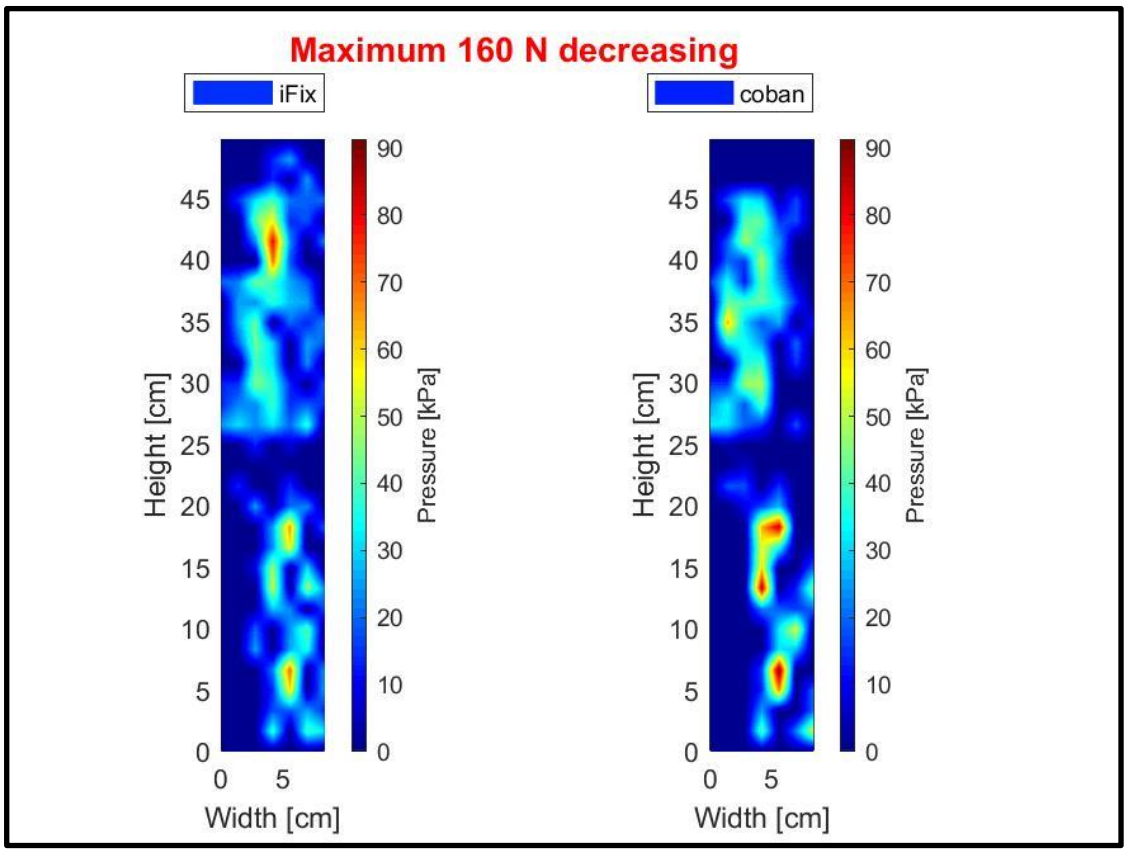
Maximum 160 N decreasing
iFix
coban
Height [cm]
Width [cm]
Pressure [kPa]
0
5
0
5
10
15
20
25
30
35
40
45
0
10
20
30
40
50
60
70
80
90

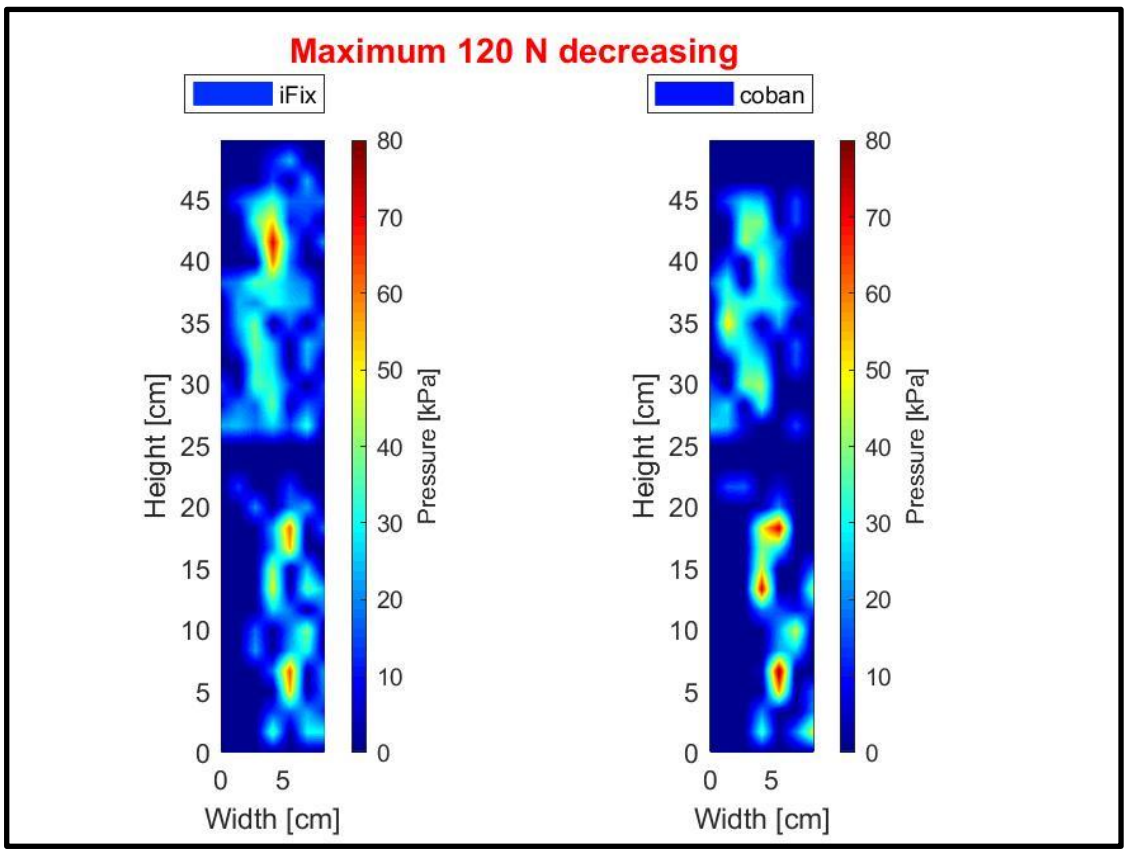
Maximum 120 N decreasing
iFix
coban
Height [cm]
Width [cm]
Pressure [kPa]
0
5
10
15
20
25
30
35
40
45
0
10
20
30
40
50
60
70
80

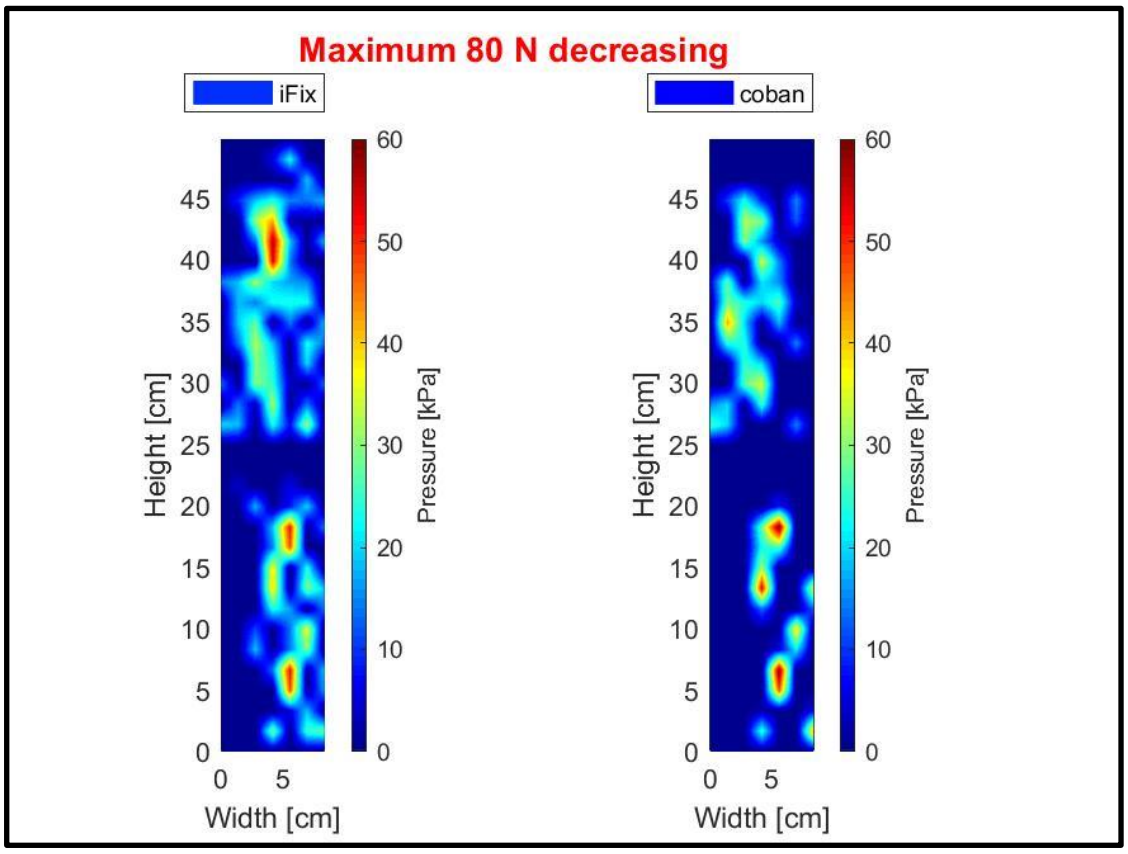
Maximum 80 N decreasing
iFix
coban
Height [cm]
Width [cm]
Pressure [kPa]
0
5
10
15
20
25
30
35
40
45
0
10
20
30
40
50
60

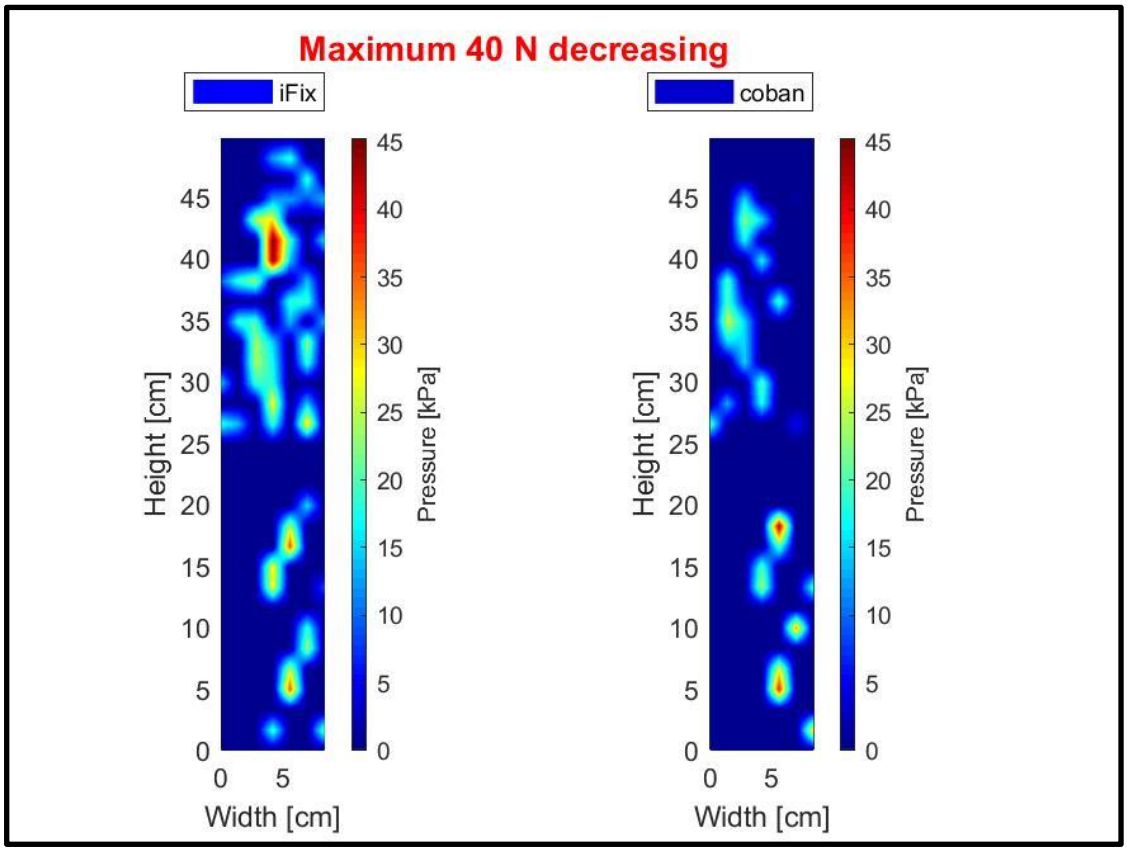
Maximum 40 N decreasing
iFix
coban
Height [cm]
Width [cm]
Pressure [kPa]
0
5
10
15
20
25
30
35
40
45

Bibliography

1. Torre M. Registro italiano artroprotesi : report 2016. 2016:28-31.
2. Jan van Houche et Al. The history of biomechanics in total hip arthroplasty. *Indian J Orthop*. 2017.
3. Mannava S, Howse EA, Stone A V, Stubbs AJ. Basic hip arthroscopy: Supine patient positioning and dynamic fluoroscopic evaluation. *Arthrosc Tech*. 2015;4(4):e391-e396. internal-pdf://120.15.79.206/basic-hip-arthroscopy.pdf.
4. Drei Fachdisziplinen, ein revolutionärer OP-Tisch: YUNO OTN.
5. Glick JM, Sampson TG, Gordon RB, Behr JT, Schmidt E. Hip arthroscopy by the lateral approach. *Arthrosc J Arthrosc Relat Surg*. 1987;3(1):4-12. doi:https://doi.org/10.1016/S0749-8063(87)80003-8
6. Dienst M, Seil R, Gödde S, et al. Effects of traction, distension, and joint position on distraction of the hip joint: An experimental study in cadavers. *Arthrosc J Arthrosc Relat Surg*. 2002;18(8):865-871. doi:https://doi.org/10.1053/jars.2002.36120
7. Ward BD, Lubowitz JH. Basic knee arthroscopy part 1: patient positioning. *Arthrosc Tech*. 2013;2(4):e497-e499. internal-pdf://159.64.26.186/basic-knee-arthroscopy-patient-positioning.pdf.
8. Ward BD, Lubowitz JH. Basic knee arthroscopy part 1: patient positioning. *Arthrosc Tech*. 2013;2(4):e497-e499. internal-pdf://159.64.26.186/basic-knee-arthroscopy-patient-positioning.pdf.
9. aofoundation. https://www2.aofoundation.org/wps/portal/!ut/p/a0/04_Sj9CPykssy0xPLMnMz0vMAfGjzOKN_A0M3D2DDbz9_UMMDRyDXQ3dw9wMDAzMjfULsh0VAbWjLW0!/?bone=Femur&classification=33-B1.1%2F2&implantstype=Lag screws&method=CRIF&preparation=Supine position for arthroscopy&redfi.
10. Romagnoli S, Verde F. L'allineamento coronale nelle protesi totali di ginocchio. *LO SCALPELLO-OTODI Educ*. 2013;27(3):126-131. doi:10.1007/s11639-013-0036-6
11. JB & JS. https://www.jbjs.org/search.php?sortby=authors&sortorder=desc&start=100&type=imagegroup&query=knee&topic=knee. Accessed September 7, 2018.
12. Daniilidis K, Tibesku CO. Frontal plane alignment after total knee arthroplasty using patient-specific instruments. *Int Orthop*. 2013;37(1):45-50. doi:10.1007/s00264-012-1732-1
13. Mako Total Knee. https://www.stryker.com/us/en/joint-replacement/systems/mako-total-knee.html.
14. Sultan A, Piuzzi N, Khlopas A, Chughtai M, Sodhi N, Mont M. *Utilization of Robotic-Arm Assisted Total Knee Arthroplasty for Soft Tissue Protection*.; 2017. doi:10.1080/17434440.2017.1392237
15. Jinnah AH, Mannava S, Plate JF, Stone A V, Freehill MT. Basic Shoulder Arthroscopy: Lateral Decubitus Patient Positioning. *Arthrosc Tech*. 2016;5(5):e1069-e1075. internal-pdf://150.66.133.94/basic-shoulder-arthroscopy-lateral-decubitus.pdf.
16. Mannava S, Jinnah AH, Plate JF, Stone A V, Tuohy CJ, Freehill MT. Basic shoulder

arthroscopy: Beach chair patient positioning. *Arthrosc Tech*. 2016;5(4):e731-e735. internal-pdf://221.0.1.68/basic-shoulder-arthroscopy-beach-chair.pdf.

17. Iamsumang C, Chernchujit B. The supine position for shoulder arthroscopy. *Arthrosc Tech*. 2016;5(5):e1117-e1120. internal-pdf://135.31.188.101/shoulder-arthroscopy-supine-position.pdf.
18. Camp CL, Degen RM, Dines JS, Sanchez-Sotelo J, Altchek DW. Basics of Elbow Arthroscopy Part II: Positioning and Diagnostic Arthroscopy in the Supine Position. *Arthrosc Tech*. 2016;5(6):e1345-e1349. internal-pdf://0.237.75.211/basic-elbow-arthroscopy.pdf.
19. Camp CL, Degen RM, Dines JS, Altchek DW, Sanchez-Sotelo J. Basics of Elbow Arthroscopy Part III: Positioning and Diagnostic Arthroscopy in the Lateral Decubitus Position. *Arthrosc Tech*. 2018;5(6):e1351-e1355. doi:10.1016/j.eats.2016.08.022
20. Aschemann D. *OP-Lagerungen Für Fachpersonal*. Springer-Verlag; 2009. internal-pdf://2.6.96.175/Buch--OP-Lagerungen_fuer_Fachpersonal--Springe.pdf.
21. Aggregate E-, Standard TG. No Title. 49(0):0-1.
22. stryker. *Leg Positioner*.
23. Partsch H, Clark M, Mosti G, et al. *Classification of Compression Bandages: Practical Aspects*. Vol 34.; 2008. doi:10.1111/j.1524-4725.2007.34116.x
24. ACE™ Brand Elastic Bandages. https://www.acebrand.com/3M/en_US/ace-brand/products/~/ACE-Brand-Elastic-Bandages/?N=4304+3294605848&rt=rud.
25. Lohmann & Rauscher GmbH. https://www.lohmann-rauscher.com/en/products/bandages/compression-therapy/long-stretch-bandages/dauerbinde-kf/.
26. SurePress® High Compression Bandage . https://www.convatec.com.au/products/pc-wound-compression/surepress-high-compression-bandage.
27. Profore +. http://www.smith-nephew.com/uk/products/wound_management/product-search/profore/profore-plus/.
28. Comprilan. http://www.bsnmedical.com/products/wound-care-vascular/category-product-search/compression-therapy/compression-bandages/comprilanr.html.
29. Rosidal K. https://www.lohmann-rauscher.com/at-de/produkte/binden/kompressionstherapie/kurzzugbinden/rosidal-kelko-rosidal-k/.
30. Pütter bandage. https://www.hartmann.info/en-DX/our-products/Compression-and-Support-Therapy/Compression-bandages/Stretch--100-/Cohesive/Pütter-haft#products.
31. Evaluating the effectiveness of the customized Unna boot when treating patients with venous ulcers. http://www.scielo.br/scielo.php?pid=S0365-05962013000100041&script=sci_arttext&tlng=pt.
32. Hearn EJ. Mechanics of materials, vols. 1 and 2 Edited by E. J. Hearn. Pp. 643. Pergamon Press, Oxford. 1978. *Endeavour*. 1978;2(4):192. doi:10.1016/0160-9327(78)90104-7
33. Weighing S, Separation C. Standard Test Method for Tensile Properties of Thin Plastic Sheeting 1. 2006;14(June 2002).
34. Yahya Gharagozlou. Instron. http://www.instron.us/en-us/testing-solutions/industry-solutions/automotive/interior/textiles-testing. Accessed August 30, 2018.
35. Iso BSEN. Textiles — Tensile properties of fabrics — This British Standard is the English language version of. 1999.

36. Partsch H. The Static Stiffness Index: A Simple Method to Assess the Elastic Property of Compression Material In Vivo. *Dermatologic Surg*. 2005;31(6):625-630. internal-pdf://230.180.248.37/Partsch_H_Dermatol_Surg.pdf.

37. Liu R, Kwok YL, Li Y, Lao TT, Zhang X. Quantitative assessment of relationship between pressure performances and material mechanical properties of medical graduated compression stockings. *J Appl Polym Sci*. 2007;104(1):601-610. doi:10.1002/app.25617

38. Suehiro K, Okada M, Yoshimura A, et al. Elastic Multilayer Bandages for Chronic Venous Insufficiency: Features of Our Technique. *Ann Vasc Dis*. 2012;5(3):347-351. doi:10.3400/avd.oa.12.00020

39. Al Khaburi JAJ. Pressure mapping of medical compression bandages used for venous leg ulcer treatment.PhD thesis, University of Leeds. 2010. internal-pdf://240.209.153.159/Thesis_Corrected.pdf.

40. O'Meara S, Cullum N, Nelson EA, Dumville JC. Compression for venous leg ulcers. 2012. doi:10.1002/14651858.CD000265.pub3

41. Assurance GI for Q. Medical Compression Hosiery. 2000;(January).

42. The Effect of Multi-Layer Bandage on the Interface Pressure Applied by Compression Bandages. *Int J Mech Aerospace, Ind Mechatron Manuf Eng*. 2011;5:1168-1174. internal-pdf://99.242.9.237/The-Effect-of-Multi-Layer-Bandage-on-the-Inter.pdf.

43. UNI Store. http://store.uni.com/catalogo/index.php/uni-en-29073-1-1993.html?josso_back_to=http://store.uni.com/josso-security-check.php&josso_cmd=login_optional&josso_partnerapp_host=store.uni.com. Published 1993. Accessed August 30, 2018.

44. Peha-haft. https://hartmann.info/en-GB/our-products/Wound-Management/Non-Adhesive-Fixation/Cohesive-Bandages/Peha-haft®-latexfree#products.

45. coban 3M. https://www.3m.com/3M/en_US/company-us/all-3m-products/~/3M-Coban-Self-Adherent-Wrap/?N=5002385+3293321980&rt=rud.

46. iFIX. https://www.interventional-systems.com/global/products/ifix/.

47. Polypropylene. http://www.bpf.co.uk/plastipedia/polymers/PP.aspx#properties.

48. polyamide. http://www.bpf.co.uk/plastipedia/polymers/Polyamides.aspx.

49. Thomas S. "The use of the Laplace equation in the calculation of subbandage pressure,." *EWMA J*. 2003;3(1):21-23.

50. Khaburi J Al, Dehghani-Sanij AA, Nelson EA, Hutchinson J. Pressure mapping bandage prototype: Development and testing. In: *2012 International Conference on Biomedical Engineering (ICoBE)*. ; 2012:430-435. doi:10.1109/ICoBE.2012.6179052

51. Rimaud D, Convert R, Calmels P. In vivo measurement of compression bandage interface pressures: The first study. *Ann Phys Rehabil Med*. 2014;57(6):394-408. doi:https://doi.org/10.1016/j.rehab.2014.06.005

52. Partsch H, Clark M, Bassez S, et al. *Measurement of Lower Leg Compression In Vivo: Recommendations for the Performance of Measurements of Interface Pressure and Stiffness*. Vol 32.; 2006. doi:10.1111/j.1524-4725.2006.32039.x

53. microlabitalia. http://www.microlabitalia.it/case-history.php?azione=show&url=pico-press. Accessed September 7, 2018.

54. Partsch H, Mosti G. *Comparison of Three Portable Instruments to Measure Compression*

Pressure. Vol 29.; 2010. internal-pdf://80.63.98.243/partschetal-comparisonofthreeportableinstrumen.pdf.

55. Gaied I, Drapier S, Lun B. Experimental assessment and analytical 2D predictions of the stocking pressures induced on a model leg by Medical Compressive Stockings. *J Biomech*. 2018;39(16):3017-3025. doi:10.1016/j.jbiomech.2005.10.022

56. Barbenel JC, Sockalingham S. Device for measuring soft tissue interface pressures. *J Biomed Eng*. 2018;12(6):519-522. doi:10.1016/0141-5425(90)90062-R

57. iconstrux. http://www.ic0nstrux.com/FlexiForce-Sensor-Demo-Kit#.W5I3fugzZEY. Accessed September 7, 2018.

58. microcontroller. http://www.microcontroller.it/Tutorials/Elettronica/capaciteq.htm. Accessed September 7, 2018.

59. Ashruf CMA. Thin flexible pressure sensors. *Sens Rev*. 2002;22(4):322-327. doi:10.1108/02602280210444636

60. Russell C. XSENSOR technology: a pressure imaging overview. *Sens Rev*. 2007;27(1):24-28. doi:10.1108/02602280710723433

61. A. Fergenbaum M, Hadcock L, M. Stevenson J, Bryant J, Morin E, Reid S. *Development of a Dynamic Biomechanical Model for Load Carriage: Phase 4, Part C2: Assessment of Pressure Measurement Systems on Curved Surfaces for the Dynamic Biomechanical Model of Human Load Carriage*.; 2005. internal-pdf://184.192.107.57/a481127.pdf.

62. Rikli DA, Honigmann P, Babst R, Cristalli A, Morlock MM, Mittlmeier T. Intra-articular pressure measurement in the radioulnocarpal joint using a novel sensor: in vitro and in vivo results. *J Hand Surg Am*. 2007;32(1):67-75. doi:10.1016/j.jhsa.2006.10.007

63. Pedar systhem. http://www.novel.de/novelcontent/pedar.

64. Anthony J. Wheeler ARG. *Introduction to Engineering Experimentation*.

65. Calibration. http://www.novel.de/novelcontent/calibration.

66. Quality_Management_of PMD_at_novel_2011_03.

67. Giacomozzi C. Appropriateness of plantar pressure measurement devices: A comparative technical assessment. *Gait Posture*. 2018;32(1):141-144. doi:10.1016/j.gaitpost.2010.03.014

68. Bonnaire R, Verhaeghe M, Molimard J, Calmels P, Convert R. Characterization of a pressure measuring system for the evaluation of medical devices. *Proc Inst Mech Eng Part H J Eng Med*. 2014;228(12):1264-1274. doi:10.1177/0954411914562871

69. Noyes FR, Grood ES. The strength of the anterior cruciate ligament in humans and Rhesus monkeys. *J Bone Joint Surg Am*. 1976;58(8):1074-1082. doi:10.2106/JBJS.M.00187

Ringraziamenti

Desidero ringraziare la prof.ssa Bignardi, relatrice di questa tesi, per la grande opportunità che mi ha dato, e il dott. Putzer per tutto l'aiuto fornitomi durante la stesura e per le conoscenze che ha messo a mia disposizione.

Un grande ringraziamento va alla mia famiglia, che con il loro incoraggiamento e vicinanza anche nei momenti di lontananza, mi hanno permesso di arrivare fino a qui.

Un particolare grazie va a Davide, il mio punto più importante di riferimento e che mi ha dato il coraggio di mettermi in gioco.

Un ultimo ringraziamento ai compagni di studio, con cui ho condiviso questo importante percorso, e che sono per me veri amici più che compagni.